

“Caspase-dependent cleavage of the mono-ADP-ribosyltransferase
ARTD10 interferes with its pro-apoptotic function”

Von der Fakultät für Mathematik, Informatik und Naturwissenschaften der RWTH
Aachen University zur Erlangung des akademischen Grades eines Doktors der
Naturwissenschaften genehmigte Dissertation

vorgelegt von

Diplom-Biologe
Nicolas Herzog

aus Aachen

Berichter: Universitätsprofessor Dr. rer. nat. Bernhard Lüscher
Universitätsprofessor Dr. rer. nat. Lothar Elling

Tag der mündlichen Prüfung: 26.02.2013

Diese Dissertation ist auf den Internetseiten der Hochschulbibliothek online verfügbar.

1 Abstract

Intracellular communication at the molecular level is mainly dependent on posttranslational modifications and interplay between those. ADP-ribosylation, the transfer of ADP-ribose from NAD⁺ to substrates and especially its polymerization, is involved in processes like signal transduction, gene transcription and DNA damage repair. The latter is mainly mediated by ARTD1/PARP1, the founding member of the group of ADP-ribosyltransferases (ARTs). Its functions through poly-ADP-ribosylation have been studied well. Mono-ADP-ribosyltransferase activity however was previously only reported for bacterial toxins and extracellular ARTs. Yet although evidence for intracellular ADP-ribosylation is still missing, ARTD10 was recently shown to possess mono-ADP-ribosylation activity *in vitro*.

First attempts to obtain insight into its physiological relevance revealed that the enzyme is implicated in transformation and proliferation. In this work we expanded on these findings and generated stable HeLa cell lines, which inducibly express ARTD10 or different constructs thereof. The expression of the wild-type protein confirmed prior observations, as it inhibited proliferation. By follow-up experiments this effect could be linked to the induction of apoptosis in those cells. This was dependent on catalytic activity, as ARTD10-G888W, a catalytic inactive mutant, was not cytotoxic. In addition, we could observe cleavage of ARTD10 during apoptosis, an observation also made for ARTD1. Processing at 'I A M D₄₀₆ S' resulted in a catalytically active fragment, which was no longer able to stimulate apoptosis. Moreover, the inflammatory caspase-1 also processed ARTD10 *in vitro* at "W T P D₅₈₁ S" potentially linking ARTD10 cleavage to a second cellular pathway involving caspases.

In both cases the RNA recognition motif as well as a glycine-rich region were separated from the catalytic center. The loss of pro-apoptotic activity alongside the separation of these domains hints towards an important function of ARTD10 in an RRM-linked process, like RNA processing or transport, or a regulation of ARTD10 itself through the RRM. Further studies are necessary to unravel the possible implications of ARTD10 in those pathways and could provide further insight into the physiological role of ARTD10 based on the findings made in this work.

2 Zusammenfassung

Die intrazelluläre Kommunikation auf molekularer Ebene ist hauptsächlich abhängig von posttranslationalen Modifikationen und ihrem Zusammenspiel. ADP-Ribosylierung, die Übertragung von ADP-Ribose von NAD^+ auf Substrate und die Generierung von ADP-Ribose-Polymeren ist an Prozessen wie Signaltransduktion, Gentranskription und DNS-Reparatur beteiligt. Letzteres wird vor allem durch ARTD1/PARP1 vermittelt, dem Gründungsmitglied der Gruppe von ADP-Ribosyltransferasen (ARTs). Die durch seine poly-ADP-Ribosylierung-Aktivität vermittelten Funktionen wurden gut untersucht. Mono-ADP-Ribosetransferase-Aktivität wurde jedoch bisher nur für bakterielle Toxine und extrazelluläre ARTs nachgewiesen. Obwohl Beweise für die intrazelluläre ADP-Ribosylierung noch fehlen, wurde kürzlich *in vitro* gezeigt, dass ARTD10 mono-ADP-Ribosetransferase-Aktivität besitzt.

Erste Versuche Einblicke in die physiologische Relevanz zu erhalten zeigten, dass das Enzym an Transformation und Proliferation beteiligt ist. Auf diesen Erkenntnissen aufbauend wurden stabile HeLa-Zelllinien generiert, die induzierbar ARTD10 oder verschiedene Konstrukte desselben herstellen. Die Expression des Wildtyp-Proteins bestätigte die früheren Beobachtungen, nach denen ARTD10 die Proliferation inhibiert. In nachfolgenden Experimenten konnte dieser Effekt auf die Induktion von Apoptose in den Zellen zurückgeführt werden. Dies war abhängig von katalytischer Aktivität, da ARTD10-G888W, eine inaktive Mutante, nicht zytotoxisch war. Zusätzlich konnte die Spaltung von ARTD10 während der Apoptose beobachtet werden, ein Effekt der auch für ARTD1 bekannt ist. Spaltung im Motiv "I A M D₄₀₆ S" führte zu einem katalytisch aktiven Fragment, welches jedoch nicht mehr in der Lage war Apoptose zu stimulieren. Analog dazu spaltete auch die inflammatorische Caspase-1 ARTD10 *in vitro* im Motiv "W T P D₅₈₁ S", ein Ergebnis welches die Spaltung von ARTD10 mit einem zweiten zellulären Caspase-regulierten Signalweg verbindet.

In beiden Fällen wird das RNA Erkennungsmotiv sowie eine Glycin-reiche Region vom katalytischen Zentrum getrennt. Der Verlust der pro-apoptotischen Aktivität durch Trennung dieser Bereiche könnte einerseits auf eine wichtige Funktion von ARTD10 in einem RRM-abhängigen Prozess, wie RNA-Prozessierung oder Transport, hindeuten oder andererseits eine Regulation von ARTD10 durch das RRM

bedeuten. Auf den Ergebnissen dieser Arbeit beruhende weitere Studien sind notwendig, um mögliche Einflüsse von ARTD10 in diese Wege zu untersuchen und tiefere Einblicke in die physiologische Rolle von ARTD10 zu ermöglichen.

3 Table of contents

1 Abstract	I
2 Zusammenfassung	II
3 Table of contents	IV
4 Introduction	1
4.1 ADP-ribosylation and relevant enzymes	1
4.1.1 Introduction	1
4.1.2 Structural features and nomenclature	2
4.1.3 PARP1/ARTD1	4
4.1.4 Binding domains and antagonists	7
4.1.5 ARTD10/PARP10	10
4.2 Apoptosis	12
4.2.1 Introduction to apoptosis	12
4.2.2 Key players in apoptosis	14
4.2.2.1 Caspases	14
4.2.2.2 BCL-2 family and IAPs	18
4.2.3 Intrinsic pathway	22
4.2.4 Extrinsic pathway	24
4.3 Inflammasome	25
5 Results & Discussion	31
5.1 ARTD10 and cell proliferation	31
5.1.1 Modell system: HeLa Flp-In T-Rex	31
5.1.2 ARTD10 influences cell growth in HeLa Flp-In T-Rex	36
5.1.3 ARTD10 induces apoptosis	41
5.2 ARTD10 is substrate of caspases	51
5.2.1 ARTD10 is cleaved by caspases during apoptosis	51
5.2.2 ARTD10 is target of caspase 1,6 and 8 <i>in vitro</i>	57
5.2.3 Definition of the caspase-6 cleavage site	62
5.2.4 Definition of the caspase-1 restriction site	65
5.3 Cleavage of ARTD10 and cell viability	68
6 Conclusions	75
7 Experimental procedures	78
7.1 Oligonucleotides	78

7.2	Plasmids.....	78
7.3	Antibodies.....	80
7.4	Work with nucleic acids.....	80
7.4.1	DNA preparation and extraction	80
7.4.2	RNA preparation, cDNA synthesis and RT-PCR.....	81
7.4.3	Molecular cloning	81
7.4.4	Agarose gel electrophoresis	81
7.4.5	Gateway cloning	81
7.4.6	Site-directed mutagenesis	82
7.5	Work with prokaryotic cells.....	82
7.5.1	Bacteria strains.....	82
7.5.2	Standard materials	82
7.5.3	Transformation	83
7.5.4	GST-purification	83
7.6	Work with eukaryotic cells (cell culture).....	84
7.6.1	Eukaryotic cell lines	84
7.6.2	Standard materials	85
7.6.3	Cell culture	85
7.6.4	Cryoconservation	85
7.6.5	Calcium phosphate transfection	86
7.6.6	Colony formation assay	86
7.6.7	Cell proliferation assays	87
7.7	Work with proteins	87
7.7.1	Cell lysis and immunoprecipitations	87
7.7.2	SDS-PAGE.....	88
7.7.3	Western Blot and Immunodetection	88
7.7.4	Coomassie staining	89
7.7.5	Tandem affinity purification	89
7.8	Enzymatic assays.....	91
7.8.1	ADP-ribosylation assay	91
7.8.2	Caspase assay	91
7.9	Immunofluorescence	92
8	References.....	93
9	Appendix.....	111
9.1.1	Abbreviations.....	111
9.2	Scientific contributions	113
9.2.1	Publications in scientific journals.....	113

9.2.2	Presentations at scientific meetings	113
9.3	Curriculum Vitae.....	114
9.4	Eidesstattliche Erklärung	115
9.5	Acknowledgements.....	116

4 Introduction

4.1 ADP-ribosylation and relevant enzymes

4.1.1 Introduction

ADP-ribosylation is a process, where ADP-Ribose (ADPr) is transferred from NAD to a substrate or to itself in an elongation reaction mechanism. The cofactor NAD is thereby hydrolyzed and the vitamin nicotinamide is released [Figure 1]. As the targets of ADP-ribosylation are proteins, it is classified as post-translational modification (PTM). Similar to ubiquitination or the well studied phosphorylation, ADP-ribosylation is involved in many cellular processes, like DNA repair, stress response, inflammation, cell division, regulation of transcription and RNA interference, with even more functions getting discovered each day (Hassa and Hottiger, 2002; Kraus, 2008; Luo and Kraus, 2012). With new information about motifs, recognition domains, new substrates and ADPr hydrolases a large cellular network of ADP-ribosylation is forming which is, although less abundant, most likely as important and complex as some other previously studied PTMs.

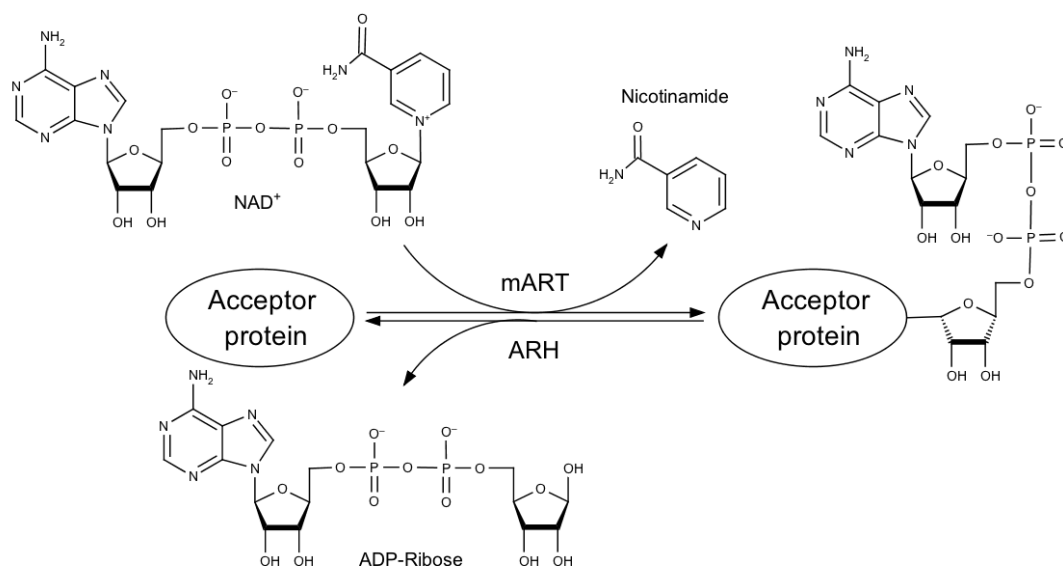


Figure 1. Schematic representation of the mono-ADP-ribosylation reaction.

The chemical structure of the mono-ADP-ribosylation reaction to an acceptor protein is shown. Mono-ADP-ribosyltransferases (mART) catalyze the addition of ADP-ribose to a substrate using nicotinamide adenine dinucleotide (NAD⁺) as cofactor, with the nicotinamide part of the molecule being released. ADP-ribosylhydrolases (ARH) remove the ADP-ribose moiety from a substrate.

ADP-ribosylation was recognized as a protein modification 50 years ago. Starting with the discovery of ADPr polymers in eukaryotic cells in 1963, the structure was solved soon after and mono-ADP-ribosylation was uncovered to be the enzymatic activity of certain bacterial toxins (Chambon et al., 1963; Gill et al., 1969; Honjo et al., 1968; Reeder et al., 1967). Over the next decades progress was made mainly in the field of poly-ADP-ribosylation. The first eukaryotic enzyme PARP was discovered, which was responsible for chromatin ADP-ribosylation upon DNA damage (Alkhatib et al., 1987; Kurosaki et al., 1987).

Mono-ADP-ribosylation in eukaryotic cells remained elusive until the end of the last century, when the so-called ecto-mARTs, mARTs located on the extracellular side of the plasma membrane, were found (Okazaki et al., 1996; Zolkiewska et al., 1992). Only recently their intracellular counterparts were identified and are now in focus of current investigations.

4.1.2 Structural features and nomenclature

ADP-ribosylation is a process, which not only exists in mammals. As mentioned earlier several bacterial toxins are classified as ADP-ribosyltransferases and a considerable number of genes encoding ADP-ribosyltransferases are found in a variety of species ranging from bacteria and fungi to plants and animals (Hottiger et al., 2010).

Despite the very different nature of these proteins, they share a common structure of their catalytic core and NAD binding region. The identification of those structures became easier with more and more catalytic domains of ARTs being crystallized with their cofactor or analogues thereof (Bell and Eisenberg, 1996). The fundamental motif of the catalytic domain is a 6-stranded β -sheet structure, which accounts for NAD-binding as well as catalytic activity. Three main motifs are responsible for these functions and are completely or partially conserved throughout all three kingdoms of life. One amino acid of each motif contributes to the formation of a catalytic triad by which ARTs can be classified. Cholera toxin-like bacterial ARTs as well as ecto-mARTs show an R-S-E motif, which is replaced by an H-Y-E motif or slight variants thereof in diphtheria toxin-like bacterial ARTs and intracellular eukaryotic ARTs.

Initially when only one intracellular mammalian enzyme was known, the reaction product gave the enzyme its name, poly-ADP-ribose polymerase (PARP). Additional enzymes were identified by *in silico* screening and numbered in ascending order (Ame et al., 2004; Otto et al., 2005). But with the growing knowledge that several of these enzymes only catalyze the addition of one ADP-ribose unit or are even inactive, a new nomenclature was proposed combining features of the catalytic activity and core structure in regard to the bacterial toxins (Hottiger et al., 2010).

The ecto-mARTs containing the catalytic R-S-E motif belong to the group of cholera toxin-like ARTs, now referred to as ARTCs. The second group comprises only of the NAD⁺-dependent tRNA 2'-phosphotransferase TpT, for which until now ADP-ribosylation activity is only postulated. The third and largest group covers the enzymes originally named PARPs. Due to the triad similarity to the bacterial toxin triad H-Y-E, they were named diphtheria toxin-like ARTs, abbreviated ARTDs. Their 17 members can be further subdivided into 2 groups according to the third amino acid in this triad, which was shown to be responsible for poly-ART activity (Marsischky et al., 1995; Rolli et al., 1997). Only in the 6 PARP1-like ARTs this glutamate is present and in addition those show also a characteristic extended loop between the β 4 and β 5 sheet, which is also found in bacterial ARTs and is thought to participate in the recognition of substrates (Sun et al., 2004). The remaining 11 enzymes, which lack the catalytic E, are currently investigated as mono-ARTs or inactive enzymes. Using a reaction mechanism called "substrate assisted catalysis" ARTD10 was the first of the ARTD family members for which mART activity was confirmed (Kleine et al., 2008).

Apart from their conserved catalytic domain the ARTDs present a great variety of structural and functional domains, like RRM, WWE, Macro, NES or ZF, which are potentially responsible for protein-protein interaction, interaction with DNA/RNA, subcellular localization and more. A list of the known human ARTDs and their characteristic features is shown in Table 1.

Table 1. The mammalian ARTD family. [adapted from (Gibson and Kraus, 2012)]

Names		Transferase*	Subclass	Size (aa)‡	Subcellular localization	Triad motif	Enzym. activity	Key functional motifs and domains
PARP	Alternative							
PARP1		ARTD1	DNA-dependent	1,014	Nuclear	H-Y-E	P/B	WGR, zinc-fingers and BRCT
PARP2		ARTD2	DNA-dependent	570	Nuclear	H-Y-E	P/B	WGR
PARP3		ARTD3	DNA-dependent	540	Nuclear	H-Y-E	<i>M</i>	WGR
PARP4	vPARP	ARTD4		1,724	Cytosolic (vault particle)	H-Y-E	<i>P</i>	BRCT
PARP5A	Tankyrase 1	ARTD5	Tankyrase	1,327	Nuclear and cytosolic	H-Y-E	P/O	Ankyrin repeat
PARP5B	Tankyrase 2 and PARP6¶	ARTD6	Tankyrase	1,166	Nuclear and cytosolic	H-Y-E	P/O	Ankyrin repeat
PARP6¶		ARTD17		322	ND	H-Y-Y	<i>M</i>	
PARP7	TIPARP and RM1	ARTD14	CCCH PARP	657	ND	H-Y-I	<i>M</i>	Zinc-fingers and WWE
PARP8		ARTD16		854	ND	H-Y-I	<i>M</i>	
PARP9	BAL1	ARTD9	macroPARP	854	ND	Q-Y-T	<i>M</i>	Macrodomain
PARP10		ARTD10		1,025	Nuclear and cytosolic	H-Y-I	M	
PARP11		ARTD11		331	ND	H-Y-I	<i>M</i>	WWE
PARP12	ZC3HDC1	ARTD12	CCCH PARP	701	Cytosolic (stress granules)	H-Y-I	<i>M</i>	Zinc-fingers and WWE
PARP13	ZC3HAV1 and ZAP1	ARTD13	CCCH PARP	902	Cytosolic (stress granules)	H-Y-V	<i>M</i>	Zinc-fingers and WWE
PARP14	BAL2 and COAST6	ARTD8	macroPARP	1,801	Cytosolic (stress granules)	H-Y-L	M	Macrodomain and WWE
PARP15	BAL3	ARTD7	macroPARP	444	Cytosolic (stress granules)	H-Y-L	<i>M</i>	Macrodomain
PARP16		ARTD15		630	ND	H-Y-I	<i>M</i>	

aa, amino acid; ARTD, ADP-ribosyltransferase; BAL, B-aggressive lymphoma protein; COAST6, collaborator of signal transducer and activator of transcription 6; ND, not determined; PARP, poly(ADP-ribose) polymerase; vPARP, vault PARP; ZAP1, zinc-finger antiviral protein 1; ZC3HAV1, zinc-finger CCCH-type antiviral protein 1; ZC3HDC1, zinc-finger CCCH domain-containing protein 1. *Based on the recently suggested revised nomenclature (Hottiger et al., 2010). ‡Number of amino acids of the human protein. §**Known** or *predicted* enzymatic activity: mono- (*M*), oligo- (*O*) or poly(ADP-ribosyl)ation (*P*), or branching (*B*). ||All PARP family members contain a PARP domain. ¶PARP6, which refers to two different proteins, is an example of the degeneracy of the PARP nomenclature in the existing literature.

4.1.3 PARP1/ARTD1

ARTD1/PARP1 is the founding member of the human intracellular ARTD family. Being responsible for approximately 85% of the cells poly-ADP-ribosylation activity it is also the most prominent enzyme (Shieh et al., 1998). It is a nuclear protein of 116 kD that is characterized mainly by 3 domains [Figure 2]. The N-terminal DNA-binding domain contains 3 zinc fingers of which 1 and 2 are responsible for ssDNA break recognition (Ikejima et al., 1990). The recently identified third zinc finger, which is separated from the first two by a nuclear localization sequence (NLS), is important

for the activation of the enzyme (Langelier et al., 2008). In addition to its obvious function the automodification domain in the center of the protein mediates protein-protein interactions with DNA repair enzymes through the BRCT (BRCA1 C-terminus) fold. The third domain at the C-terminus contains the conserved ADP-ribosyltransferase domain with the catalytic H-Y-E motif and is therefore responsible for the catalytic function of the protein.

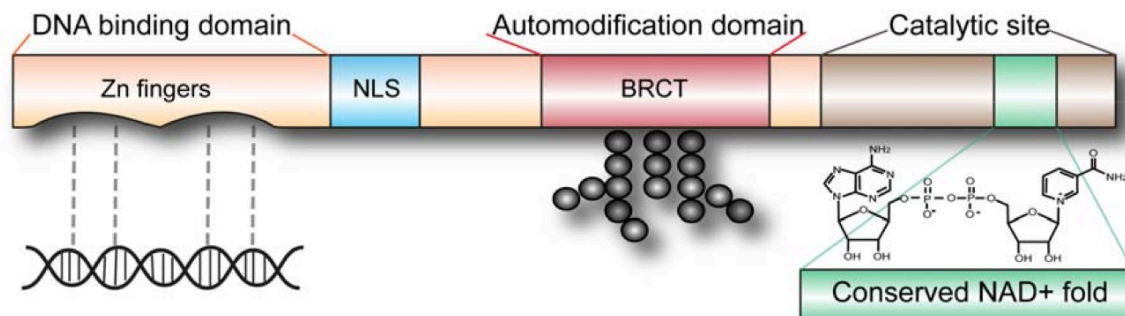


Figure 2. ARTD1, the bona-fide poly-APDr transferase [adapted from (David et al., 2009)].

ARTD1, formerly PARP1, is the founding member of the ADPr-transferase superfamily. The schematic picture shows the domain organization of this multifunctional protein. At the N-terminus it contains two functional zinc-fingers that cooperate in DNA binding, followed by an NLS, the domain responsible for the nuclear localization of ARTD1. The protein center is characterized by a BRCT fold that mediates protein-protein binding and in addition serves as target for extensive automodification. The catalytic domain common to all family members is the catalytic active part of the protein and is localized at the far C-terminus. NLS, nuclear localization signal; BRCT, BRCA1 C-terminus.

ARTD1 is best known for its function in the base excision pathway during DNA damage repair. As mentioned above it senses single strand breaks through the N-terminal zinc fingers, which activates the enzyme. But also other DNA structures like hairpins, cruciform DNA and unusual loops are recognized (Lonskaya et al., 2005). Binding of the zinc fingers leads to a conformational change in the protein and subsequently to its activation, followed by extensive automodification as well as modification of histones H1 and H2B (Langelier et al., 2012; Poirier et al., 1982). This occurs in combination with PARP2/ARTD2, which not only heterodimerizes with ARTD1 and shares different binding partners, but also seems to compensate for some ARTD1 functions, as ARTD1/2 knockouts are embryonically lethal compared to the single knockouts (Menissier de Murcia et al., 2003; Schreiber et al., 2002). The synthesized PAR chains have a length of up to 200 ADP-ribose units and can be branched every 20-50 units (Kiehlbauch et al., 1993). The elongation occurs through an $\alpha(1-2)$ -O-glycosidic bond between the nicotinamide proximal ribose and the

adenine proximal ribose of the growing poly-ADPr (PAR) chain. In a branching reaction the nicotinamide proximal ribose of the PAR chain is likewise used as an acceptor. The extensive ADP-ribosylation has two effects. On one hand it results in decondensation of chromatin as the PAR chains displace histones (Poirier et al., 1982; Zahrada and Ebisuzaki, 1982). On the other hand the PAR chains function as binding platform for DNA repair enzymes, like XRCC1, which thereby accumulate at the site of DNA damage (Masson et al., 1998). The growing number of negative charges added to ARTD1 itself through automodification leads to an electrostatic repulsion from the DNA and subsequent loss of activity. This is followed by a degradation of the PAR chains through PAR hydrolyzing enzymes like PARG (poly-ADP-ribose glycohydrolase) (D'Amours et al., 1999; Zahrada and Ebisuzaki, 1982). Apart from this well-known function in DNA repair, ARTD1 is also involved in inflammation and apoptosis, findings that were made using ARTD1 knockout mice or the *in vivo* application of inhibitors (Altmeyer et al., 2010; Liaudet et al., 2002). In inflammatory diseases it is implicated in pathogen associated as well as in noninfectious inflammation, for example in the ischemia reperfusion model or allergy-associated inflammation (Ba et al., 2010; Oumouna et al., 2006; Thiernemann et al., 1997). Studies indicate that ARTD1 influences inflammation at different levels. Analogue to the function during base excision repair, extensive PAR chains can relax the chromatin and lead to a different gene expression pattern. Other groups reported, that ARTD1 regulates the inflammatory response by modifying key enzymes in signaling cascades involved in inflammation, like RELA/p65, a subunit of the NF- κ B signaling pathway. PARylated p65 cannot bind to the nuclear export factor Crm1 and is thereby retained in the nucleus, leading to prolonged signal transduction (Zerfaoui et al., 2010). In addition inactive ARTD1 also binds directly to promoters, prevents NF- κ B from binding and thereby inhibits transcription, like it is the case for the C-X-C-motif chemokine ligand 1 gene. When stimulated, the PARylation of ARTD1 leads to its dissociation from the promoter and the subsequent activation of the gene (Amiri et al., 2006).

A field of investigation, which is related to inflammation, is ARTD1's implication in cell death. Active promotion of cell death takes place in situations with extensive amounts of DNA damage or oxidative stress. From the point of hyperactivation of ARTD1 the rapid degradation and resynthesis of PAR chains can lead to NAD and subsequently ATP depletion, which results in a necrotic cell death called parthanatos (Andrabi et

al., 2008). Another path leads the cell into regulated breakdown and apoptosis, which is nonetheless caspase independent (Yu et al., 2002). The key component of this mechanism is the apoptosis-inducing factor (AIF), an oxidoreductase, which resides in the mitochondrial intermembrane space (IMS) (Otera et al., 2005). Due to the strong activation of ARTD1 in combination with the also endoglycosidic activity of PARG, PAR chains are formed and translocate throughout the cell. At mitochondria those PAR chains lead to the conversion of membrane bound to free AIF and its subsequent release. However the exact mechanism by which the PAR chains function is not clear yet (Yu et al., 2006). When released AIF travels to the nucleus, where it stimulates chromatin condensation and further promotes cell death which shows hallmarks of apoptosis, like phosphatidylserine exposure and mitochondrial membrane depolarization, but is caspase independent (Susin et al., 1999).

Apart from these active implications in cell death, ARTD1 is also targeted by caspases as well as granzymes during normal apoptotic events (Lazebnik et al., 1994; Tewari et al., 1995; Zhu et al., 2009). ARTD1 is cleaved at D₂₁₄ by caspase-3, an apoptotic executioner caspases, as well as by the inflammatory caspases 1 and 7 (Malireddi et al., 2010; Zhu et al., 2009). The protein is thereby inactivated and fragments can even exhibit a dominant negative effect. The hypothesis is that in cases where the damage to the cell is too severe, the repair pathways are inactivated to spare remaining energy for the ordered breakdown. The analysis of ARTD1 fragmentation is commonly used as evidence for apoptosis, i.e. the activation of caspases.

4.1.4 Binding domains and antagonists

ADP-ribose modifications, introduced in the preceding chapters, are involved in a variety of processes through regulation of intermolecular interaction, scaffolding and connection to other posttranslational mechanisms. The resulting influence on a cell has to be tightly controlled, to prevent errors, malfunction and overreaction; incidents that would otherwise lead to disturbed cell function or even cell death. Not long after the discovery of ARTD1, PARG was identified, an enzyme capable of hydrolyzing PAR chains (Miwa et al., 1974). It cleaves both at the end and inside the polymers, but with prevalence to endohydrolyzation resulting in the production of mono-ADP-ribose as well as oligomers and is therefore important for the normal turnover and

metabolism of ADPr (Davidovic et al., 2001; Kim et al., 2005). On the other hand PARG is also involved in ARTD1 related cell death, as it facilitates the extensive NAD consumption of ARTD1 in parthanatos and produces ADP-ribose oligomers, which mediate AIF translocation to the nucleus (Andrabi et al., 2008; Yu et al., 2006). The pivotal role of PARG in cellular processes and ADP-ribosylation homeostasis is strengthened by findings obtained from knockout experiments. Mice depleted of PARG die at embryonic day 3.5 and murine embryo fibroblasts (MEFs) that lack PARG accumulate PAR and show a strongly increased sensitivity to DNA damage (Koh et al., 2004). With findings in the early 90s a second class of enzymes came into play. The ADP-ribose glycohydrolase ARH was found to reverse mono-ADP-ribose modifications on arginine, an enzymatic activity that was not seen with PARG (Moss et al., 1992; Takada et al., 1993). *In silico* screening revealed two additional members of the ARH family (Glowacki et al., 2002). ARH2 does not possess catalytic activity, but ARH3 was shown to have PARG-like activity, hydrolyzing PAR but not mADPr (Oka et al., 2006). Except for indications that ARH3 is involved in PAR degradation at mitochondria, little is known of its *in vivo* functions (Niere et al., 2012). The same is true for the third class of proteins with ADP-ribosylhydrolase activity. The NUDIX class of enzymes contains 24 human genes and catalyzes the cleavage of the pyrophosphate in nucleoside-diphosphate-containing molecules, which includes PAR chains (McLennan, 2006). NUDIX proteins were early on defined as housecleaning enzymes as they play a role in the recycling of metabolites and reaction intermediates, but their role in opposing ADP-ribosylation has to be clarified (Bessman et al., 1996).

Apart from the interplay between ARTs and hydrolases the process of recognizing and binding of ADPr has become a research focus in the last decade. Much like other posttranslational modifications of proteins, ADP-ribosylation also has its binding domains integrating it in recognition and signaling processes. The first domain to bind PAR was described in 2000, a 20 amino acid consensus sequence containing a basic-residue rich cluster and a hydrophobic part containing single basic amino acids (Pleschke et al., 2000). Several DNA damage checkpoint proteins were revealed that contained this PAR-binding motif (PBM). A more recent *in silico* screen broadened the range of proteins containing a PBM to proteins mostly involved in DNA damage repair, chromatin remodeling and RNA processing (Gagne et al., 2008). Among PBM

proteins are known PAR binders like XRCC1 and DNA ligase III as well as AIF, the factor involved in ARTD1 induced cell death (Wang et al., 2011). The PBM, as the name states, is rather a motif that can be interspersed in other domains than a structural domain itself. Therefore it is likely that it controls the functionality of those domains that contain such a motif due to the potential interaction with PAR (Kalisch et al., 2012). The first protein structure to bind ADPr, the so-called macrodomain, was initially recognized in the early 90s in the core histone macroH2A1.1, without knowing its function (Pehrson and Fried, 1992). Later on a study focusing on the protein Af1521 from *Archaeoglobus fulgidus* proved that its macrodomain as well as macrodomains from macroH2A1.1 and other proteins bind ADPr (Karras et al., 2005). The structure of specific macrodomains revealed that these domains bind ADPr in PAR chains. Thus macrodomains are interaction partners of poly-ADPr and possibly of mono-ADP-ribosylated substrates (Timinszky et al., 2009). In humans 11 proteins are predicted to contain a macrodomain, a 130-190 amino acid residue motif, either as single domain or up to a triple repeat (Kalisch et al., 2012). The implication in the recruitment of factors to sites of DNA damage is currently best understood. For example the former mentioned macroH2A1.1 as well as the helicase ALC1 bind to PAR upon ARTD1 activation and remodel the chromatin, resulting in facilitation of DNA repair (Ahel et al., 2009; Timinszky et al., 2009). Two additional PAR-binding domains are the PAR-binding zinc fingers (PBZ) and the WWE domain. PBZs were only found in 3 proteins where they are essential for the binding within PAR molecules. The interstrand crosslink repair protein SNM1 contains only one PBZ whereas the two DNA damage response proteins APLF and CHFR contain a cooperative tandem repeat, which was shown to increase binding affinity (Ahel et al., 2008; Li et al., 2010). The mitotic checkpoint protein CHFR is linking two posttranslational modifications, as it contains a RING domain and is able to ubiquitinate ARTD1 upon mitotic stress and also upon ARTD1 activation, leading to its degradation (Kashima et al., 2012). WWE domains were likewise recognized in molecules involved in ubiquitination and ADP-ribosylation by sequence profiling (Aravind, 2001). Three groups published independently that the WWE containing E3 ligase RNF146 binds to PAR (Andrabi et al., 2011; Kang et al., 2011; Zhang et al., 2011). Upon interaction with bound or free PAR RNF143 polyubiquitinates itself, automodified ARTD1, and other DNA repair factors, thereby targeting the substrates for proteasomal degradation (Kang et al.,

2011). In contrast to the macro domain, the WWE domain recognizes the internal iso-ADPr rendering it specific for PAR (Wang et al., 2012).

4.1.5 ARTD10/PARP10

ARTD10, the former PARP10, is a mammalian mono-ART. The putative protein was found through *in silico* screening together with other members of the former mentioned seventeen PARP family members (Ame et al., 2004). Evidence for the actual mRNA/protein was found and the protein was further characterized. Its gene is located to chromosome 8q24.3 in a head-to-tail fashion with the plectin 1 gene (Lesniewicz et al., 2005; Yu et al., 2005). The gene consists of 11 exons and has a length of more than 9.3 kb. It is transcribed as a 3.4 kb mRNA which encodes for 1025 amino acids of human ARTD10. Although the calculated molecular mass is 110 kD, the protein has an apparent mass in SDS-PAGE of 150 kD. Until now no isoforms through alternative start codons or splice variants are described.

As mentioned in the introductory chapter to the ART family ARTD10 is a confirmed mono-ART. The catalytic glutamate in the H-Y-E triad, which is required for elongation in ARTD1, is exchanged for an isoleucine thereby abolishing polymerization reactions (Kleine et al., 2008; Marsischky et al., 1995). The transfer of the single ADP-ribose unit is mediated through a reaction called substrate assisted catalysis, wherein the target glutamate of the receptor protein is replacing the absent glutamate in the active center of the protein. As the modified amino acid is afterwards not available for another round of catalysis, the reaction stops. Despite this straightforward mechanism, it is still discussed if glutamates are the target amino acids.

The main research focus at the moment is directed towards the targets of ARTD10 to elucidate its cellular functions. Beside itself ARTD10 also modifies all four core histones, which are currently the only published substrates. ProtoArrays with more than 8000 proteins spotted are currently used to provide further insight into ARTD10 targets (Feijs et al. submitted). The detection of ADP-ribosylation within these arrays is realized through biotinylated NAD and the subsequent application of fluorescently labeled avidin, as there are no antibodies available to identify mono-ADP-ribosylation.

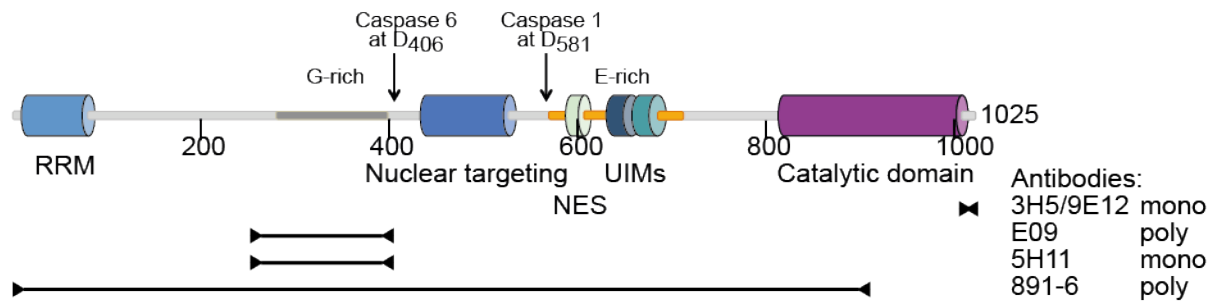


Figure 3. Domain structure of ARTD10.

ARTD10 protein composition is schematically shown together with the amino acid count. The RRM was found *in silico* with no available *in vitro* data yet. Caspase restriction sites mapped in this thesis at D₄₀₆ by caspase-6 and at D₅₈₁ by caspase-1 are indicated. The total length of the protein is 1025 amino acids. Names and binding regions of mono- and polyclonal antibodies are shown. RRM, RNA recognition motif; G-rich, glycine-rich region; Nuclear targeting, sequence responsible for nuclear import; NES, nuclear export sequence; E-rich, glutamate-rich region; UIM, ubiquitin interacting motif.

ARTD10's domain structure, with the exception of its catalytic domain at the C-terminus, is rather unique within the ARTD group [Figure 3]. At the N-terminus ARTD10 has a putative RRM (11-85) followed by a glycine rich region, a combination which is also present in other RNA binding proteins (Burd and Dreyfuss, 1994). In a further C-terminal glutamate rich region (588-697) (which is also responsible for the aberrant mobility on SDS-PAGE) one can find a nuclear export sequence (NES) as well as two functional ubiquitin interaction motifs (UIMs). Studies with Leptomycin B, a potent inhibitor of the nuclear export protein Crm1, revealed that the NES is functional. A nuclear targeting region was mapped to amino acids 435-528 and extensive live cell imaging experiments showed that ARTD10 shuttles between the nucleus and cytoplasm (Kleine et al., 2012). Moreover ARTD10 localizes to distinct cytoplasmic foci, which in part colocalize with the ubiquitin adapter molecule p62.

The regulation of ARTD10 proves to be rather complex as it is, like most other ART family members, a target of ubiquitination, phosphorylation, acetylation and also ADP-ribosylation. Yet despite the evidence that those modifications exist, little is known about their function and implication in the physiological role of ARTD10.

As ARTD10 was discovered in a screen for interaction partners of MYC, binding to MYC and influence on MYC's cellular functions was investigated. The interaction interface was mapped to amino acids 700-907, a region stretching into the catalytic domain of ARTD10. The same study revealed, that expression of ARTD10 inhibited MYC/HA-RAS-dependent transformation of rat embryo fibroblasts. This effect was

independent of ART activity, but was abolished when nuclear export was repressed by mutations in the NES. A similar effect was observed in 3T3-L1 murine fibroblasts, where the cells were unable to progress into S-phase when ARTD10 was overexpressed. Although these findings strongly suggested an overall implication of ARTD10 in cell growth or cell cycle control, overexpression in other cell lines, like HEK293 and U2OS, did not reduce cell numbers (Yu et al., 2005).

4.2 Apoptosis

4.2.1 Introduction to apoptosis

Apoptosis is a regulated form of cell death in which the cell is actively broken down in apoptotic bodies, which subsequently can be phagocytized. The phenotype was originally observed and described by three scientists at the University of Aberdeen in the early 70s. In their publication in 1972 they proposed the term apoptosis, which originates from a Greek word describing “leaves falling of a tree” (Kerr et al., 1972). Apoptosis is important for ordered cell homeostasis in healthy tissues and during development, not only in the model organism *Caenorhabditis elegans*, but also for example in the differentiation of fingers and toes. Nowadays many more physiological processes are known, which are influenced by apoptosis. Defects in apoptosis pathways are implicated in the development of diseases, including cancer (Elmore, 2007; Lowe and Lin, 2000).

The classic phenotype of apoptosis is characterized by shrinkage of the cell and nucleus (pyknosis), chromatin condensation and nuclear fragmentation (karyorrhexis), the so-called membrane-blebbing and finally the formation of apoptotic bodies. These morphologic changes were defined as the hallmarks of apoptosis, which were used to discriminate this process from the other two main forms of cells death: necrosis and autophagy. But as more and more intermediate forms of cell death became apparent, the focus shifted towards characterizing cell death forms by biochemical features rather than by the classic organization into the three groups mentioned above (Kroemer et al., 2009). In agreement with this, Table 2 shows an overview of biochemical processes involved in apoptosis and standard methods of detection.

Table 2. Biochemical features and detection methods of apoptosis [adapted from (Kroemer et al., 2009)].

Biochemical feature	Methods for detection
Activation of caspases	Colorimetric/fluorogenic substrate-based assays in live cells
	Colorimetric/fluorogenic substrate-based assays of lysates in microtiter plates
	FACS/IF microscopy quantification with antibodies specifically recognizing the active form of caspases
	FACS/IF microscopy quantification with antibodies specific for cleaved caspase substrates
	FACS/IF microscopy quantification with fluorogenic substrates
	Immunoblotting assessment of caspase-activation state
	Immunoblotting assessment of the cleavage of caspase products (e.g. ARTD1)
$\Delta\Psi_m$ dissipation	Calcein-cobalt technique (FACS/IF microscopy)
	FACS/IF microscopy quantification with $\Delta\Psi_m$ -sensitive probes
	Oxygen-consumption studies (polarography)
MMP	Colorimetric techniques to assess the accessibility of exogenous substrates to IM-embedded enzymatic activities
	FACS-assisted detection of IMS proteins upon plasma membrane permeabilization
	FACS-assisted detection of physical parameters of purified mitochondria
	HPLC-assisted quantification of mitochondrial alterations in purified mitochondria
	IF microscopy colocalization studies of IMS proteins (e.g., Cyt c) with sessile mitochondrial proteins (e.g., VDAC1)
	IF (video) microscopy with Cyt c-GFP fusion protein
	Immunoblotting detection of IMS proteins (e.g., Cyt c) upon cellular fractionation
Oligonucleosomal DNA fragmentation	DNA ladders
	FACS quantification of hypodiploid cells (sub-G1 peak)
	TUNEL assays
Activation of proapoptotic Bcl-2 family proteins	IF microscopy localization studies
	Immunoblotting with conformation-specific antibodies
Plasma membrane rupture	Colorimetric/fluorogenic substrate-based assays of culture supernatants in microtiter plates to determine the release of cytosolic enzymatic activities (e.g., LDH)
	FACS quantification with vital dyes
PS exposure	FACS quantification of Annexin V binding
ROS overgeneration	FACS/IF microscopy quantification with ROS-sensitive probes
ssDNA accumulation	FACS quantification with ssDNA-specific antibodies

Abbreviations: $\Delta\Psi_m$, mitochondrial transmembrane permeabilization; Cyt c, cytochrome c; FACS, fluorescence-activated cell sorting; GFP, green fluorescent protein; HPLC, high-pressure liquid chromatography; IF, immunofluorescence; IM, mitochondrial inner membrane; IMS, mitochondrial intermembrane space; LDH, lactate dehydrogenase; MMP, mitochondrial membrane permeabilization; PS, phosphatidylserine; ROS, reactive oxygen species; TUNEL, terminal deoxynucleotidyl transferase-mediated dUTP nick-end labeling; VDAC1, voltage-dependent anion channel 1.

The implication of apoptotic proteins, caspases and mitochondria as well as pathways that lead to apoptosis will be introduced in the next chapters.

4.2.2 Key players in apoptosis

4.2.2.1 Caspases

Caspases are a family of proteases, which are involved in a huge variety of cellular processes, but are best known for their function in cellular apoptosis. The name 'caspase' is an abbreviation of *cysteine-dependent aspartate-directed proteases*, describing their catalytic functionality. The founding member caspase-1 was originally named ICE (IL-1 β converting enzyme), as it is required for the maturation of this cytokine (Thornberry et al., 1992). The connection to apoptosis was made when a homology to ced-3 (cell death protein-3) was discovered, a key component in the regulated cell death during *Caenorhabditis elegans* maturation (Yuan et al., 1993). As the family of ICE/ced-3 related proteins grew the nomenclature was unified in 1996 and in humans it consists of 11 proteins (Alnemri et al., 1996; Fan et al., 2005). In regard to their structure and function these 11 proteases can be further subdivided into three groups [Table 3]. The so-called initiator caspases are characterized by their N-terminal protein-protein interaction domain, by which they are clustered upon apoptosis stimulation. They are the first to be activated and in turn cleave in a process called caspase cascade the effector caspases. The latter only have a very short N-terminal domain and are the proteases responsible for most of the apoptotic phenotype, as they cleave a large number of different cellular proteins (Taylor et al., 2008). The third group of caspases encompasses the inflammatory caspases. These proteases are not involved in apoptosis at all, but rather function in inflammatory processes.

Table 3. The human caspase family.

Subfamily	Role	Members	Domains	P4 \rightarrow P1 *
I	Initiator caspases	Caspase-2	CARD	DEHD
		Caspase-8	DED	LETD
		Caspase-9	CARD	LEHD
		Caspase-10	DED	
II	Executioner caspases	Caspase-3		DEVD
		Caspase-6		VEHD
		Caspase-7		DEVD
III	Inflammatory caspases	Caspase-1	CARD	IEPD
		Caspase-4	CARD	WEHD
		Caspase-5	CARD	WEHD
	Mediator of keratinocyte differentiation (Denecker et al., 2008)	Caspase-14		

DED, death effector domain; CARD, caspase-recruitment domain; *amino acid consensus recognition motif (Thornberry et al., 1997)

All caspases are produced as inactive zymogens or pro-caspases. Activation occurs as mentioned above through oligomerization and subsequent reciprocal cleavage or cleavage by other members of the caspase family. Apart from the N-terminal pro-domain the structure of the caspases is similar throughout the family. Two domains separated by a small linker sequence will later on form the large (p20) and small (p10) subunit of the active caspase [Figure 4]. When the zymogen is processed the resulting p20 and p10 fragments form a heterodimer, which again combined with another dimer forms the active hetero-tetramer (Fuentes-Prior and Salvesen, 2004). The catalytic center of the caspases is located in the p20 subunit and features a highly conserved 'QACXG' motif (where X can be R, Q or D) with a cysteine in the middle, which is crucial for catalytic activity (hence their name) (Fan et al., 2005).

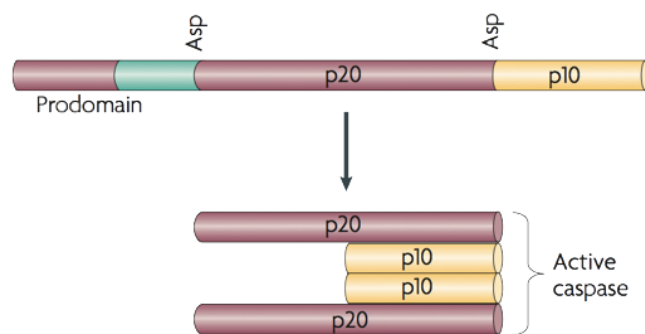


Figure 4. Structural changes during caspase activation [adapted from (Clarke and Tyler, 2009)].

The domain structures of an inactive and active caspase are depicted. During maturation caspases are cleaved at two aspartic acids, resulting in the removal of the pro-domain and the separation of the large (p20) and small (p10) catalytic subunit. Subsequently two p20 subunits containing the catalytically essential 'QACXG' motif (X being R, Q or D) bind two p10 units to form the active hetero-tetrameric caspase.

The substrate specificity is different in every caspase, although cleavage of many substrates is redundant [Table 3]. As caspases are proteases their cleavage sites were analyzed using the standard nomenclature from Schechter and Berger (Schechter and Berger, 1967). The amino acids surrounding the cleavage site are named and counted N-terminally P1, P2, P3 etc. whereas the C-terminal amino acids are marked with an apostrophe (P1') [Figure 5].

Although various exceptions complicate the identification of precise consensus sequences for target motifs of each caspase, all caspases prefer a glutamate at P3 and the aspartate at P1, which led to their name (Thornberry et al., 1997; Timmer and Salvesen, 2007). Although the specific binding groove of caspases prefers an

aspartate at P1 to a glutamate with up to 4 magnitudes higher specificity, there are exceptions reported where substrates are cleaved following a glutamate (Krippner-Heidenreich et al., 2001; Stennicke et al., 2000). Positions P4, P2 and P1' are also important and differ for each caspase (Talanian et al., 1997). At position P1' for example charged or bulky amino acids are known to inhibit restriction, whereas smaller amino acids seem not to interfere (Stennicke et al., 2000). More recent approaches even take the amino acid range from P10 to P10' into account to specify caspase restriction sites. (Shen et al., 2010). Commercial substrate peptides and inhibitors for caspases are available, which claim to target specifically each caspase.

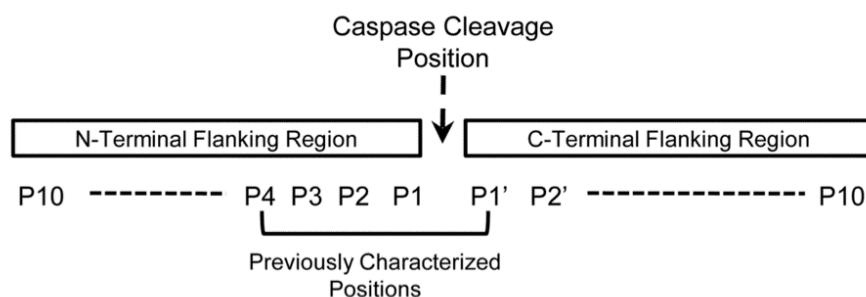


Figure 5. Nomenclature of the amino acid positions of caspase cleavage sites [adapted from (Shen et al., 2010)].

The cleavage site nomenclature, originally developed by Schechter and Berger (Schechter and Berger, 1967), and the extended version are used to define and communicate the amino acid prevalence of different caspases. Amino acid frequencies in known caspase cleavage sites can be integrated in algorithms to predict and determine new sites.

As mentioned earlier caspases are the key components in apoptosis by cleaving a variety of cellular proteins, which finally leads to the apoptotic phenotype (Martin and Green, 1995). Until now several hundred caspase substrates have been identified and many of those show either a gain- or a loss-of-function phenotype upon proteolytic processing, but the functional relevance of the cleavage remains unknown for most of the targets (Luthi and Martin, 2007; Taylor et al., 2008; Timmer and Salvesen, 2007). Nonetheless there is strong believe that most of them are targeted on purpose as a lot of caspase sites separate domain-containing parts of proteins and a great part of generated fragments are very stable (Johnson and Kornbluth, 2008).

There are several substrates, for which the function of proteolysis by caspases is understood in more detail. Lamins are targeted by caspase-6 and their breakdown

contributes to the condensation of chromatin and the subsequent breakdown of the nuclear envelope (Cowling and Downward, 2002; Takahashi et al., 1996). The decomposition of the cytoskeleton on the other hand is mediated by the cleavage of actin and fodrin (Janicke et al., 1998; Mashima et al., 1999). Two substrates and examples for the loss-of-function category are ARTD1 and ICAD, which are involved in the degradation of the DNA. ARTD1 as mentioned above is inactivated in its function as DNA repair enzyme by the processing through caspase-3 (Lazebnik et al., 1994). ICAD is under normal physiological conditions the inhibitor of the endonuclease CAD (caspase-activated DNase). Upon cleavage by caspase-3 its binding capabilities are lost and active CAD translocates to the nucleus and cleaves the DNA in oligonucleosomal fragments (Liu et al., 1999; Sakahira et al., 1998). This finally leads to chromatin condensation and formation of apoptotic bodies, as the absence of CAD results in defects in those processes (Liu et al., 1997).

Phosphatidylserine is a phospholipid normally found on the inner leaflet of the plasma membrane, where it is kept by a translocase (Verhoven et al., 1995). Its presentation on the outer membrane side during apoptosis is one of the early phenotypes in apoptosis. Although the exact mechanism controlling the externalization is unknown, it is at least partially caspase dependent (Ferraro-Peyret et al., 2002; Huigsloot et al., 2001). Its presentation to the surrounding cells is a key step in the prevention of inflammation due to secondary necrosis, as it stimulates macrophages to engulf the apoptotic cell and apoptotic bodies that are formed (Verhoven et al., 1995). The receptors T cell immunoglobulin mucin (TIM) proteins 1 and 4 are responsible for PS binding and promote the signal in macrophages and dendritic cells (Santiago et al., 2007). In addition to this “eat-me” signal, other molecules on living cells, like CD31 or CD46, have the opposing effect and prevent phagocytosis (Brown et al., 2002; Elward et al., 2005). Figure 6 summarizes the apoptotic targets and their effect on cellular morphology.

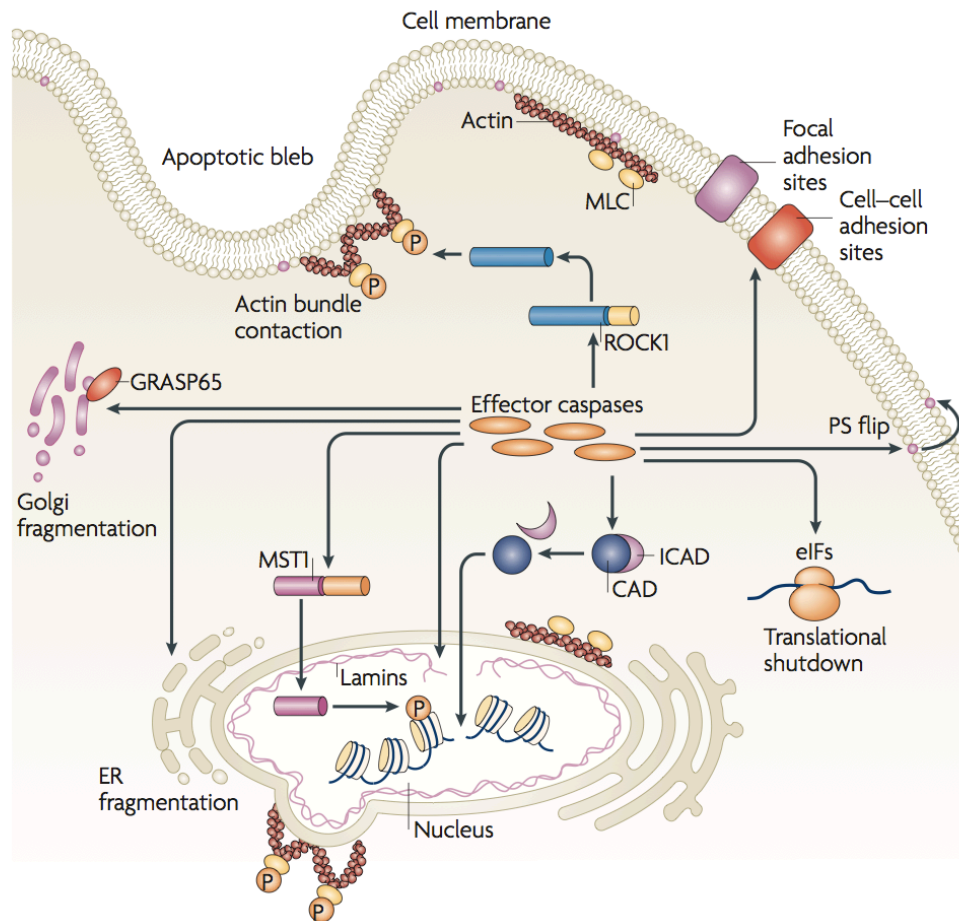


Figure 6. Caspase mediated degradation of cellular integrity [adapted from (Taylor et al., 2008)].

The apoptotic phenotype of a cell is mediated by the activity of the effector caspases, which cleave a variety of proteins leading finally to the ordered cellular breakdown. Nuclear decomposition is promoted by cleavage of the DNA through CAD, phosphorylation and condensation of the chromatin by MST1 and nuclear envelope fragmentation due to the cleavage of lamins. ROCK1 and GRASP65 processing promotes GOLGI fragmentation and dissolves actin bundles, resulting in membrane destabilization. Also processes like cell-cell detachment, the exposure of phagocytic signals as well as the shutdown of translation due to cleavage of eIFs are effects of the proteolytic capabilities of caspases. CAD, caspase-activated DNase; ICAD, inhibitor of caspase-activated DNase; MST1, mammalian STE20-like protein kinase 1; ROCK1, Rho-associated protein kinase 1; GRASP65, Golgi reassembly-stacking protein 1; eIFs, eukaryotic initiation factor; ER, endoplasmic reticulum; MLC, myosin light chain; PS, phosphatidyl serine.

4.2.2.2 BCL-2 family and IAPs

The initiated caspase cascade in apoptosis is a powerful process that is not reversible and therefore has to be tightly controlled. Two families of proteins contribute to this matter, the BCL-2 and IAP family, their founding members being discovered in the early 90s (Crook et al., 1993; Vaux et al., 1992). The connection to apoptosis was again made in *Caenorhabditis elegans*, where the single BCL-2 homolog ced-9 was found together with the caspase homolog ced-3 (Hengartner and Horvitz, 1994). The B-cell lymphoma protein 2 family grew rapidly. Their members

are characterized by four B-cell homology (BH) domains, with BH3 as the only domain that is present in all members (Yin et al., 1994). According to the number of BH domains the family can be further subdivided into 3 groups. Members containing all four known domains, among those BCL-2 itself, are anti-apoptotic. The BH domains 1-3 as well as an additional transmembrane domain characterize the second group. Together with the last group, the BH3-only proteins, they are promoters of apoptosis [Figure 7].

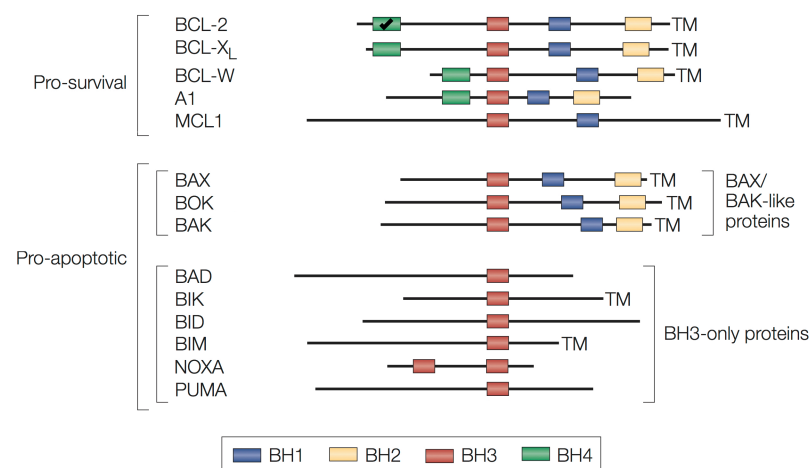


Figure 7. Classification of the mammalian BCL-2 family members [adapted from (Strasser, 2005)].

BCL-2 family members are essential for the regulation of apoptosis. They can be subdivided by a combination of functional as well as structural features. Members containing all four BH domains are anti-apoptotic. The remaining pro-apoptotic proteins contain the BAX/BAK-like proteins, involved in mitochondrial membrane permeabilization, and the BH3-only proteins. The latter is the largest group and functions as intermediate between stress signals and apoptosis induction. Homology searches revealed additional family members, who are not listed here, as a requirement or involvement in apoptosis induction or prevention has yet to be shown. BCL-2, B-cell lymphoma 2; BAX, BCL-2-associated X protein; BAK, BCL-2-antagonist/killer; BAD, BCL-2-antagonist of cell death; BIK, BCL-2-interacting killer; BID, BH3-interacting domain death antagonist; BIM, BCL-2-interacting mediator of cell death; PUMA, p53-upregulated modulator of apoptosis.

The BH1-3 group of proteins is key to induction of mitochondria-dependent apoptosis by controlling their outer membrane permeability (Martinou and Green, 2001). As mentioned above they all contain the BH1-3 as well as a hydrophobic transmembrane (TM) domain. BAK (BCL-2 antagonist killer) is localized in the outer membrane of mitochondria, whereas the TM domain of BAX (BCL-2-associated protein X) is hidden inside the protein, leading to its cytosolic localization (Suzuki et al., 2000). Both are essential for apoptosis in response to several death stimuli and in normal tissue development (Lindsten et al., 2000; Wei et al., 2001). The precise initiation of outer membrane permeabilization by BAX/BAK however is not well understood. The 3D structure of BAX revealed α -helices similar to pore forming

bacterial toxins and the translocation domain of diphtheria toxin (Suzuki et al., 2000). Interestingly this structure is also conserved in anti-apoptotic family members, like BCL-2 and BCL-X_L (Muchmore et al., 1996). The deletion or exchange of the specific α -helix in those proteins *in vitro* or by caspases completely changes their function to promotion of apoptosis (Cheng et al., 1997; George et al., 2007).

The current understanding of the activation of BAX is that upon certain apoptotic stimuli, be it stress signals or toxic agents, its conformation is changed leading to the exposure of its transmembrane domain and the subsequent insertion into the mitochondrial outer membrane (Nechushtan et al., 1999). Especially BH3-only proteins are believed to influence this structural modification of BAX, which is strengthened by experiments with BH3 peptides derived of BIM and BID or tBID directly (Desagher et al., 1999; Gavathiotis et al., 2008; Walensky et al., 2006). Following insertion BAX oligomerizes with BAK and itself to form pores in the outer mitochondrial membrane leading to the efflux of apoptosis promoting proteins like cytochrome C or SMAC/DIABLO (Kroemer et al., 2007; Vaux, 2011). This process is again strongly promoted by the BH3-only proteins BID/BIM (Eskes et al., 2000; Kuwana et al., 2002). Opposing the BH1-3 proteins, the anti-apoptotic BCL-2 like proteins inhibit pore formation by binding to BAX/BAK [Figure 7] (Cheng et al., 2001). They contain all four known BH domains and a transmembrane domain, which leads to a localization at mitochondria, the nucleus and the endoplasmatic reticulum (Reed, 2006).

Most proteins containing multiple BH domains seem to interact with members of the BH3-only group (Cheng et al., 2001). With until now 18 discovered genes in humans this group is the largest in the BCL-2 family (Reed et al., 2004). They function as regulators and transmitters of apoptotic signals, by inhibiting anti-apoptotic proteins or in the case of BIM/BID by stimulating the pro-apoptotic proteins BAX/BAK (Lomonosova and Chinnadurai, 2008). They are therefore classified as “sensitizers” or direct “activators” (Martinou and Youle, 2011). The BH3-proteins themselves are activated and controlled by different mechanisms. NOXA as well as PUMA are inducible by the transcription factor p53, which is a mediator of DNA damage associated apoptosis (Clarke et al., 1993; Lowe et al., 1993; Nakano and Vousden, 2001; Oda et al., 2000). BID is cleaved by caspases or calpains to the shorter form tBID, is then myristoylated and subsequently integrates into the outer mitochondrial

membrane were it facilitates the oligomerization of BAX (Desagher et al., 1999; Strasser, 2005). Additional ways of regulation are the stress-induced dephosphorylation and subsequent stabilization of BIM or the Ca^{2+} -dependent dephosphorylation of BAD (Puthalakath et al., 2007; Wang et al., 1999).

A second group of proteins involved in the negative regulation of cell death is the inhibitor of apoptosis (IAP) family (Shi, 2004a). They were originally discovered in the baculoviral genome, which led to the name of their common domain, the baculoviral IAP repeat (BIR) (Crook et al., 1993). These BIR domains are stretches of about 70 amino acids with a cysteine/histidine containing core motif (Hinds et al., 1999). They occur in repeats of 1-3 domains, facilitate protein-protein interactions and are essential for the anti-apoptotic function of IAPs (Srinivasula and Ashwell, 2008). In addition to the BIR domains the best studied human IAPs c-IAP1, c-IAP2 and XIAP contain a RING (really interesting new gene) domain, which confers E3 ligase activity, and in the case of the c-IAPs an additional CARD (caspase activation and recruitment domain) [Figure 8] (Srinivasula and Ashwell, 2008). All IAPs bind several caspases through their BIR2/3 domains, but only XIAP is able to directly inhibit the executioner caspase 3 and 7 as well as the initiator caspase 9 using two different interaction sites (Eckelman and Salvesen, 2006; Eckelman et al., 2006). The direct inhibition by c-IAPs was only shown in vitro so far and is about 100 fold weaker than the effect of XIAP (Deveraux and Reed, 1999). The BIR1 domain is an exception to the binding pattern of BIR2/3, as it confers binding to mainly signaling molecules (Srinivasula and Ashwell, 2008). Although the CARD domain in other proteins is linked to the binding of apoptotic and inflammatory proteins containing the same domain, its function in the c-IAPs is not well understood. Recently it was reported that the CARD domain has an auto-inhibitory effect on the RING domain, controlling the enzymatic functions of c-IAP1/2 (Lopez et al., 2011). This E3 ligase activity is at the moment a focus of research and several groups reported not only implications in apoptosis prevention, but also in regulating signaling cascades. c-IAPs as well as XIAP ubiquitinate caspase 3 and/or 7 leading to their degradation. c-IAP1/2 in addition ubiquitinate their inhibitor SMAC/DIABLO and thereby contribute to its turnover (Choi et al., 2009; Hu and Yang, 2003; Suzuki et al., 2001). SMAC/DIABLO originally identified in 2000 is released from the mitochondrial inner membrane space

and binds to IAPs through a four amino acid long N-terminal IAP binding motif (IBM) thereby reverting their inhibitory effect (Chai et al., 2000; Du et al., 2000; Shi, 2002; Verhagen et al., 2000). Interestingly the same functional binding peptide can be found in proteolytically activated caspase-9, leading to opposing effects in activation of the caspase cascade, as caspase-9 is inhibited first by binding to XIAP until SMAC/DIABLO replaces it (Srinivasula et al., 2001). Ubiquitination by IAPs not only confers degradation, but c-IAP1/2 also seem to play a role in different pathways involved in inflammation and apoptosis, like NF- κ B and MAPK signaling, by K63-linked ubiquitination of key proteins, leading to a binding scaffold for other proteins (Bertrand et al., 2008; Li et al., 2002; Matsuzawa et al., 2008; Varfolomeev et al., 2008).

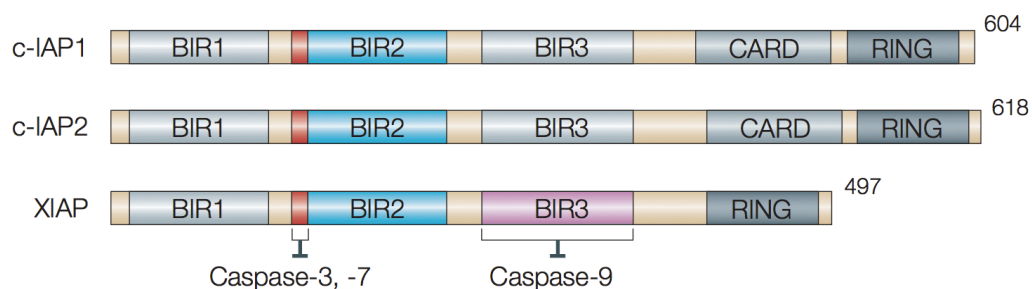


Figure 8. The inhibitor of apoptosis family [adapted from (Riedl and Shi, 2004)].

Schematic representations of the most prominent members of the inhibitor of apoptosis (IAP) family are shown. The conserved sequence that is important for binding of caspase-3 and -7 is marked in red in all three proteins. In contrast only the BIR3 domain of XIAP is able to bind and inhibit caspase-9. The roles of the CARD and RING domain have yet to be elucidated, but it seems that the E3-ligase function of the RING domain is involved in protein degradation and the CARD in controlling its activity. c-IAP, cellular IAP; XIAP, X-linked IAP; BIR, baculoviral IAP repeat; CARD, caspase-recruitment domain.

4.2.3 Intrinsic pathway

Two major pathways lead to the induction of apoptosis, which are also partly linked to each other. Signals from within the cell activate the intrinsic pathway of apoptosis, with the BCL-2 family and the mitochondria as key players [Figure 9]. The signals can comprise all sorts of 'stress signals' ranging from environmental factors like hypoxia or growth factor withdrawal to extensive DNA damage or disturbance in the protein biosynthesis (Pereira and Amarante-Mendes, 2011). Depending on the stimulus different sensors are involved in finally promoting mitochondrial outer membrane permeabilization, which marks the point of no return. Certain cytotoxic substances can damage the mitochondria themselves; other signals involve the

members of the BCL-2 family. DNA damage for instance activates the transcription factor p53, which enhances transcription of a wide variety of genes including the pro-apoptotic PUMA, BAX and BID, but at the same time has a repressing effect on anti-BCL-2 transcription (Nakano and Vousden, 2001; Vousden and Lu, 2002; Wu et al., 2001). Although different routes are taken, ultimately the mitochondria are damaged, either by pore formation through the BCL-2 family members BAX/BAK alone or in combination with the so-called permeability transition pore complex. The latter is a multiprotein complex spanning the outer and inner mitochondrial membrane and is involved in the loss of inner mitochondrial membrane potential. Core subunits of this large complex are the voltage-dependent ion channel (VDAC), the adenine nucleotide translocase (ANT) and cyclophilin D (Zamzami et al., 2005). Its role in apoptosis is not fully understood, but it seems that opening of this channel leads to efflux of Ca^{2+} and solutes smaller than 1.5 kD, influx of water and finally swelling and membrane rupture (Orrenius et al., 2011). The pore formed by multimerization of BAX/BAK on the other hand only opens the outer mitochondrial membrane, followed by the efflux of proteins from the mitochondrial inter-membrane space, with pro-apoptotic proteins, like cytochrome c, AIF, endonuclease G, SMAC/DIABLO and HtrA2/OMI among them (Patterson et al., 2000; Wei et al., 2001). Cytochrome c, normally part of the electron transport chain in the inter-membrane space (IMS), is commonly recognized as the main factor promoting apoptosis (Bernardi and Azzone, 1981). Upon release to the cytoplasm cytochrome c binds dATP as well as apoptotic protease activating factor 1 (APAF-1) in a heptameric structure called the apoptosome [Figure 11] (Acehan et al., 2002; Yuan et al., 2010; Zou et al., 1999). A conformational change in the APAF-1 and subsequent exposure of a CARD domain promotes the CARD-CARD interaction with pro-caspase-9 and subsequent auto-activation of the latter. The presence of cytochrome c in the cytoplasm alone is enough to trigger apoptosis (Vaux, 2011). The active caspase-9 as initiator caspase now processes effector caspases triggering the caspase cascade.

Other pro-apoptotic factors released from IMS like the flavoprotein apoptosis-inducing factor (AIF) and endonuclease G are involved in the caspase independent breakdown of genomic DNA (Cande et al., 2002; Kroemer and Martin, 2005; Li et al., 2001). SMAC/DIABLO as well as HtrA2/OMI function through inhibition of the IAP family members (Verhagen et al., 2000; Verhagen et al., 2002). Opposed to SMAC/DIABLO, the contribution of HtrA2 to IAP inhibition is currently on debate.

The apoptotic effects of the serine protease HtrA2 could be due to the sudden protease activity in the cytoplasm, whereas the IAP inhibition plays a minor role, which would explain the missing effect on apoptosis in mice lacking HtrA2 (Saelens et al., 2004; Vaux, 2011).

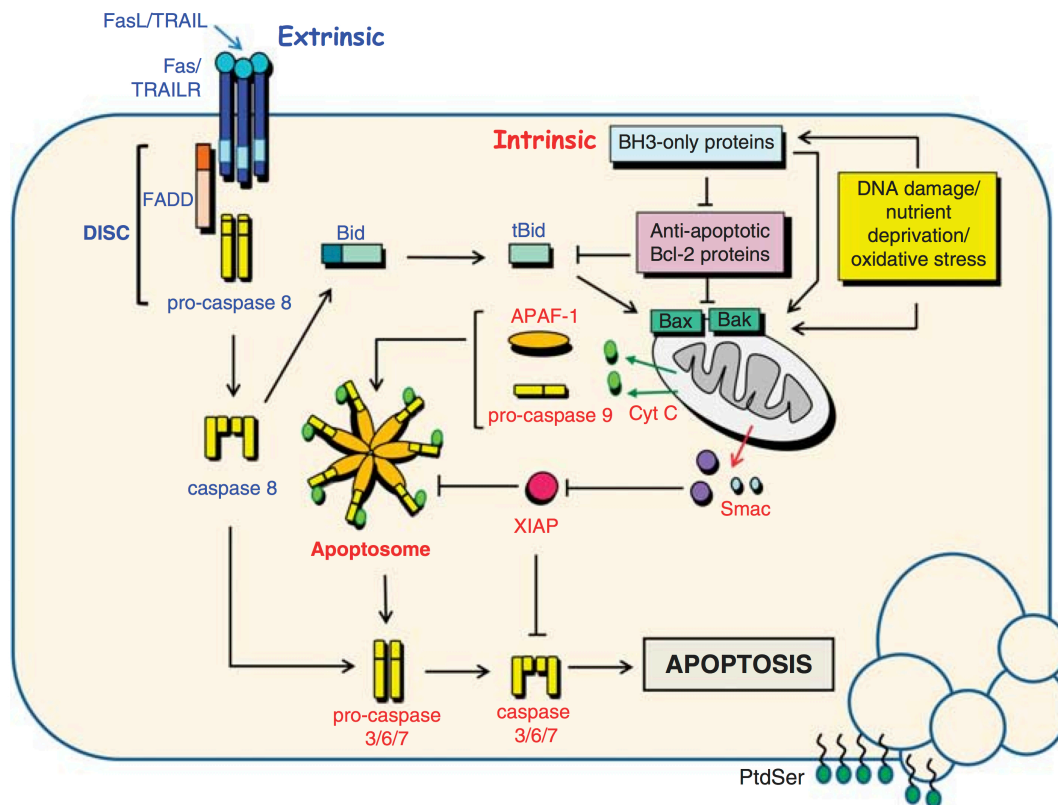


Figure 9. The intrinsic and extrinsic induction of apoptosis [adapted from (Long and Ryan, 2012)].

The two pathways that lead to apoptosis are shown in this diagram. The intrinsic pathway is triggered by cell stress like DNA damage, nutrition deprivation or oxidative stress, incidents that are sensed by proteins of the BCL-2 family. Oligomerization of BAX/BAK leads to mitochondrial membrane permeabilization (MMP) and the subsequent release of apoptotic mediators such as cytochrome c and SMAC/DIABLO. The latter inhibits the anti-apoptotic XIAP, whereas the ATP-dependent binding of cytochrome c to APAF-1 and pro-caspase-9 results in the formation of the apoptosome, a complex that activates downstream effector caspases. External death stimuli through receptors like FAS and TRAIL-R induce a homologous complex through binding of adapter molecules like FADD and the initiator pro-caspase-8. This death-inducing signaling complex (DISC) triggers the auto-activation of caspase-8 and the subsequent progression of the caspase cascade. The BCL-2 family member BID connects the two pathways as it promotes BAX oligomerization at the mitochondria after cleavage by caspase-8. SMAC/DIABLO, second mitochondria-derived activator of caspase/Direct IAP-binding protein with low pI; XIAP, X-linked inhibitor of apoptosis FADD, FAS-associated protein with a death domain; BAX, BCL2-associated X-protein.

4.2.4 Extrinsic pathway

The extrinsic pathway leading to apoptosis relies on members of the TNF-receptor family to initiate the death signal, like CD95/FAS, TNF-R1 or TRAIL receptors. These

receptors contain a cysteine-rich extracellular and a cytoplasmic death domain and are involved in immunology, differentiation and survival (Debatin and Krammer, 2004; Gaur and Aggarwal, 2003). The TNF-R1 and FAS pathways were focus of research over several years. Both are activated through trimerization when the specific trimeric ligands TNF or FASL bind and subsequently stimulate protein interactions at their death domains (DD). FASL/FAS recruit the FAS-associated death domain protein (FADD), whereas TNF/TNF-R recruit TNF-R1-associated death domain protein (TRADD), both of which are adapter molecules to pro-caspase-8 or its homolog pro-caspase-10 through their death effector domains (DED) (Chinnaiyan et al., 1995; Hsu et al., 1995). At this point a regulatory mechanism can come into action involving the cellular FLICE-like inhibitory protein (cFLIP), which also binds via a DED and thereby prevents the caspase recruitment, a mechanism that is also exploited by viruses and tumor cells (Benedict et al., 2002; Krueger et al., 2001; Shirley and Micheau, 2010). The assembled complex of receptor, adapter and caspase is termed death-inducing signaling complex (DISC) (Wilson et al., 2009). Similar to the before mentioned apoptosome, caspases are brought into close proximity and are subsequently auto-activated, resulting in the initiation of the caspase cascade (Salvesen and Dixit, 1999; Shi, 2004b).

For FASL/FAS complexes different modes of activation were described depending on the cell types. In type I cells the pathway follows the standard route also seen for TNF-R1 or TRAIL-R. Type II cells are defined by an involvement or rather amplification through the intrinsic pathway. In this case DISC assembly is less prominent and activated caspase-8, instead of initiating the caspase cascade, cleaves the pro-apoptotic BID to tBID. tBID in return integrates into the mitochondrial membrane, recruits BAX and leads to the activation of the intrinsic apoptosis pathway (Fulda et al., 2001; Scaffidi et al., 1998).

4.3 Inflammasome

The inflammasome is a multimeric complex, which leads to the activation of inflammatory caspases, the third group of the caspase family. It is part of the innate immune response and forms upon encounter of pathogen-associated molecular patterns (PAMPs) as well as danger-associated molecular patterns (DAMPs). The result of its activation is the processing of pro-inflammatory cytokines like IL-1 β and

IL-18 by caspases and their subsequent secretion, the mechanism of which is still unknown [Figure 10]. Due to the involvement in inflammation and the homology to the apoptosome, Martinon et al. coined the term inflammasome in 2002 [Figure 11] (Martinon et al., 2002). Host defense and the decision between foreign and self is mediated in the innate immune response through a variety of receptors, encompassing the membrane spanning families of Toll-like receptors (TLRs) and C-type lectin receptors (CLRs) as well as the cytosolic RIG-I-like receptors (RLRs) and NLRs (nucleotide-binding-and-oligomerization domain [Nod] and leucine-rich-repeat-containing receptors), with members of the latter being part of inflammasomes (Bauernfeind et al., 2011a). Other families, like the TLR or TNFR family, promote expression of inflammasome components as part of a priming step (Bauernfeind et al., 2009).

The human NLR family until now contains 22 members with the defining leucine rich repeats (LRRs) and NACHT domain (also NOD [nucleotide-binding-and-oligomerization domain] or NBD [nucleotide-binding domain]), which are classified into 5 groups according to their additional domains: The NLRA group contains an acidic activation domain, NLRBs a BIR domain, and NLRCs a CARD domain whereas NLRPX lack a defined domain. The largest subgroup, NRLPs, comprises of proteins with a C-terminal pyrin domain, another member of the death fold protein-protein interaction domains (Fairbrother et al., 2001; Ting et al., 2008a). Most of the NLRs are involved in diverse inflammatory signaling processes, whereas NLRP1, NLRP3 and NLRC4 are key components of different inflammasomes. The LRRs of these proteins are thought to be the sensing part of the protein, although no direct binding to an activator could be shown until now (Bella et al., 2008). The NACHT domain resembles a motif of APAF-1, the central apoptosome unit, binds ATP and is thought to oligomerize upon this interaction, which is key to the activation of the caspases [Figure 11] (Bauernfeind et al., 2011a; Duncan et al., 2007). As only the ARTC subgroup contains a CARD domain to recruit inflammatory caspases directly, an adapter molecule is needed to propagate the signal for NLRP1 and NLRP3, respectively. PYCARD (or ASC [apoptosis-associated speck-like protein containing a CARD]), a protein containing a pyrin domain (PYD) as well as a CARD, was found as a promoter of apoptosis (Masumoto et al., 1999; McConnell and Vertino, 2000). A few years later the connection to the inflammasome was made and ASC has turned out to be involved in all known inflammasomes, including NLRC4, for which the exact

mechanism still has to be discovered, as NLRC4 lacks the PYD (Agostini et al., 2004; Manji et al., 2002; Mariathasan et al., 2004; Srinivasula et al., 2002).

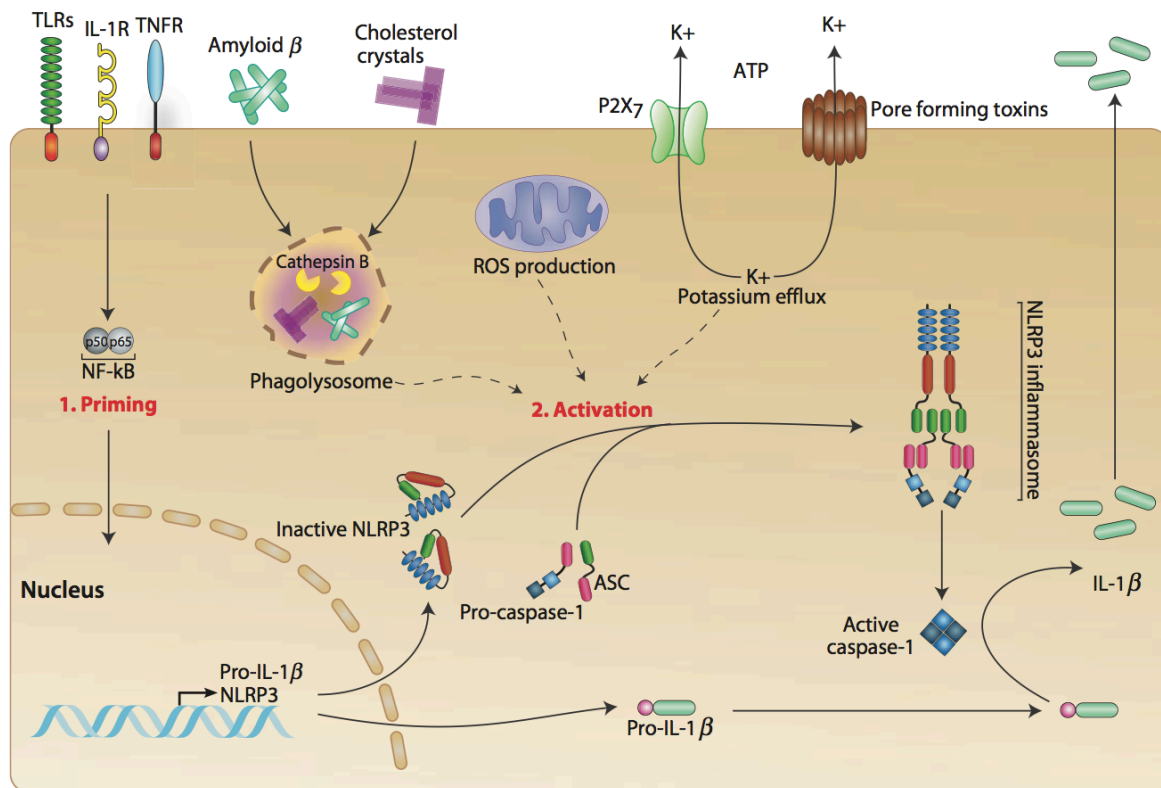


Figure 10. Priming and activation of the NLRP3 inflammasome [adapted from (Horvath et al., 2011)].

The NLRP3 inflammasome activation is a two-step mechanism. At first inflammatory signaling through NF- κ B stimulates the expression of NLRP3 itself and the proteolytic target of caspase-1 IL-1 β . Upon sensing a second signal such as ROS, potassium efflux or lysosomal damage, by mechanisms yet to be discovered, NLRP3 oligomerizes with ASC and pro-caspase-1. The assembled inflammasome results in the proximity-induced activation of caspase-1 and subsequent cleavage of IL-1 β . NF- κ B, nuclear factor 'kappa-light-chain-enhancer' of activated B-cells; IL-1 β , interleukin-1 β ; ROS, reactive oxygen species; ASC, apoptosis-induced speck-like protein.

The NLRP1 inflammasome was the first to be described to form apoptosome-like structures (Martinon et al., 2002). Unlike other NLRs, NLRP1 also contains a FIIND (function to find domain) and CARD in addition to the classifying PYD, which allows the direct binding of caspases (Martinon et al., 2002). It is activated by lethal toxin (LT) of *Bacillus anthracis* as well as the peptidoglycan muramyl dipeptide (MDP), which is a component of bacterial cell walls (Faustin et al., 2007; Hsu et al., 2008). In the presence of MDP or LT NLRP1 forms oligomers, the basis for the inflammasome, and recruits caspase-5 through its CARD domain as well as caspase-1 through the collaboration with ASC (Martinon et al., 2002). A direct interaction between NLRP1 and its activators could not be shown, but recent work suggests that another family member, NLRC2, is also involved in cooperation with NLRP1 (Hsu et al., 2008).

Regulation of NLRP1 seems to be realized through binding of BCL-2 and BCL-X_L to its LRR and subsequent inhibition of caspase-1 activation, which represents another parallel to apoptosis (Bruey et al., 2007).

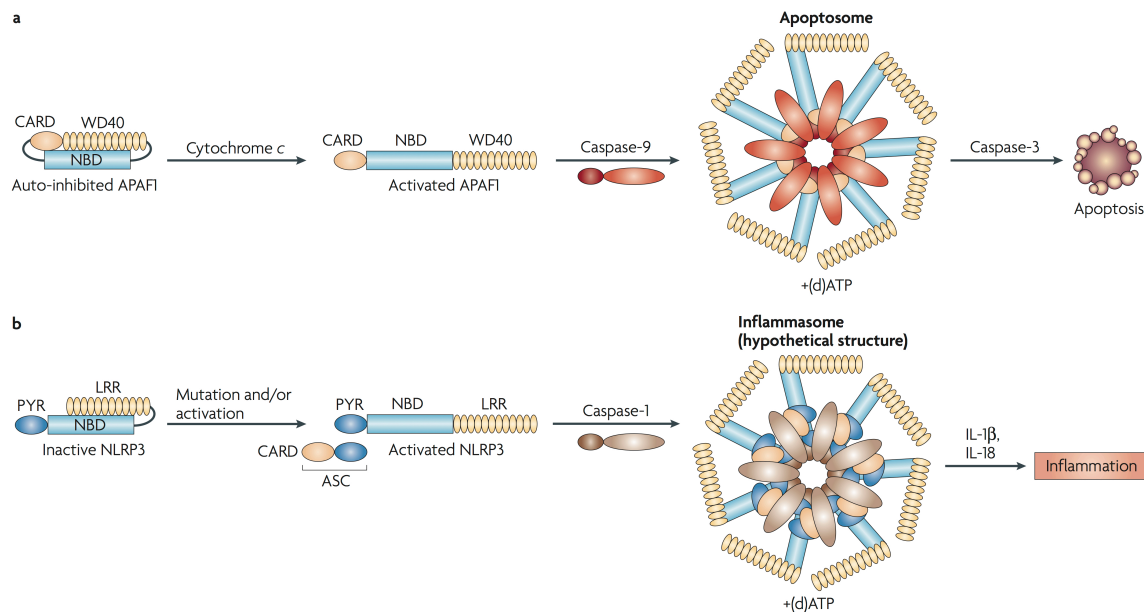


Figure 11. The apoptosome and inflammasome are homologue structures [adapted from (Ting et al., 2008b)].

The two proposed heptameric complexes involved in the inflammatory response to DAMPs/PAMPs and in the intrinsic apoptotic pathway are similar. Both structures contain a protein capable of ATP-dependent oligomerization (APAF-1 and NLRP3) and a caspase as effector. The apoptosome (a) assembles upon binding of cytochrome C to APAF-1 and pro-caspase-9, leading to activation of the latter and finally to apoptosis. The inflammasome (b) relies on NLRP3 as sensor of DAMPs/PAMPs and contains in addition the adapter molecule ASC and pro-caspase-1 in its functional state. The subsequent processing of IL-1 β and IL-18 further enhances the inflammatory milieu surrounding the cell. CARD, caspase-recruitment domain; NBD, nucleotide-binding domain; DAMPs/PAMPs, danger/pathogen associated molecular patterns; LRR, leucine-rich repeats; ASC, apoptosis-induced speck-like protein.

Although the NLRP1 inflammasome was the first to be described, the NLRP3 inflammasome is the most extensively studied, most likely due to its broad range of activators. These include PAMPs, like bacterial RNA, bacterial cell wall components and pore forming toxins as well as DAMPs, like metabolites, aggregates or crystals (Bauernfeind et al., 2011a; Kanneganti et al., 2006; Martinon et al., 2004). The latter includes endogenous deposits like uric acid crystals and amyloid β fibrils and exogenous materials like asbestos, silica and alum (Dostert et al., 2008; Eisenbarth et al., 2008; Halle et al., 2008; Hornung et al., 2008; Martinon et al., 2006). Therefore it is believed that the NLRP3 inflammasome acts as a defect and disturbance sensor in general. As part of its regulation, its expression is controlled via the NF- κ B pathway and relies on activation by other pattern recognition receptors like TLRs

(Bauernfeind et al., 2009). NLRP3 lacks a CARD and the propagation of the signal to caspases happens through PYD-PYD interactions with ASC. The mechanism on the other hand by which NLRP3 detects its various activators is still not clearly understood, but three main theories are being pursued [Figure 10]. The first involves the purinergic receptor P2X7, which upon ATP binding opens a pore together with its partner protein pannexin-1 (Ferrari et al., 2006; Pelegrin and Surprenant, 2006). The resulting potassium efflux or influx of DAMPs/PAMPs seem to activate the NLRP3 inflammasome (Kanneganti et al., 2007; Petrilli et al., 2007). Although it could explain the sensing of for instance necrotic cell death by the inflammasome, the ATP levels needed *in vitro* are much higher than levels released *in vivo* (Bauernfeind et al., 2011a). The second observation to explain NLRP3 activation was made in phagocytes. Upon engulfment of DAMPs, such as silica crystals, lysosomal rupture can occur with leakage of compounds like cathepsin B into the cytosol triggering NLRP3 activation (Hornung et al., 2008). This mechanism defines the inflammasome as watchman of lysosomal integrity. In a third scenario reactive oxygen species were proposed as common denominator of NLRP3 activation, but recent findings suggest that this occurs most likely by affecting gene transcription (Bauernfeind et al., 2011b; Dostert et al., 2008; Zhou et al., 2011).

The third of the well-studied NLR inflammasomes utilizes the CARD containing NLRC4 as signal sensor, which directly binds to caspase-1 (Poyet et al., 2001). It is activated by flagellin and components of the type III secretion system of gram⁻ bacteria, which both exhibit a common motif, but similar to NLRP1 and NLRP3 direct interaction could not be proven (Franchi et al., 2006; Miao et al., 2006; Miao et al., 2010). Surprisingly NLRC4 discriminates between flagellins, e.g. *Escherichia coli* flagellin fails to activate, which is explained by the importance of discriminating between commensal and pathogenic bacteria (Ren et al., 2006).

In addition to the receptors of the NLR family another receptor was postulated in 2008, when it was observed that double-stranded DNA (dsDNA) led to the processing of IL-1 β without the involvement of NLRP3/NLRC4 (Muruve et al., 2008). The responsible protein AIM2 (absent in melanoma 2), a member of the PYHIN (pyrin domain and HIN domain containing) family, was identified a year later (Hornung et al., 2009). This cytosolic protein directly binds dsDNA with its HIN-200 domain and ASC through the PYD, which makes it so far the only known member of the inflammasome sensors directly binding to its activator (Fernandes-Alnemri et al.,

2009). As it contains no oligomerization domain in contrast to the NLRs, the assembly of the inflammasome is thought to be due to the multiple binding sites in the DNA polymer. This is strengthened by the observation, that shorter fragments of dsDNA are unable to trigger the inflammasome activation (Roberts et al., 2009).

5 Results & Discussion

5.1 ARTD10 and cell proliferation

ARTD10 was discovered only recently and therefore the work in our group so far was focused mainly on the basic characterization, like chromosomal localization, gene organization, domain structure and catalytic mechanism. Apart from those important findings, experiments with ARTD10 in rat embryo fibroblasts (REFs) showed a potential for inhibition of fibroblast transformation by MYC/HA-RAS. This was dependent rather on nuclear export than on catalytic activity. In addition overexpression of ARTD10 in 3T3-L1 murine fibroblasts led to failed G1/S transition. Although HEK293 and U2OS cells were unaffected, HeLa cells displayed a similar result in colony formation assays (Schuchlautz, 2008; Yu et al., 2005). To further elucidate the role of ARTD10 in cell proliferation HeLa cells with an incorporated inducible expression system were used in this work.

5.1.1 Modell system: HeLa Flp-In T-Rex

The Invitrogen Flp-In T-Rex system is designed to integrate a target gene at a specific site in the genome of a cell under the control of a tetracycline, i.e. doxycycline inducible promoter. Directed integration is achieved by the use of the Flp recombinase, which recognizes FRT sites in the expression vector and an integrated FRT site in the host cell. In a first step the latter has to be introduced into the cell using the pFRT/lacZeo vector. Cells were screened for a single integration and analyzed for a normal phenotype, as this insertion is not directed and can disrupt essential parts of the genome. The resulting Flp-In cell line contained a single FRT site and was Zeocin resistant. To complement the cells to be able to use a doxycycline controlled expression system, a TET repressor vector was additionally transfected and cells that propagated this pcDNA6/TR were selected with Blasticidin S. This cell line is now referred to as the Flp-In T-Rex host cell line and can be used for inducible expression of the desired target protein. A scheme of the further procedures is depicted in Figure 12A. There are different expression vectors containing the FRT site that are compatible with this modular system. The vector pcDNA5/FRT/TO was used in here. A CMV promoter containing TET operator sites

to which the TET repressor binds controlled the expression of the target gene. It was transfected together with the plasmid encoding the recombinase, which then promoted integration of the transgene into the FRT site in the genome. It thereby disrupted the Zeocin ORF and instead resulted in a hygromycin resistance, by which cells with successful integration could be selected. The complete system could now be activated by the addition of doxycycline, a tetracycline antibiotic that binds to the TET repressor, induces a conformational change and thereby prevents binding to DNA. The advantage of the Flp-In T-Rex system over other stably integrated expression vectors is the single targeted insertion. As the impact of the integration on the genome and the cell itself is explored prior to the integration of the target protein all resulting stable cell lines have the same background. The variation between clones is kept to a minimum and the establishment of single clones could even be omitted. S. Taylor from the University of Manchester provided the HeLa Flp-In T-Rex (HFT) cell line used here.

The influence of ARTD10 on cell growth and transformation was dependent on the cell system and seemed to be in part dependent on either the catalytic activity or a functional NES (Schuchlautz, 2008; Yu et al., 2005). Therefore different ARTD10 constructs were used to generate stable cells [Figure 12b]. The mutation of glycine at position 888 to a tryptophan (G888W or GW) renders the wild type protein (wt) inactive, whereas the replacement of three leucines to alanines abolishes nuclear export (Kleine et al., 2008; Yu et al., 2005). Changing all 9 lysines (ΔK) leaves ARTD10 unable to be ubiquitinated, whereas the mutation of the UIMs (ΔUIM) leads to the loss of K63-linked ubiquitin binding (Chauvistré, 2008; Milke, 2007). The ARTD10 construct lacking the amino acids 219-502 ($\Delta 219-502$) misses the glycine-rich region, a feature that is commonly found in RNA binding proteins [see Figure 3](Burd and Dreyfuss, 1994; Dreyfuss et al., 1993).

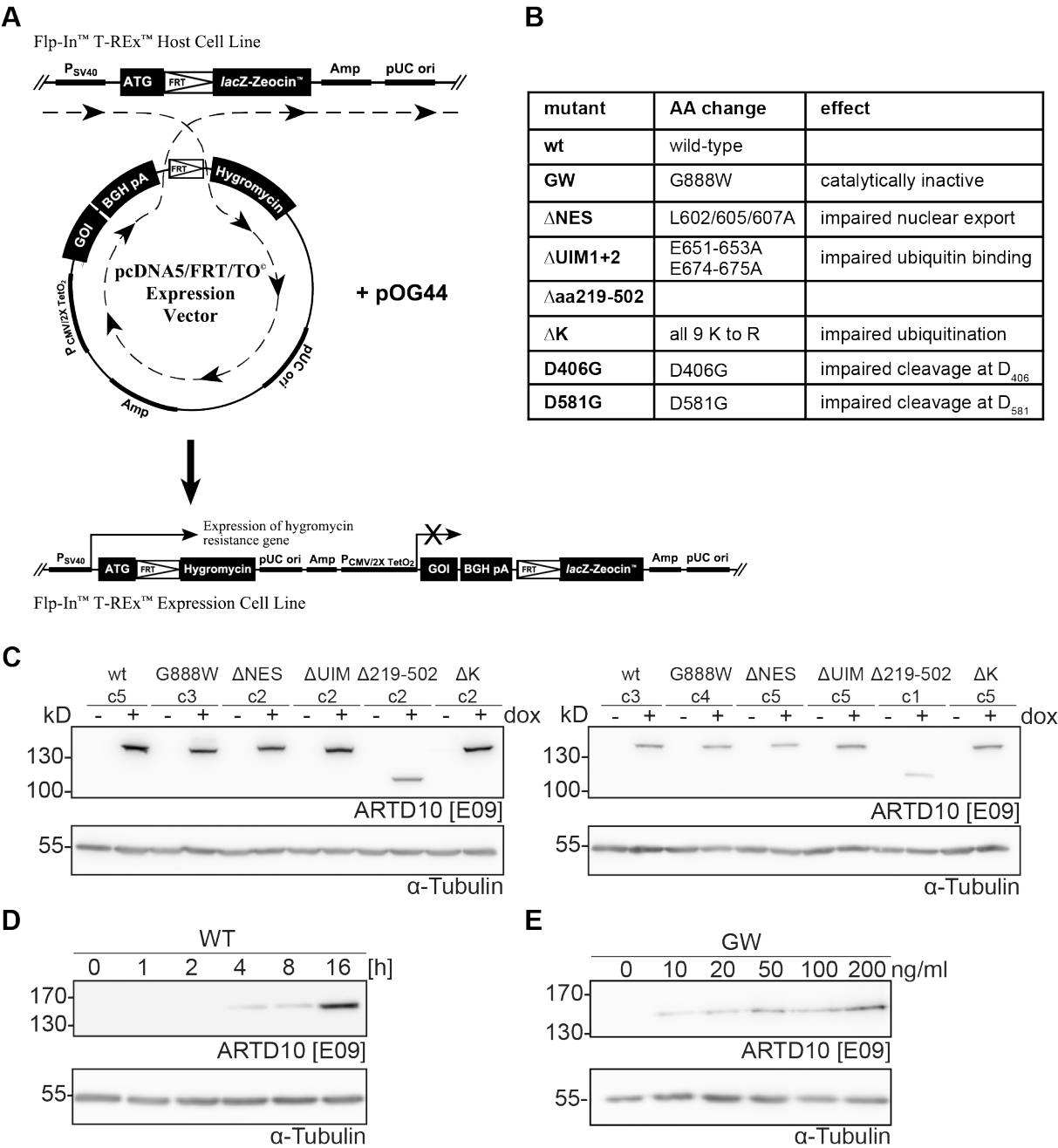


Figure 12. Establishing HeLa cell lines inducibly expressing ARTD10.

(A) Schematic representation of the workflow to generate a Flp-In T-Rex expression cell line using the vector pcDNA5/FRT/TO. The co-transfection of the recombinase encoding vector pOG44 leads to an integration of the expression vector into the FRT site of the host cell. Due to this incorporation the lacZ-Zeocin reading frame is destroyed whereas an hygromycin reading frame is established, rendering the cells now Zeocin sensitive and hygromycin resistant. The expression of the target gene is achieved by addition of doxycycline an antibiotic that inactivates the Tet-repressor blocking the CMV promoter.

(B) Table describing the modifications made in ARTD10 constructs and the resulting effect on the protein. AA, amino acid

(C) Expression test of all established HeLa Flp-In T-Rex ARTD10 cell lines. Of each construct two different clones (c) were induced for expression with 1 μg/ml doxycycline (dox) and analyzed via SDS-PAGE and western blot using the polyclonal E09 antibody. An α-tubulin antibody was used as loading control.

(D) Time course experiment with wt3 cells induced for expression of ARTD10 using 1 μg/ml doxycycline for the indicated times. The samples were analyzed via SDS-PAGE and western blot using the polyclonal E09 antibody. Tubulin was detected as loading control.

(E) Dose-response experiment with GW4 cells. The indicated amounts of doxycycline were used to induce expression of ARTD10 for 16 hours. The samples were analyzed via SDS-PAGE and western blot using the polyclonal E09 antibody. Tubulin was detected as loading control.

After transfection and integration of the pcDNA5/FRT/TO constructs single HFT cell clones were established for every construct. Throughout this work the HFT lines are named using the abbreviations introduced above indicating the protein that was expressed and the clone number. Unnumbered lines represent the polyclonal cell population. Although the Flp-In T-Rex system, due to the directed single integration site of the transgene, should result in a homogenous cell population after integration, the single clones were established to nonetheless analyze possible differences between individual clones. Expression of the proteins was tested by SDS-PAGE and western blotting with a polyclonal antibody as all available monoclonal antibodies available during the initial characterization of the HFT clones recognized ARTD10 in the region missing in the $\Delta 219-502$ construct. All clones showed the expected ARTD10 band of 150 kD and a comparable expression level except for ARTD10- $\Delta 219-502$, which ran at about 110kD [Figure 12C]. The 40 kD higher molecular weight of ARTD10 compared to the calculated theoretical weight is thought to be due to the highly positive charged glutamate-rich region ranging from amino acid 588 to 697. Comparing the expression levels between the constructs and clones it can be stated that at the level of protein production the Flp-In T-Rex system is highly constant. The slightly weaker signal for the ARTD10- $\Delta 219-502$ could be due to the polyclonal antibody used, as it might also detect epitopes in the deleted region. Only minimal differences in protein expression could be observed and qualified this system as a tool to study the impact of different proteins on the cells. It is worth noting that the endogenous level of ARTD10 in HeLa cells is very low and with currently available antibodies the detection on a western blot of whole cell lysates was not possible, which explained the lack of a band in the uninduced samples [Figure 12C]. Dynamics of the expression level were explored using wt3. Therefore the protein levels, following either variations of the induction time [Figure 12D] or the quantity of doxycycline used, were monitored [Figure 12E]. The amount of ARTD10 increased with time, with first traces being detectable by western blotting after 4 hours of induction. The manufacturer's guide recommended the initial use of 1 $\mu\text{g/ml}$ tetracycline to induce expression of the protein of interest. As the analogue

doxycycline has a half-life of 48h, which is double the half-life of tetracycline, it was used in these experiments. The titration of doxycycline in a culture with GW4 cells showed detectable levels of ARTD10 with as low as 10 ng/ml and a dependence on the doxycycline quantity ranging up to 200 ng/ml [Figure 12E]. This concentration was used in all experiments if not indicated otherwise, to ensure constant expression even over longer time periods, taking into account the former mentioned half-life of doxycycline.

ARTD10 was reported to be preferentially cytoplasmic due to its NES. Further experiments revealed, that it extensively shuttles between the nucleus and cytoplasm (Kleine et al., 2012). The region responsible for the necessary nuclear import was localized to a part of ARTD10 encompassing amino acids 435-528. The functional NES is dependent on the Crm1 export receptor, as its inhibitor Leptomycin B leads to nuclear accumulation of ARTD10 due to the NLS region (Fornerod et al., 1997; Yu et al., 2005). HeLa Flp-In T-Rex cells expressing wild-type or mutant ARTD10 were subjected to immunofluorescence analysis to check for changes in the subcellular localization [Figure 13]. In addition Leptomycin B was used to ensure the functionality of the NES and to facilitate the localization analysis by blocking one component responsible for the localization. Staining of Δ 219-502 was unfortunately not possible, as the polyclonal antibody was not specific enough for immunofluorescence and the epitope recognized by the 5H11 antibody lies within the deleted region. The localization of this construct would have been interesting, as a part of the proposed nuclear localization signal is missing.

All constructs except for Δ NES showed a similar localization with the majority of the protein staining in the cytoplasm, a finding that was in line with results obtained from transient expression experiments [Figure 13]. Also as expected the ARTD10 without functional NES was distributed equally or with a preference for the nucleus, varying slightly in each individual cell. Upon Leptomycin B treatment all constructs showed localization comparable to the Δ NES construct. The residual staining in the cytoplasm could be either due to the continuous overexpression of the protein or a relatively weak nuclear targeting. In addition ARTD10 localized to specific dots in cells, the function of which are not fully understood. Colocalization experiments however rule out RNA associated structures like P-bodies and stress granules as well as Golgi, ER and endosomes. The poly-ubiquitin adapter molecule p62/SQSTM1

however, which is involved in cargo targeting to autophagosomes, did colocalize (Kleine et al., 2012). None of the domain modifications seemed to influence the overall cellular distribution of ARTD10 [Figure 13]. The G888W mutant however is the only construct resulting in extensive dot formation after 4 hours an outcome also seen in transient experiments. This may suggest, that catalytic activity is needed to antagonize accumulation of ARTD10 in those structures.

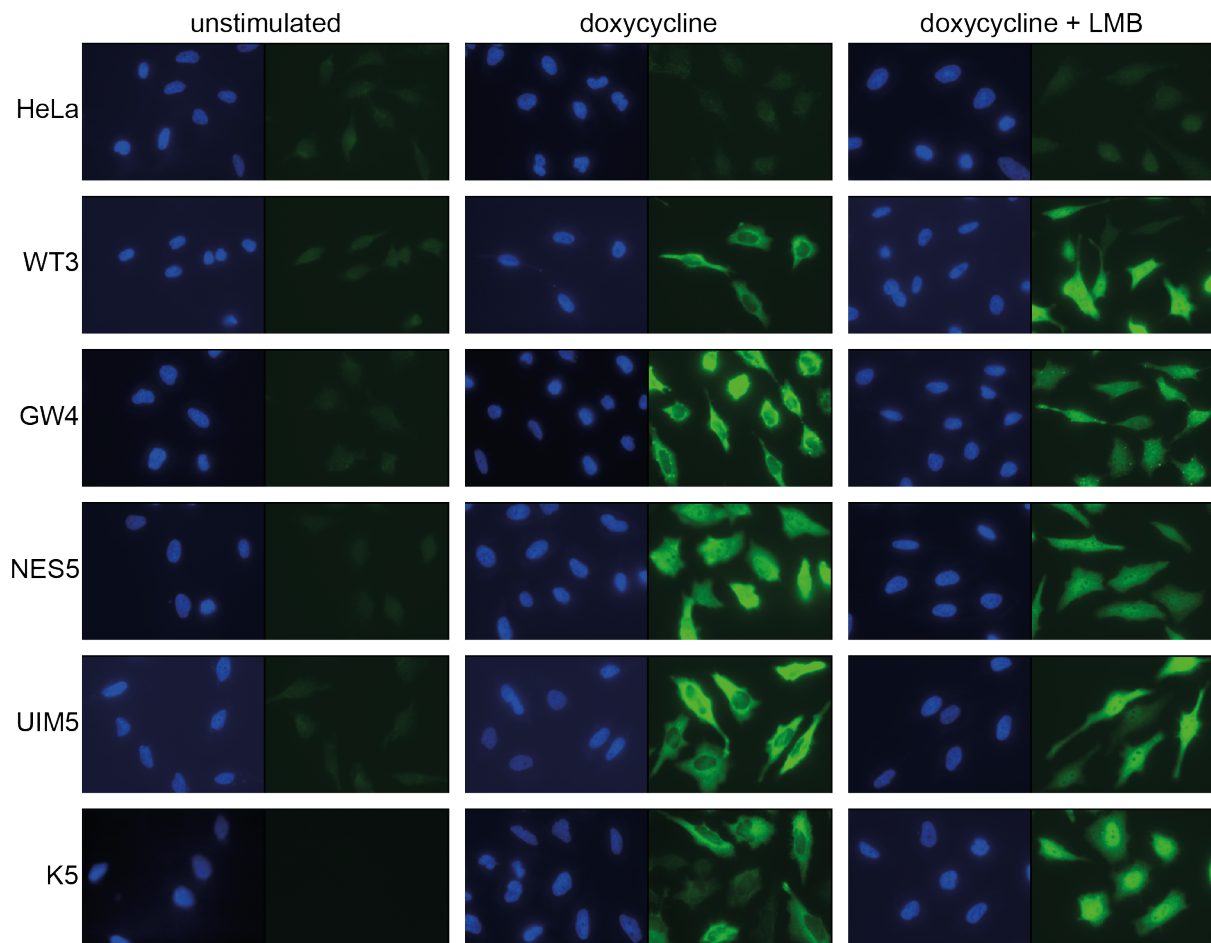


Figure 13. Subcellular localization of ARTD10 and ARTD10 mutants in stable HeLa cells.

The indicated cell lines were seeded on coverslips and protein expression was induced with 1 µg/ml doxycycline for 4 h with or without the addition of 20 nM Leptomycin B. Cells were fixed with PFA and ARTD10 was stained using the monoclonal antibody 5H11. Nuclei were stained using Hoechst 33342.

5.1.2 ARTD10 influences cell growth in HeLa Flp-In T-Rex

Initial characterization of the cell growth behavior was done using colony formation assays. 100 cells were seeded in 6-well dishes, the expression of the different proteins induced and the colonies were fixed and stained with methylene blue after 11 days. Additional proteins could be introduced the day after seeding by transfection

of their expression vector. Figure 14A shows the outcome of a colony formation with the different HFT ARTD10 cells as well as control HFT without a transgene to control for doxycycline effects. Without induction the size of the single colonies varied slightly, but the amount of colonies was equal, an effect that was most likely due to different basal growth rates of the clones. Addition of doxycycline however completely abolished colony formation in the case of wt3, an outcome which is consistent with previous findings in transient colony formation assays (Schuchlautz, 2008). Cells overexpressing ARTD10 mutants did not show this effect, an indication that the integrity of the full-length protein is very important, as each mutation represents most likely a drastic impact on the proteins morphology or functionality. Unfortunately this complicated the research for the underlying factors leading to the diminished cell growth, as no domain's implication can be ruled out.

Although it is an easy method to obtain an overview on the overall cell growth rate, the experiments measure an end point, i.e. the final amount of cells. Further conclusions on the underlying cause, be it delayed or blocked cell cycle or even cell death, was not possible.

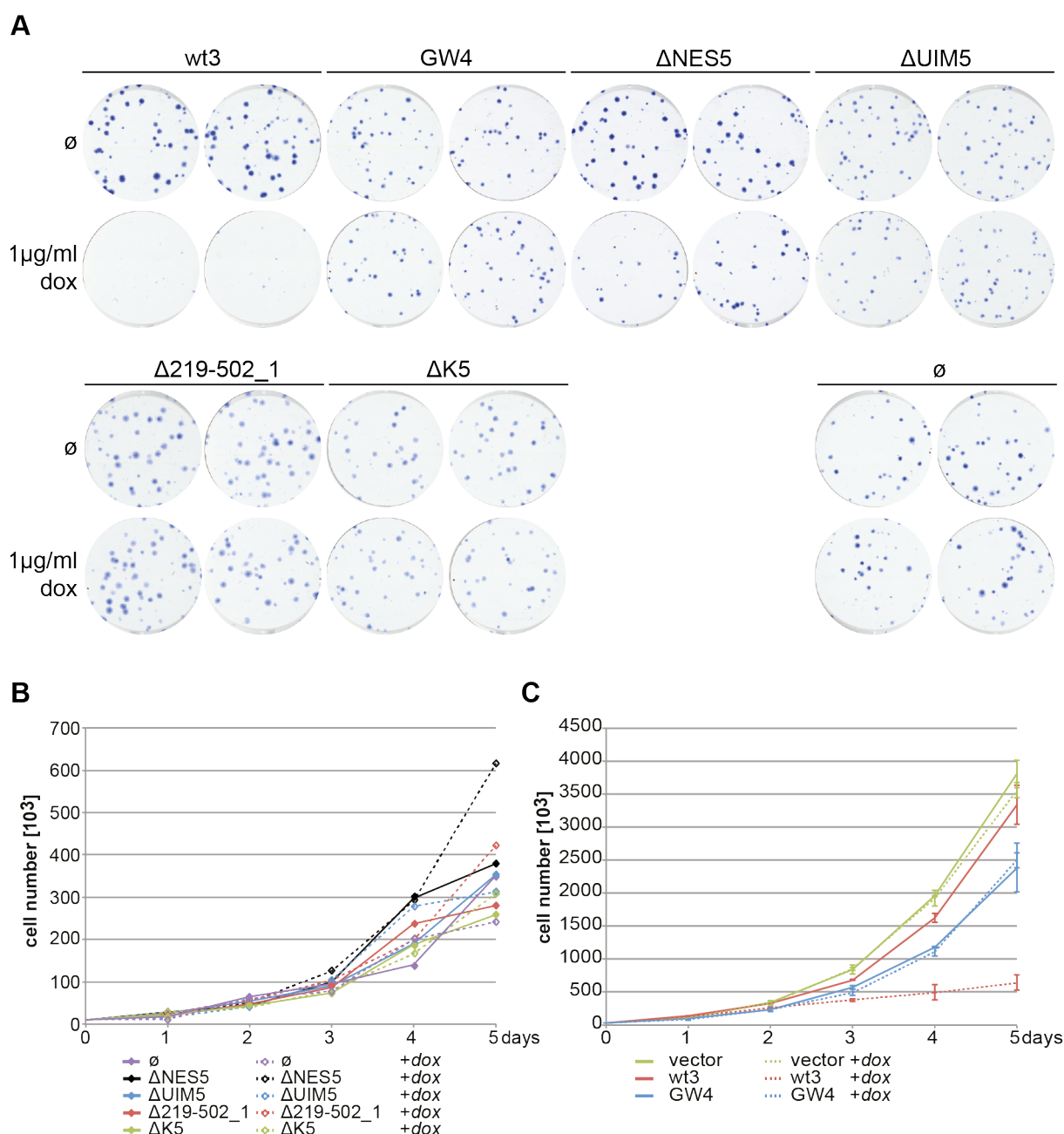


Figure 14. ARTD10 inhibits cell growth in HeLa Flp-In T-Rex cells.

(A) Colony formation experiment using clones of the established HFT ARTD10 cell lines with Ø indicating control HFT cells. 100 cells were plated and grown with and without addition of 1 µg/ml doxycycline for 11 days and subsequently stained with methylene blue. The experiment was performed in duplicates.

(B) Growth curves of different HFT ARTD10 cell constructs with Ø indicating control HFT cells. 10,000 cells were seeded, grown with and without doxycycline and counted over 5 days.

(C) Growth curves of different wt3, GW4 and empty HFT cells. 30,000 cells were seeded, grown with and without doxycycline and counted over 5 days. The experiment was performed in a triplicate.

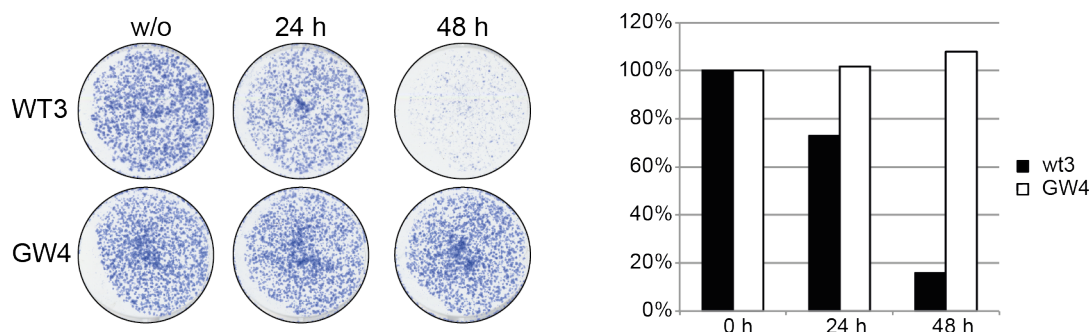
The different colony size in uninduced samples could be an indication for a different overall growth rate of each cell line [Figure 14A]. To address this question cell proliferation of an exponentially growing culture was assessed as shown in Figure 14B and C. The cells were seeded at a low density in 5 plates. The cells of individual

plates were counted at each time point using the CASY cell counter. For clarity control HFT as well as wt3 and GW4 are arranged together. As expected the cells show a slightly different growth rate even in the uninduced state, which could be explained by the use of single clones. Upon induction however only wt3 cells grew significantly slower [Figure 14]. In analogy to the findings above in the colony formation assays, mutated ARTD10 did not have this impact on the cells. The Δ NES, Δ UIM, Δ 219-502 and Δ K proliferated at the same rate with or without doxycycline [Figure 14B]. Therefore those ARTD10 mutants were not used in further experiments and we concentrated on wt or GW cells.

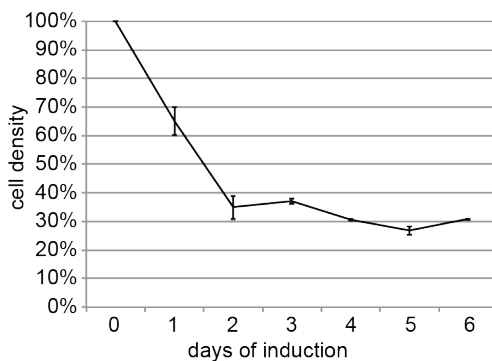
To further elucidate the nature of the inhibitory effect, especially if the prolonged and continuous expression of ARTD10 was needed, colony formation assays were performed with a time-restricted induction of ARTD10. In an initial experiment wt3 and GW4 cells were treated with doxycycline for 24 or 48 hours followed by growth in normal medium. The plates and their quantification in Figure 15A showed a slight decrease in the number of colonies after 24 hours as well as even less colonies after expression of ARTD10 over two days, while the catalytic inactive ARTD10 showed no effect. Subsequent experiments extending the time of doxycycline application revealed that indeed at 2 days the maximum effect was achieved and prolonged ARTD10 expression from this point on did not further decrease colony number [Figure 15B]. An explanation for this non-linear effect could be a continuous apoptosis in a small number of cells throughout the experiments. On the other hand induction of the apoptotic effect only in the first 48 hours in a percentage of cells would result in a delayed onset of exponential cell growth and smaller, invisible colonies in colony formation assays. These two mechanisms could not be distinguished with the assays used. A third possibility would be that ARTD10 was required at a certain level within the cell and had to accumulate over time to trigger the inhibitory effect. As shown in Figure 12E the exogenous ARTD10 was detectable even with 10 ng/ml doxycycline. To determine the influence of the protein amount on the growth inhibiting effect, a dose response assay was performed using the colony formation assay. Dosages from 5 to 1000 ng/ml were applied to the HFT containing the wild-type form of ARTD10 during the whole growth period. Quantification revealed that while 5 ng/ml were sufficient to reduce the colony number, the application of 5 times the amount of doxycycline lowered it to a minimum [Figure

15C]. Further increase of the antibiotic did not have an additional effect. Although the quantification of the colony formation assays resulted in high standard deviations, the tendency was the same in each experiment. To further elucidate the nature of ARTD10's growth inhibiting effect one would have to combine time and amount of applied doxycycline. It would be interesting to see whether the combination of the minimal values, in this case 2 days and 25 ng/ml doxycycline, is still sufficient to induce the limited cell growth.

A



B



C

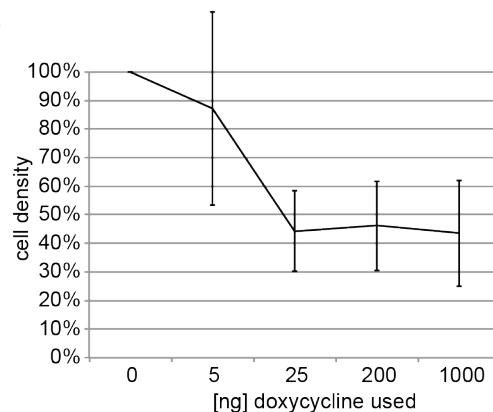


Figure 15. Influence of time and concentration of doxycycline treatment on cell growth.

(A) Colony formation (CF) experiment with wt3 and GW4 cells, in which either ARTD10 expression was uninduced or induced for 24 or 48 h. After 7 days the cells were stained with methylene blue (left panel). A quantification of the CF is shown on the right.

(B) Quantification of an extended induction colony formation with wt3 cells. Again the cells were either uninduced or induced for the indicated times. After 8 days the cells were stained with methylene blue and quantified. The experiment was performed in duplicates.

(C) Quantification of a colony formation experiment with wt3 cells induced with different amounts of doxycycline. The cells were grown for 8 days with the indicated antibiotic amount and subsequently stained with methylene blue and quantified. The experiment was performed in duplicates.

Taken together the results shown in Figure 14 and Figure 15 strongly suggested a negative effect of ARTD10 on cell growth in HFT cells. This effect was both reliant on strength as well as length of induction, with defined points of maximum efficiency. Regarding the nature of this negative effect the conducted experiments were not sufficient to make further conclusions. The elucidation of this issue will be addressed in the next chapter.

5.1.3 ARTD10 induces apoptosis

Throughout the preceding experiments the observation of HFT, expressing the wild-type ARTD10, using an optical microscope revealed an increase in dead and non-adherent cell. To elucidate whether the growth inhibitory effect described in the last chapter was due to dying cells and not inhibition of cell proliferation per se, the number of dead cells in the samples was quantified. Propidium iodide (PI) is a widely used chemical to distinguish viable from dead cells. It is a DNA intercalating as well as fluorescent substance that can be excited at a wavelength of 488 nm. It is excluded from viable cells, as it cannot penetrate cells with an intact cell membrane. When cell membrane integrity is lost during cell death, PI is taken up by the cells and intercalates into the DNA. PI containing cells are easily detectable by various methods, e.g. FACS analysis. Figure 16 shows two FACS histograms of wt3 and GW4 cells stained with PI after expression of ARTD10 for 3 days. The background level of dead cells in culture was at about 4 percent for both constructs, which was comparable to viability scores obtained with the CASY cell counter. Expression of ARTD10 led to an increase of dead cells to about 36%, whereas no increase in PI positive cells was measurable for GW4.

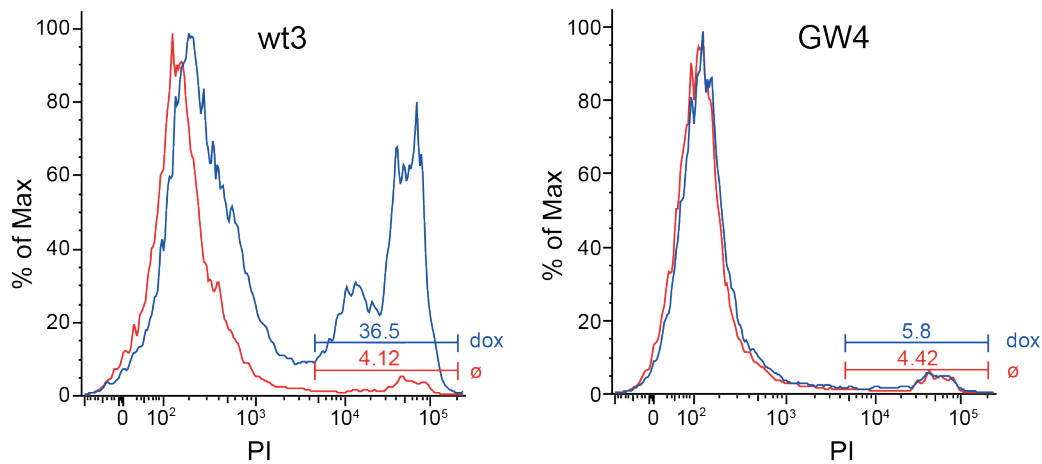


Figure 16. Overexpression of ARTD10 induces cell death.

FACS analysis of dead cells after ARTD10 expression in wt3 and GW4 cells. The cells were grown for three days with or without doxycycline and afterwards stained with propidium iodide. The cells were counted and analyzed using FACS.

The outcome of this experiment confirmed the initial observations made in cell culture using light microscopy. The effects seen in colony formation and proliferation assays seemed to be in large part due to the death of the cells. The analysis in Figure 16 represents an end point analysis of cells that lost the integrity of the plasma membrane. However cells that died early in the experiment and disintegrated were not analyzed. Therefore these measurements could not be compared directly to those obtained in the colony formation and proliferation assay experiments. In addition the quantification of dead cells as measured here by FACS did not contribute to the understanding of why and how those cells died. In order to understand the functions ARTD10 might have had and how it led to cell death, it had to be distinguished what kind of death these cells undergo.

The form of a cell's death can be characterized by various biochemical features as described in chapter 4.2. A list of those features and methods of detection is provided in Table 2 for apoptosis. The apoptotic phenotype is very distinct and is characterized by membrane-blebbing and apoptotic bodies, which can also be observed by light microscopy. But as stated in chapter 4.2 with new forms of cell death intermediates emerging more and more it is more suitable to characterize those forms by experimental quantification of their biochemical features.

A method widely used for determination of apoptotic cells is annexin V staining of the cells (Vermes et al., 1995). Annexin V is a protein that Ca^{2+} -dependently binds phosphatidylserine (PS), a phospholipid that is exposed on the outer cell membrane during early apoptosis [see chapter 4.2.2.1]. Using FACS a fluorescently labeled annexin V marks cells exposing PS. But as loss of membrane integrity leads to the diffusion and binding of annexin V to intracellular PS and subsequently to a false positive signal, the cells have to be counterstained with PI to exclude already dead cells. Control HFT cells as well as wt3 and GW4 were subjected to an annexin V assay to detect PS exposure. Following a three day induction of expression of ARTD10 or ARTD10-G888W the cells were trypsinized and stained with FITC labeled annexin V and PI before FACS analysis was carried out. The topoisomerase inhibitor etoposide, an agent known to induce apoptosis, was used as positive control. Figure 17A shows histograms of the annexin V signal measured by FACS with PI positive cells gated out. All three samples showed an increase in PS exposure following the etoposide treatment. Expression of wild-type ARTD10 also induced the translocation of PS to the outer membrane leaflet, though not as strong as the cytotoxic agent. Control cells and GW4 however were not affected by doxycycline addition. Compared to the positive control the actual shift was not that distinct, meaning that apparently not as much PS was exposed at the surface. The cytotoxic effect of etoposide seemed to cause a stronger apoptotic response within the cell. As the explicit pathways regarding PS exposure during apoptosis are not known conclusions on the cause cannot be made.

To further ensure the form of cell death a second biochemical approach was used. The cleavage of the bona-fide PARP ARTD1 during apoptosis by caspase-3 guarantees the shutdown of DNA repair (Lazebnik et al., 1994; Tewari et al., 1995). Processing of the 113 kD protein at D₂₁₄ results in a 24 kD N-terminal and an 89 kD C-terminal part, which can be detected using fragment specific antibodies. A western blot of ARTD1 cleavage in wt3 compared to GW4 cells is shown in Figure 17B. In wt3 cells consistent with the so far established time frame of cell death a weak signal for the 89 kD fragment at 24 h of ARTD10 induction could be seen [compare Figure 15 and Figure 16]. With continuous expression over 48 h the signal increased. The catalytic inactive mutant of ARTD10 did not cause any cleavage of ARTD1 above background. In comparison to other apoptotic stimuli like UV [Figure 22 and Figure

23] the full length ARTD1 amount seemed not to be altered, an indication that apoptosis was induced only in a subset of cells, whereas others were still viable. This was consistent with the data seen in Figure 15 and Figure 16 where depending on the experimental setup, especially the time frame, the rate of dead cells ranged from 30 to 70%.

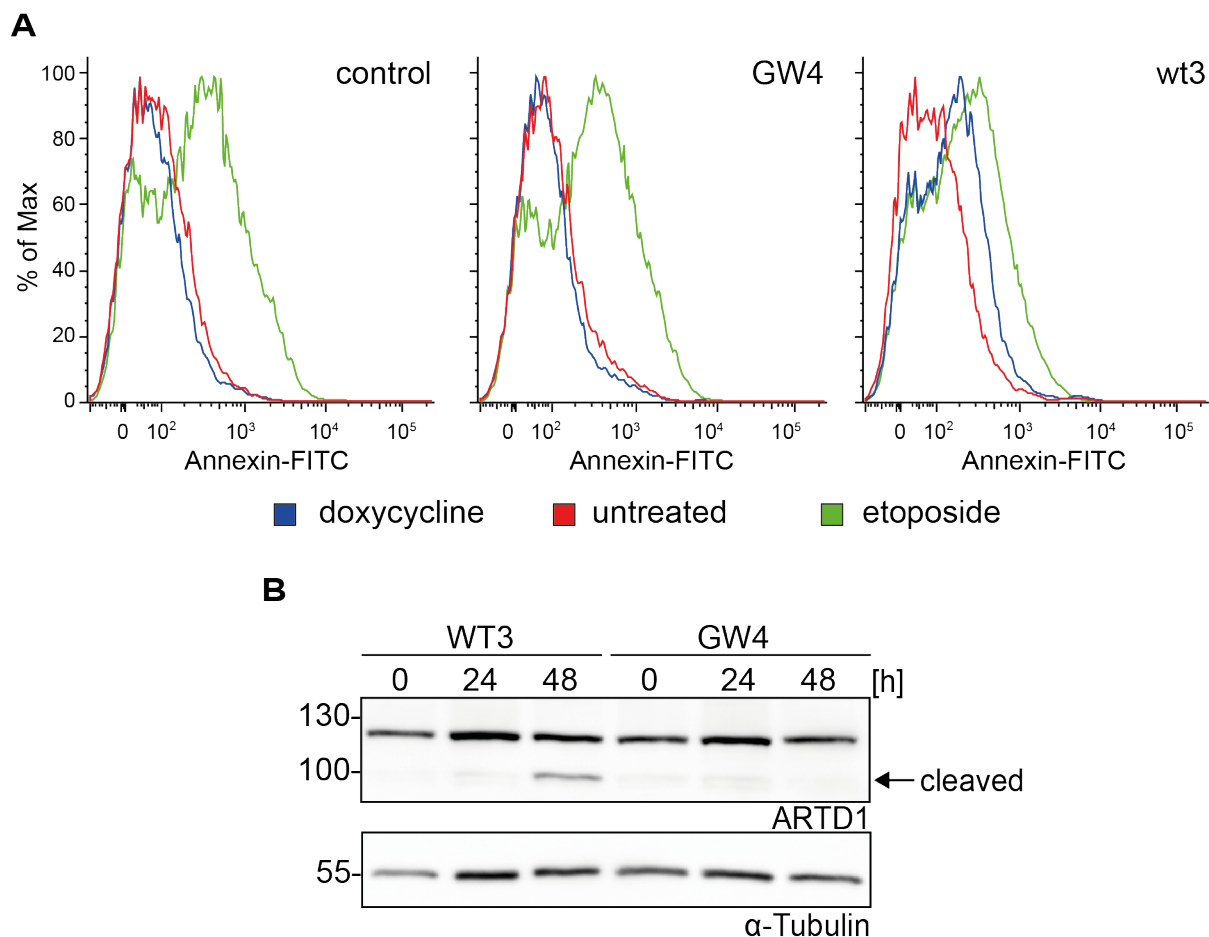


Figure 17. ARTD10 overexpression induces PS exposure and ARTD1 cleavage in HFT cells.

(A) wt3, GW4 and control cells were treated with or without doxycycline for three days. In addition the cells were treated with 20 μ M etoposide for 48 hours. The cells were then stained for annexin V and PI and analyzed by FACS. PI positive cells were gated out and histograms of the annexin-V-FITC intensity are shown.

(B) wt3 and GW4 cells were induced with doxycycline for the indicated times and the cleavage of ARTD1 analyzed by immunoblotting. The cleaved fragment of ARTD1 at 89 kD is indicated. Tubulin was detected as loading control.

With the analysis of PS exposure and activation of caspases two methods described in Table 2, the results pointed towards apoptosis as underlying mechanism of cell death. A third method was used to confirm this interpretation. Cells undergoing programmed cell death loose their DNA and nuclear integrity. Nucleosomal fragmentation and DNA degradation contribute to the lower nucleic acid content

resulting in hypodiploid cells, which can be measured in FACS analysis (Telford et al., 1991, 1992). During this assay cells were trypsinized and stained with Vybrant DyeCycle Violet stain, a DNA intercalating, fluorescent substance, which in contrast to PI is plasma membrane permeant. The molecule is taken up into the cell, binds DNA and can be subsequently used to quantify the DNA content in living cells. Histograms of the FACS analysis conducted after staining represent the cells cell cycle stages. A G_0/G_1 peak ($2n$ DNA) is followed by a broader range of cells in S-phase containing variable amounts of DNA. The right side of the cell cycle diagram shows in an additional peak the G_2 /pre-mitotic cells with double the amount of DNA ($4n$ DNA). Counted events outside this cell cycle area are cell aggregates, hyperploid cells or at lower intensity cell debris and hypodiploid cells. After exclusion of the cell debris by size the hypodiploid population, appearing in the so-called sub- G_1 peak left from the $G_{0/1}$ peak, can be quantified. Using this assay with wt3 and GW4 cells a normal cell cycle distribution with all three phases could be observed [Figure 18]. The impact of ARTD10 expression on those cells was monitored over 2 days. Whereas the GW4 cell cycle did not show any change during the experiment time frame, the wild-type samples showed a loss of viable cells and the appearance of the above-mentioned sub- G_1 peak with up to 20% of apoptotic cells.

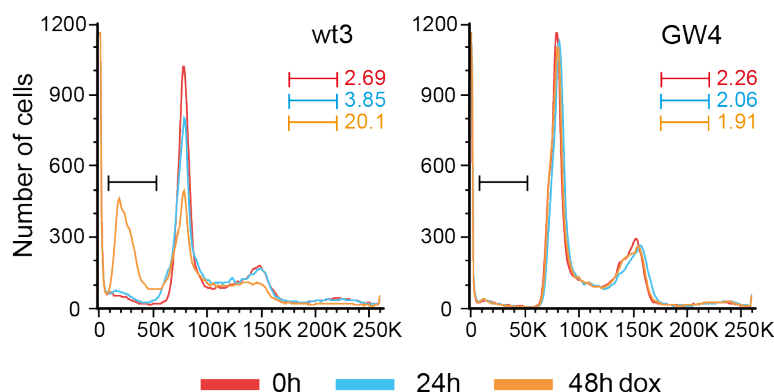


Figure 18. ARTD10 overexpression induces the formation of a sub-G1 peak.

wt3 and GW4 cells were induced for ARTD10 expression for the indicated times. The DNA content was stained with Vybrant DyeCycle Violet stain and the cells were analyzed using FACS. Representative histograms are shown with percentages of cells in the sub-G1 peak.

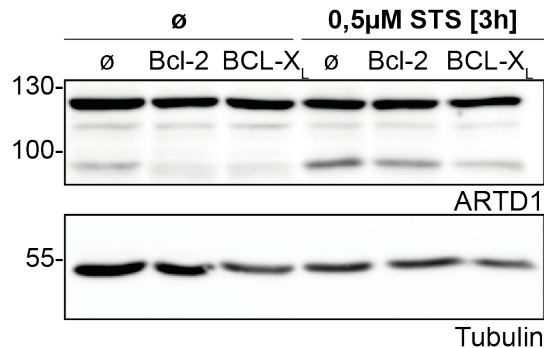
With the detection of the sub-G1 peak, indicating DNA breakdown, the cleavage of ARTD1 by caspases and the PS exposure, three independent biochemical methods confirmed hallmarks of apoptosis. Although more methods are available to verify

apoptosis further [Table 2], it can be stated that expression of ARTD10 induces apoptosis in HeLa cells, an outcome that is not visible with the catalytically inactive mutant.

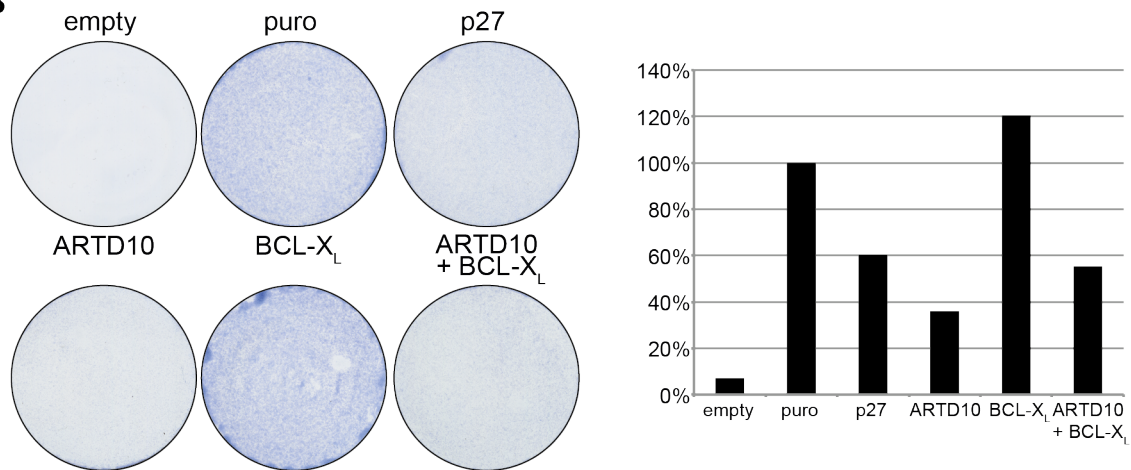
In a first approach to obtain insight into how ARTD10 induces apoptosis, colony formation assays were conducted after transfection of two anti-apoptotic BCL-2 family members, namely BCL-2 as well as BCL-X_L. To control their function, the proteins were overexpressed in HeLa cells, the intrinsic pathway was induced by addition of staurosporine and apoptosis was monitored subsequently by detection of ARTD1 cleavage [Figure 19B]. Especially BCL-X_L was able to reduce the cleavage of ARTD1 and was therefore used in a further colony formation experiment. BCL-X_L as member of the BCL-2 family belongs to their pro-survival subgroup, which contain all four BH domains and function as antagonists to the BH1-3 proteins by binding to BAX/BAK and inhibition of their pore forming abilities (Cheng et al., 2001; Ruffolo and Shore, 2003; Strasser, 2005). BCL-X_L is also able to inhibit apoptosis when BAX/BAK binding is impaired through mutations, potentially through the ability to bind tBID, BIM or BAD (Cheng et al., 1996; Cheng et al., 2001). Use of BCL-X_L resulted in an increase of colony numbers around 20% when it was co-expressed with HA-tagged ARTD10 in HeLa cells [Figure 19B]. To transfer these results to the HFT cells and at the same time facilitate the quantification, wt3 cells were seeded, transfected with BCL-X_L or the correspondent backbone vector and let grown for 5 days with or without induction of ARTD10 expression. Finally cells were counted using the CASY cell counter. Expression of BCL-X_L in those cells led to an increase of more than 2 times the cell number. This effect could also be observed when ARTD10 expression was induced [Figure 19C]. To better compare the reduction of cell number the results for the samples without BCL-X_L were set to 100 % and plotted accordingly [Figure 19C, right panel]. The population of surviving cells was with 33 % in the sample expressing BCL-X_L 10 % higher than in the sample lacking the anti-apoptotic protein. Although the effects were rather small, cell growth was recovered to a certain extend when BCL-X_L was overexpressed. This suggests at least in part the involvement of the mitochondrial pathway of apoptosis. Although no external stimuli were applied to the HFT cells it is still possible that ARTD10 engages the extrinsic apoptosis pathway downstream of those receptors, circumventing the intrinsic pathway. Additional

experiments with other members of the BCL-2 or IAP family or inhibitory proteins like FLICE would facilitate further interpretations.

A



B



C

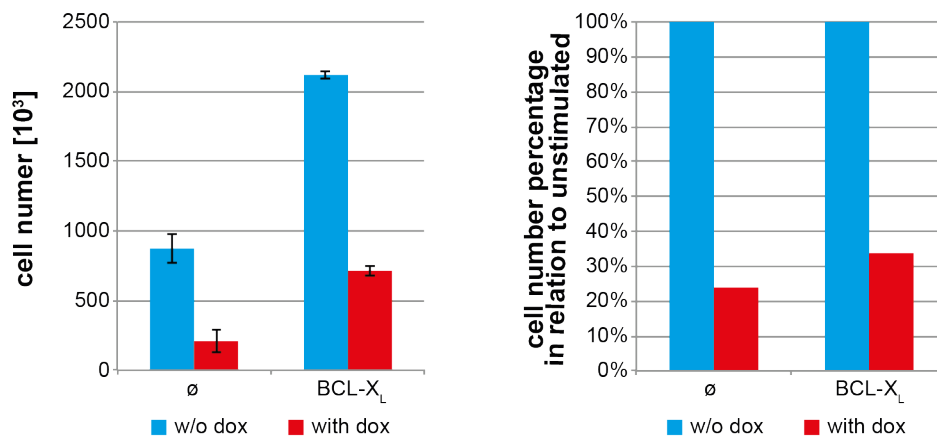


Figure 19. BCL-X_L partially rescues the apoptotic effect of ARTD10.

(A) HeLa cells were transfected with plasmids expressing BCL-2 or BCL-X_L and apoptosis was induced by addition of staurosporine for 3 hours. ARTD1 cleavage was monitored using SDS-PAGE and western blotting.

(B) Colony formation assay showing HeLa cells transfected either with pBabePuro and pEVRF0-HA-ARTD10 alone or in combination with pMSCV-BclXL-GZ, a mammalian expression vector for the anti-apoptotic protein BCL-X_L. Cells without transfection (empty) and cells transfected with a p27 expression plasmid were used as controls. The cells were stained with methylene blue and subsequently quantified (right panel).

(C) HFT wt3 cells were transfected with either pH2B-YFP or pMSCV-BclXL-GZ with and without the induction of ARTD10 expression. After 4 days the cells were counted (left panel). To focus on the BCL-X_L effect cell numbers were calculated in relation to the uninduced sample (right panel). The experiment was performed in triplicates.

The question of how ARTD10 induces apoptosis is still in need of further investigations, but several findings help to link ARTD10 to apoptotic events observed in other fields of molecular research. An interaction that was found recently describes the partial co-localization of ARTD10 with p62/SQSTM1, an adapter protein that links poly-ubiquitinated proteins to autophagosomes (Johansen and Lamark, 2011; Kleine et al., 2012). Its interaction with LC3-II and its UBA domain are essential for this function, the latter of which is also required for the mentioned ARTD10 co-localization (Kirkin et al., 2009). This connection to autophagy has still to be elucidated and possible implications of ARTD10 on autophagy or whether the interaction is due to turnover of ARTD10 is not yet known. However p62 apart from its function in autophagy was initially characterized as molecule involved in signaling processes of cell survival and apoptosis through its ability to oligomerize and bind poly-ubiquitin chains (Moscat and Diaz-Meco, 2009). In inflammatory pathways mediated through ligands like IL-1 β and TNF- α p62 is a critical factor in propagating the NF- κ B signal. Binding and clustering of RIP-1 and TRAF6 in p62-speckles facilitate the propagation (Sanz et al., 2000; Sanz et al., 1999). During IL-1 β signaling p62 positively influences the auto-ubiquitination of TRAF6 and thereby the following downstream events [Figure 20] (Sanz et al., 2000). Recently established data revealed that ARTD10 is also linked to NF- κ B signaling. Overexpression of the protein leads to a decrease in NEMO ubiquitination (a TRAF6 substrate), blocked p65 translocation to the nucleus and repressed NF- κ B target gene expression (Verheugd et al. submitted). Co-immunoprecipitation experiments in addition show a weak interaction with p62, but where performed without any stimuli to the cells (Kleine et al., 2012). At this point it is worth mentioning that p62 was not confirmed as target of ARTD10. Taken together the data could explain the apoptotic effect in HeLa cells, as the NF- κ B pathway regulates proliferation and apoptosis and is upregulated in many tumors (Rayet and Gelinas, 1999). A shutdown of any residual NF- κ B activity in those cells through ARTD10, either direct through inhibition of NEMO ubiquitination or through a possible influence on p62, enhanced by the local enrichment of interaction in p62/ARTD10 bodies, could possibly result in the observed cell death.

p62 is also connected to TRAIL, an apoptosis inducing ligand, that stimulates the extrinsic pathway through formation of the DISC involving the initiator caspase 8 (Wilson et al., 2009). Upon ligand binding the caspase activation is amplified through p62 in a mechanism similar to the one described above for NF- κ B [Figure 20]. The E3 ligase CUL3 poly-ubiquitinates the recruited caspase-8, p62 binds through its UBA domain and aggregates the caspase in the former mentioned speckles, leading to enhanced activation (Jin et al., 2009; Moscat and Diaz-Meco, 2009). Although in the stable HeLa cells no external death stimulus is applied and caspase-8 might not be ubiquitinated, the p62-speckles as signaling hubs for caspase-induction are of interest and provide another link between ARTD10 and apoptosis.

TNF signaling in contrast to TRAIL is capable of inducing an anti-apoptotic, inflammatory response as well as mediating cell death through a secondary complex (Muppidi et al., 2004). Upon stimulation a complex I is formed mediating the NF- κ B signal through the IKK complex (Zhang et al., 2000). This complex consists of the receptor itself, TRADD, RIP-1 and TRAF2. Those proteins can also dissociate together from the receptor. The death domain (DD) of TRADD, now free from TNFR DD interaction, can recruit FADD and subsequently caspase-8 building the so-called complex II, which facilitates the apoptotic response. Under normal circumstances the protein FLIP, which is expressed in response to the NF- κ B pathway, blocks the pro-apoptotic function of complex II. Failed induction of this pathway by complex I therefore would lead to sustained complex II activity and finally to apoptosis and clearing of the cell from the system (Micheau and Tschopp, 2003). Although no external TNF- α stimulation occurs in the HFT cells, the inhibiting effect of ARTD10 on NF- κ B could be enough to push residual TNF- α signaling in cell culture towards complex II activity in the stable cell lines explaining the apoptosis. All of these models could be investigated using the mentioned external apoptotic stimuli like TRAIL or TNF- α in combination with ARTD10 overexpression or knockdown to evaluate a possible increased or diminished apoptosis induction by those ligands. To exclude the toxic effect of ARTD10 itself these experiments should be conducted in different cell lines.

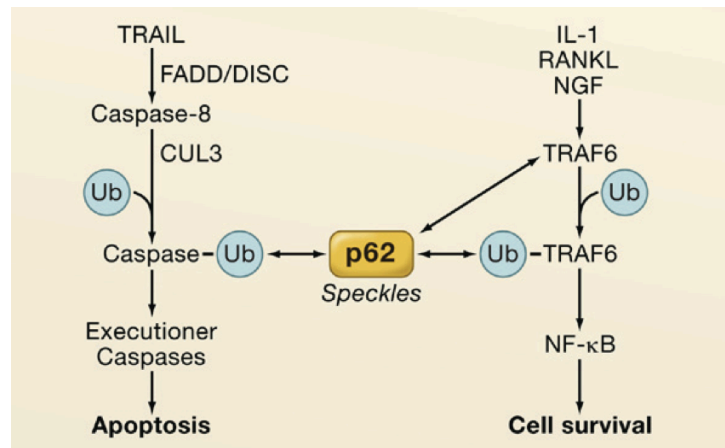


Figure 20. Implication of p62 in TRAIL and NF- κ B signaling [adapted from (Moscat and Diaz-Meco, 2009)]. K63-linked poly-ubiquitination of core components of the TRAIL and NF- κ B pathways allows the binding of p62. The adaptor protein aggregates the essential signaling molecules in hubs and potentiates interaction and the resulting signal.

Another connection between ARTD10 and p62 is based on the observation, that p62 is essential in RAS mediated tumor transformation again due to influence on NF- κ B. The activation of the pro-survival NF- κ B pathway through RAS is important during RAS-mediated transformation because it counteracts RAS-induced p53-independent cell death (Mayo et al., 1997). p62 in this pathway seems to be the link between RAS and IKK activation and subsequent downstream events, as loss of p62 reduces NF- κ B activation and transformation (Duran et al., 2008). The inhibition of oncogenic RAS-mediated transformation was also observed in a setup where ARTD10 was overexpressed in rat embryonic fibroblasts (Yu et al., 2005). The decreased transformation is not dependent on ARTD10 activity but on its localization, as the Δ NES mutant of ARTD10 abrogates this effect. An alternative mechanism apart from catalytic activity, perhaps through the interaction shown in co-immunoprecipitation experiments, seems therefore to be likely (Kleine et al., 2012). A direct inhibition of its function by modification can be excluded, as p62 could not be confirmed as ARTD10 substrate. These data reveal another interesting connection between ARTD10 and p62 in an NF- κ B pathway background and further strengthen the idea that ARTD10 regulates this signaling process resulting in decreased cell survival.

In contrast to p62, which is not modified by ARTD10, several proteins involved in mitosis regulation were identified as strong hits in our substrate screen (Feijs et al. submitted). This is especially interesting as the so-called mitotic catastrophe is an often-observed outcome of deregulated or failed mitosis, wherein the cell finally

succumbs to DNA damage or checkpoint errors. The precise definition of this process is highly discussed, but several publications link mitotic catastrophe to apoptosis, as it can show several hallmarks of the latter (Castedo et al., 2004; Kroemer et al., 2009; Vakifahmetoglu et al., 2008). As mentioned above ARTD10 modified different kinases that control mitosis in a substrate array screen, among them PLK1, Aurora-A and NEK6, all three of which are known to be involved in processes like mitotic spindle establishment or centrosome regulation. (Loffler et al., 2006; Ma and Poon, 2011; O'Regan and Fry, 2009). Deregulation of these kinases is fatal as reported by several groups and could provide a link back to ARTD10 induced apoptosis. Overexpressed dominant negative PLK-1 induces mitotic catastrophe in HeLa cells and apoptosis in several other cancer cell lines (Cogswell et al., 2000; Mundt et al., 1997). Similar observations were made for the NIMA related kinase NEK6, where depletion of the protein or the overexpression of a kinase-dead version triggers an apoptotic response in epithelial cell lines, among them HeLa (Yin et al., 2003). A model wherein apoptosis is induced by ARTD10 through a disturbed mitosis would fit to the observation that the onset of apoptosis in the HFT cells is rather late after approximately 24 hours. In addition errors during chromosome segregation and subsequent aneuploidy would only result in the death of particular cells and could explain remaining cells after several days of ARTD10 induction (Castedo et al., 2004).

In conclusion many recent findings connect ARTD10 in several ways to apoptosis inducing pathways, but still the actual point of action in one of those has to be elucidated.

5.2 ARTD10 is substrate of caspases

5.2.1 ARTD10 is cleaved by caspases during apoptosis

ARTD10 as shown in the last chapter induced apoptosis and with it the activation of caspases as seen in the ARTD1 western blot in Figure 17B. The processing of hundreds of substrates by caspases is the key to the process of programmed cell death [4.2.2.1 Caspases](Taylor et al., 2008; Timmer and Salvesen, 2007). During time course experiments with the HFT ARTD10 cells western blot analysis of the protein revealed an additional band at around 50 kD, which was only visible in the

cells expressing wild-type ARTD10 [Figure 21]. With the knowledge that ARTD10 induced apoptosis it became obvious to ask, whether the appearance of the protein band was dependent on this process and if it was really a fragment of ARTD10 or rather an artifact of the antibody. In addition the overexpression in HFT resulted in a variety of smaller fragments during western blot analysis that could be due to different transcriptional start sites or degradation. Those possibilities could be excluded for the 50 kD band, as the catalytically inactive mutant did not show this and a stabilization of the protein through one amino acid change seemed unlikely.

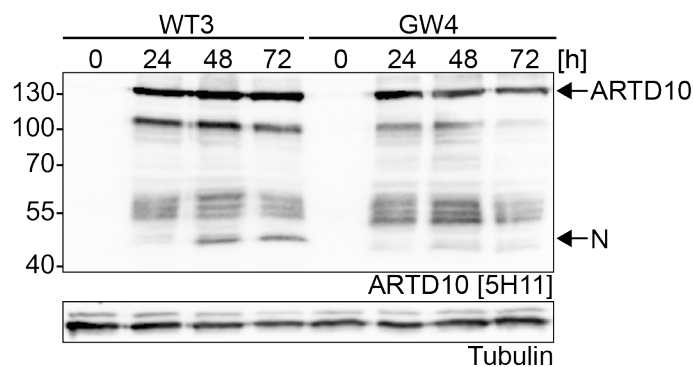


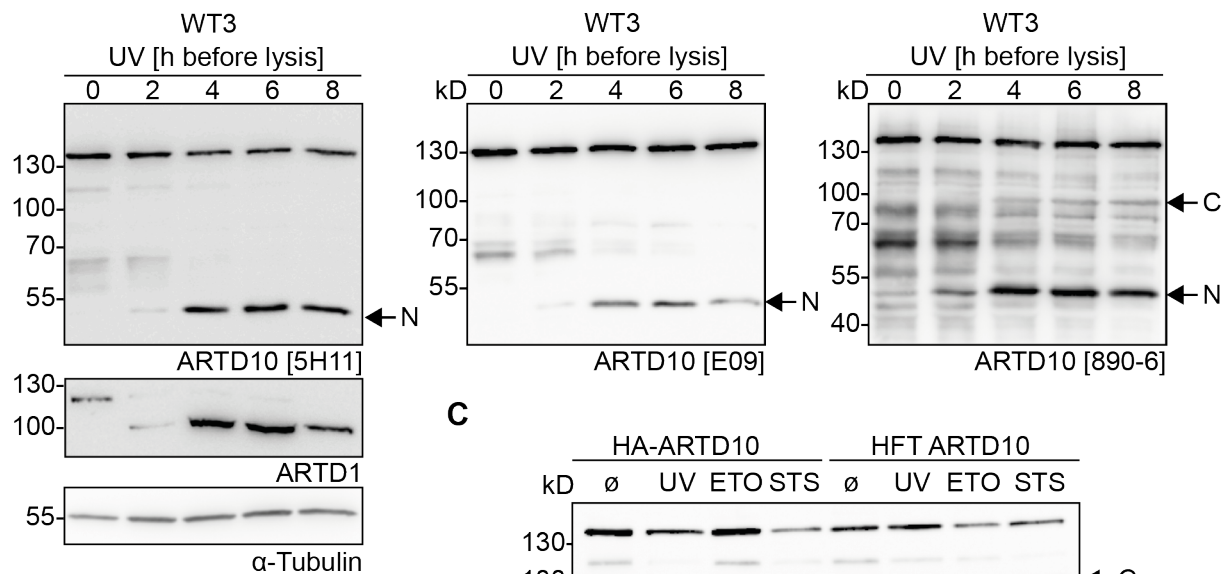
Figure 21. ARTD10 induction leads to fragment appearance.

ARTD10 expression was monitored in wt3 and GW4 cells in response to doxycycline. Expression of ARTD10 was induced for the indicated times and the samples were analyzed by immunoblotting using the monoclonal 5H11 antibody. Tubulin was detected to ensure equal loading.

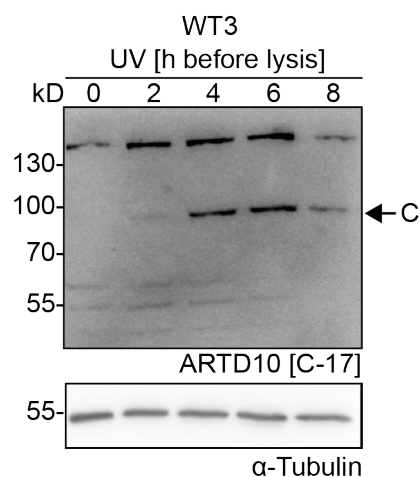
To link the fragmentation to apoptosis HFT cells expressing the wild-type form of ARTD10 were irradiated with UV light, which triggered the internal death program through massive DNA damage. Application of 20 mJ/cm² at 254 nm was sufficient to induce apoptosis in the HFT cells as monitored by ARTD1 cleavage, which appeared already 2 hours after the stimulus. The same dynamic could be seen in the case of the ARTD10 fragment [Figure 22a, left panel]. Using different mono- and polyclonal antibodies that recognize different epitopes [see Figure 3] the possibility of an antibody-related artifact could be ruled out. Recognition by the rat monoclonal antibody 5H11 suggested that it was an N-terminal fragment. Moreover the polyclonal rabbit serum 890-6, raised against amino acids 1-907, detected a second signal increasing over time at around 90 kD, which was not recognized by 5H11 [Figure 22A, right panel]. This suggested that it represented a rather C-terminal part of ARTD10 downstream of the 5H11 binding site. To verify this observation an antibody against the last 17 amino acids of ARTD10 (C-17) was used [Figure 22B]. A

protein species at the estimated size became apparent in parallel to the smaller N-terminal fragment. With the evidence of N-terminal and C-terminal protein fragments detected upon apoptosis induction, which added up to the length of the full protein, a cleavage of ARTD10 into two parts became likely. The cleavage at the same time as ARTD1 suggested that ARTD10 is a target of executioner caspases as ARTD1 is cleaved by caspase-3 and -7 (Boucher et al., 2012; Lazebnik et al., 1994).

A



B



C

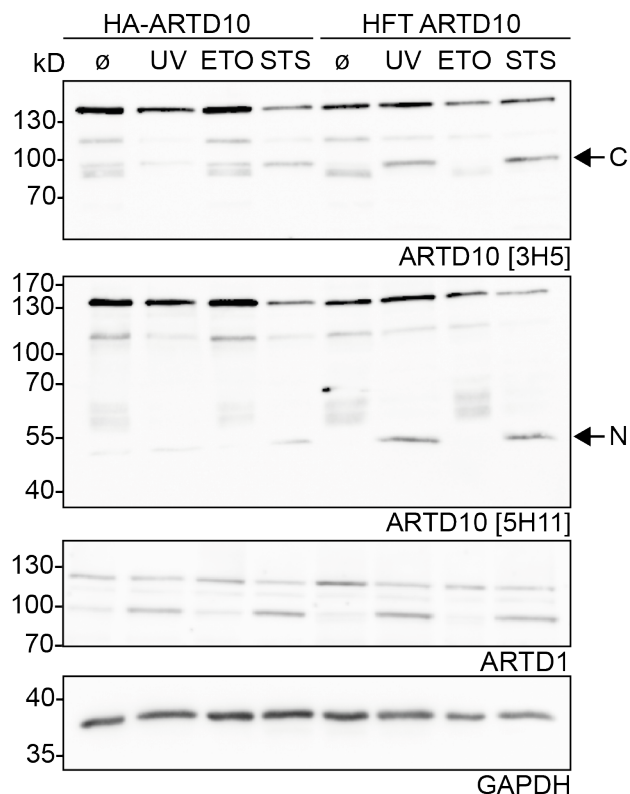


Figure 22. ARTD10 fragment appearance is consistent with apoptosis.

(A) wt3 cells with induced ARTD10 expression (16 h) were treated with UV (20 mJ/cm², 254 nm) for the indicated times. The cells were subjected to immunoblotting and ARTD10 was analyzed with the monoclonal antibody 5H11 as well as the polyclonal antibodies E09 and 890-6 (see Figure 3). The appearing of N- as well as C-terminal bands are indicated. Detection of ARTD1 was used to monitor the induction of apoptosis, whereas tubulin served as loading control.

(B) Immunoblot with samples like in (A) using a C-terminal antibody (C-17). Tubulin was detected as loading control.

(C) HeLa cells transfected with HA-ARTD10 as well as induced wt3 cells were subjected to different apoptotic stimuli (\emptyset , no treatment; UV, 100 mJ/cm² at 254 nm; ETO, 30 μ M etoposide; STS 0,5 μ M staurosporine) 6 hours prior to lysis. After immunoblotting the N- (5H11) as well as the C-terminal (3H5) fragment of ARTD10 were detected using the respective antibodies. ARTD1 cleavage was detected to ensure induction of apoptosis. GAPDH served as loading control.

To further strengthen the idea of an apoptosis dependent process additional stimuli were used to induce the death of the cell. Etoposide, the topoisomerase inhibitor already used in Figure 17A as positive control, as well as staurosporine, a broadband kinase inhibitor known to trigger the intrinsic self-destruction program, were used (Belmokhtar et al., 2001; Karpinich et al., 2002). Upon application to induced wt3 cells as well as transiently transfected HeLa cells the fragments at 50 and 90 kD appeared with staurosporine treatment similar to the findings in response to UV. Etoposide on the other hand failed to induce efficient ARTD10 cleavage [Figure 22C]. As ARTD1 analysis also did not show any cleavage in the case of etoposide, the induction of apoptosis did not seem to work in the first place.

Although the likelihood of an antibody caused artifact was limited due to different antibodies, there was still the possibility the bands being an overexpression phenomenon. To address this concern endogenous protein had to be monitored. While the HFT cells represented a good model for studies with exogenous ARTD10, the endogenous level was too low to be detected in a straight western blot. The monocytic leukemia cell line THP-1 shows higher levels of ARTD10 and was used for further characterization of its fragmentation (Tsuchiya et al., 1980). As those cells grow in suspension apoptosis was induced with staurosporine and ARTD10 fragments were monitored over 8 hours using western blot analysis [Figure 23A]. Consistent with the previous overexpression studies 4 hours after the apoptotic stimulus ARTD1 processing as well as fragmentation of ARTD10 could be observed. In contrast to the exogenous protein, which seemed to be resynthesized very rapidly, the amount of full length ARTD10 decreased with the appearance of the fragments. The fragments themselves were stable during the time course of the experiment. Similar to Figure 22A/B the protein fragments stayed visible up to the last time point at 8 hours. The drawbacks of the polyclonal 891-6 serum were numerous background bands and a weak signal for the bigger fragment and therefore monoclonal antibodies with epitopes in the N- (5H11) and C-terminus (3H5) were

used [Figure 23B]. As equal irradiation with UV light was not applicable to suspension cells, etoposide as another stimulus was used. Both treatments were able to induce the same ARTD10 fragmentation with an N- and C-terminal fragment [Figure 23B] and seemed to be sufficient to induce apoptosis in THP-1 cells.

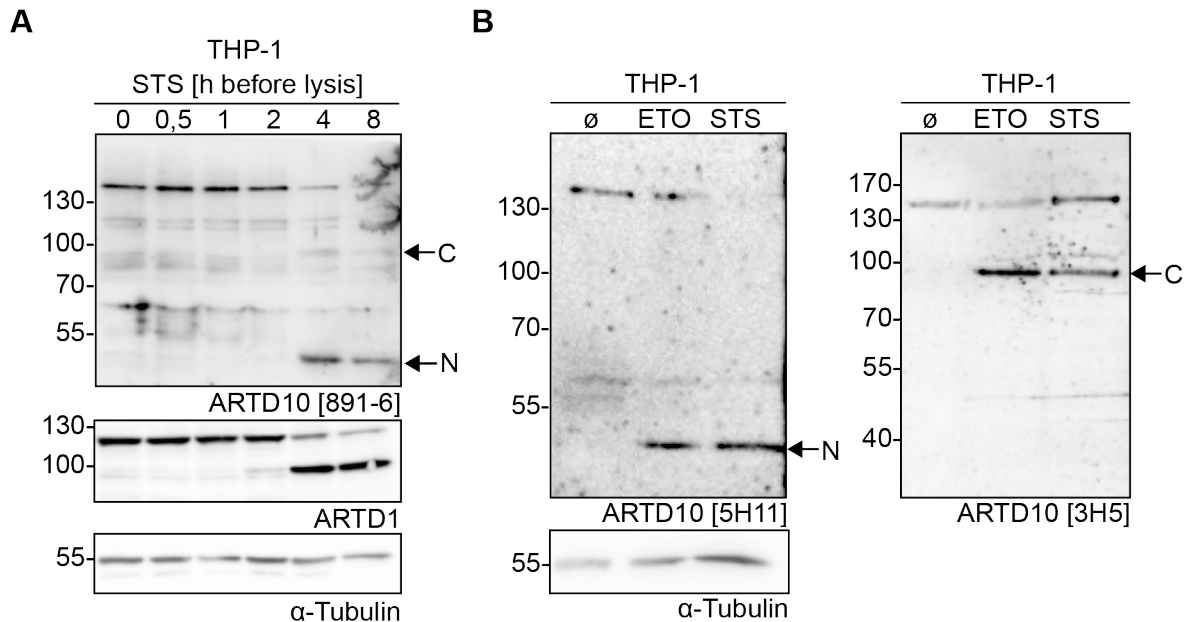


Figure 23. Induction of apoptosis leads to ARTD10 fragmentation in THP-1.

(A) Apoptosis was induced in THP-1 cells by application of staurosporine (1 μ M) for the indicated times. Endogenous ARTD10 was analyzed by immunoblotting using the polyclonal 891-6 antibody. ARTD1 was detected to monitor induction of apoptosis, whereas α -tubulin detection served as loading control. The N- as well as the C-terminal ARTD10 fragment are indicated.

(B) In addition to staurosporine another set of cells was treated with 30 μ M etoposide for 3 h. ARTD10 was analyzed after immunoblotting where it was detected by an N- (5H11) and C-terminal (3H5) monoclonal antibody. The appearing fragments are indicated. The detection of α -tubulin served as loading control.

The results of the experiments shown in Figure 22 and Figure 23, i.e. the decrease of endogenous ARTD10 and the fact that two fragments complementary in size appeared simultaneously with ARTD1 cleavage, pointed towards proteolytic cleavage during apoptosis. To validate that ARTD10 is processed by caspases, the proteolytic key factors during apoptosis, the pan-caspase inhibitor Z-VAD-fmk was used to inactivate those enzymes [Figure 24]. Z-VAD-fmk is a cell permeant peptide inhibitor that inside the cell irreversibly binds to the catalytic site of caspases rendering them inactive and thereby preventing apoptosis (Zhu et al., 1995). HeLa cells transiently transfected with HA-tagged ARTD10 as well as induced wt3 cells were irradiated with UV to induce apoptosis with and without the simultaneous application of the inhibitor

to the medium. The cells were harvested and analyzed using SDS-PAGE and western blotting.

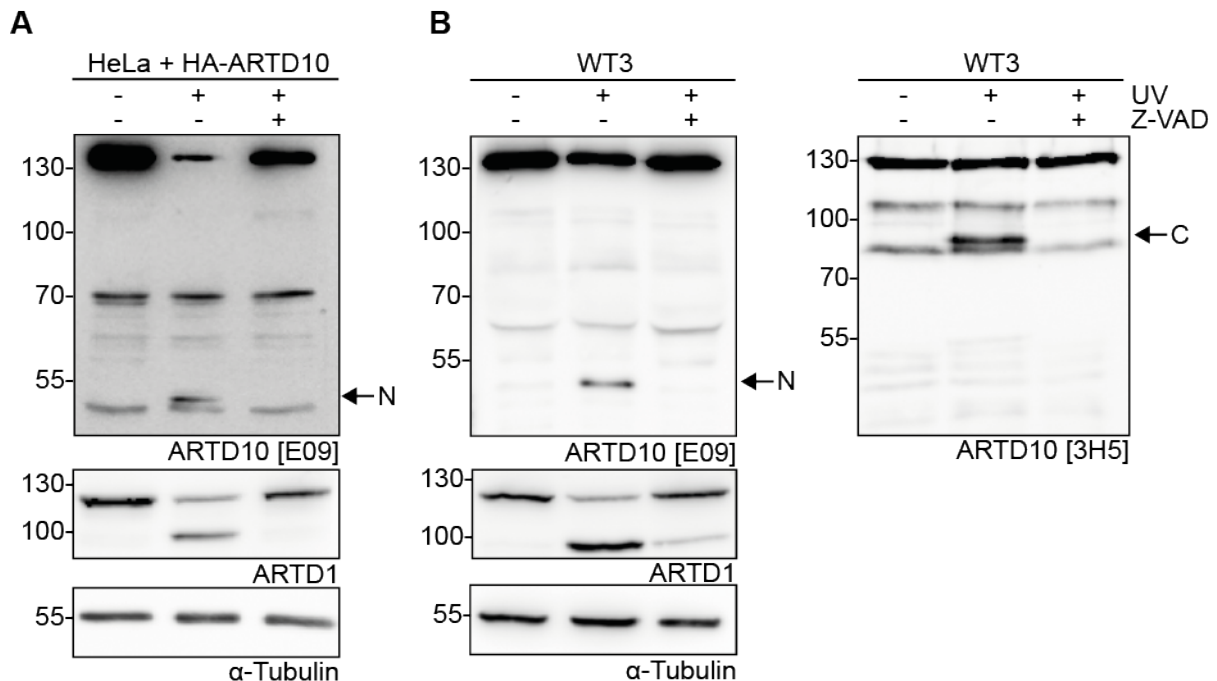


Figure 24. Fragmentation of ARTD10 is blocked by the caspase inhibitor ZVAD-fmk.

(A) Apoptosis was induced in HeLa cells transfected with pEVRFO-HA-ARTD10 using UV (20 mJ/cm² at 254 nm) 4 h prior to lysis. Caspases were blocked using the inhibitor Z-VAD-fmk (20 μM). ARTD10 was detected using the polyclonal E09 antibody. ARTD1 detection served as monitor for apoptosis induction and α-tubulin detection was used as loading control.

(B) HFT wt3 cell were treated like described in panel (A). In addition to the N-terminal fragment, the bigger C-terminal part was detected using the 3H5 antibody.

ARTD1 cleavage as positive control for the induction of apoptosis could be observed in both cases [Figure 24A/B]. As expected both fragments, as detected by N- (E09) and C-terminal (3H5) antibodies, appeared in parallel to ARTD1 processing [Figure 24B]. Application of Z-VAD-fmk to the cells abolished ARTD1 fragmentation in normal HeLa as well as HFT cells [Figure 24A/B]. At the same time both ARTD10 fragments vanished, leading to the assumption that indeed ARDT10 was targeted by caspases during the apoptotic process. The emerging question as to which caspase was responsible will be addressed in the next chapter.

5.2.2 ARTD10 is target of caspase 1,6 and 8 *in vitro*

ARTD10 was cleaved during apoptosis, a process in which the initiator as well as executioner caspases are fundamentally important (Fan et al., 2005). Although the third group of inflammatory caspases [Table 3] is not involved in apoptotic cell death, all caspases were purchased as purified proteins in order to conduct *in vitro* caspase cleavage assays. In a first assay *in vitro* purified TAP-tagged ARTD10-G888W was used as substrate and incubated in the suitable caspase reaction buffer with each caspase. The samples were separated by SDS-PAGE and subsequently blotted to detect the N-terminal ARTD10 fragment using the monoclonal antibody 5H11. Caspases 1, 6, 7 and 8 seemed to be able to cut, but only caspases 1, 6 and 8 showed a fragment of the expected size at around 50 kD comparable to the *in vivo* recognized fragment [Figure 25A]. Caspase-1 produced an additional piece at 70 kD, whereas the incubation with caspase-7 resulted only in one large fragment at 110 kD. It was not possible to detect the corresponding C-terminal fragments with the antibodies available. Further degradation or instability could be the cause of this. In addition the potential of the *in vitro* purified caspases to cleave a substrate was dependent on its origin. Immunoprecipitated endogenous ARTD10 from THP-1 was only cut by caspase-1 at a second site or by caspase-6 [Figure 26]. This could be due to *in vivo* modifications or different folding of ARTD10, which prevented the cleavage.

The conducted experiments however showed that full length ARDT10 was *in vitro* targeted by caspases 1, 6 and 8 most likely at the same site, whereas caspase-7 only and caspase-1 additionally cleaved at a secondary site.

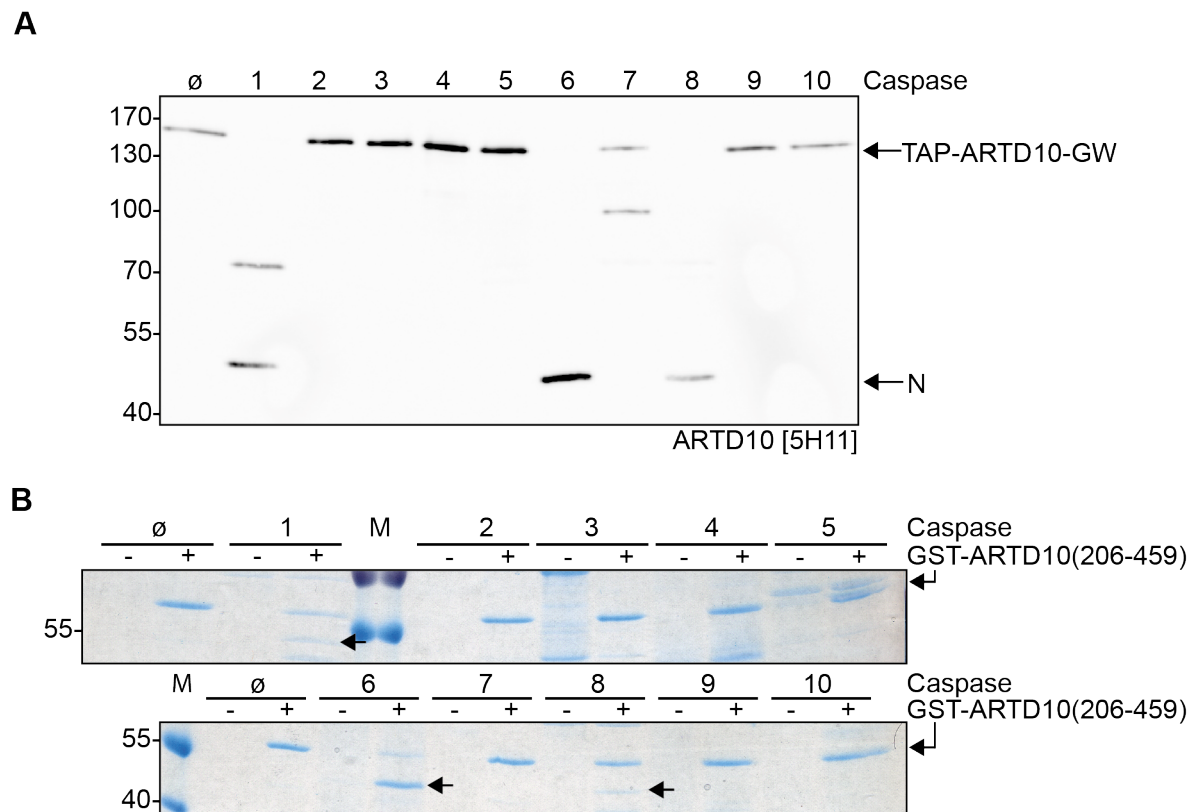


Figure 25. *In vitro* caspase assay with purified TAP-ARTD10-GW and GST-ARTD10 fragments.

(A) *In vitro* caspase assay with TAP-tagged ARTD10-G888W and recombinant caspases. The assay was stopped with addition of sample buffer and subjected to gel electrophoresis and immunoblotting with the N-terminal 5H11 antibody. The *in vivo* observed fragment is indicated.

(B) *In vitro* caspase assay with a GST tagged recombinant fragment of ARTD10 containing the amino acids 206-459 and recombinant caspases. The assay was stopped using sample buffer and proteins were separated by SDS-PAGE and stained with coomassie brilliant blue. Arrows indicate cleaved proteins.

As only the 50 kD fragment could be observed *in vivo*, the focus turned to finding this specific restriction site. The size of the fragment and recognition by the 5H11 antibody, which recognized an epitope between amino acids 259 and 408, led to the conclusion that the cleavage occurred C-terminal of amino acid 400. To confirm this a GST-purified ARTD10 fragment of amino acid 206-459 was used in a caspase assay. Control samples without GST-protein were run to ensure that bands resulted from cleavage, as the protein background in the acquired caspases was high. The experiment showed that indeed incubation with caspases 1, 6 and 8 resulted in a truncated form of the protein, which was around 5-7 kD smaller and predominantly produced by caspase-6 [Figure 25B]. This was in line with the caspase assay performed with TAP-purified protein. The fact that Caspase-7 did not process the GST-fragment was expected, as the larger fragment suggested a cleavage site not present within the used protein. The same was true for the larger fragment observed

using caspase-1. Nonetheless the experiment helped to narrow down the major cleavage site to a region around amino acid position 420.

Until now ARTD10 was tagged, overexpressed and purified from *E. coli* and HEK293 cells. In follow up experiments endogenous protein was immunoprecipitated from THP-1 cells and subsequently used in caspase assays to obtain the protein in its most natural condition. In contrast to the experiments before incubation of the protein with caspase-1 only resulted in the larger 70 kD fragment whereas the 50 kD fragment could only be produced using caspase-6. None of the other utilized caspases resulted in cleavage of immunoprecipitated ARTD10 [Figure 26]. An explanation could be conformational changes of the protein due to longer purification times, different buffers or storage, when one compares the immunoprecipitation with TAP-purification protocols. An unnatural folding could prevent recognition and cleavage. Although a possibility, the repeated use of TAP-purified protein in PARP assays showed that ARTD10 is active and the TAP-purification as a method used to identify interaction partners suggests a natural confirmation within these conditions. Phosphorylation as posttranslational modification could also block cleavage site recognition in ARTD10 like it is the case for BID or other caspase substrates (Desagher et al., 2001; Duncan et al., 2011). Such modifications could be lost while preparing and storing the sample rendering the cleavage site accessible for less active or less specific caspases.

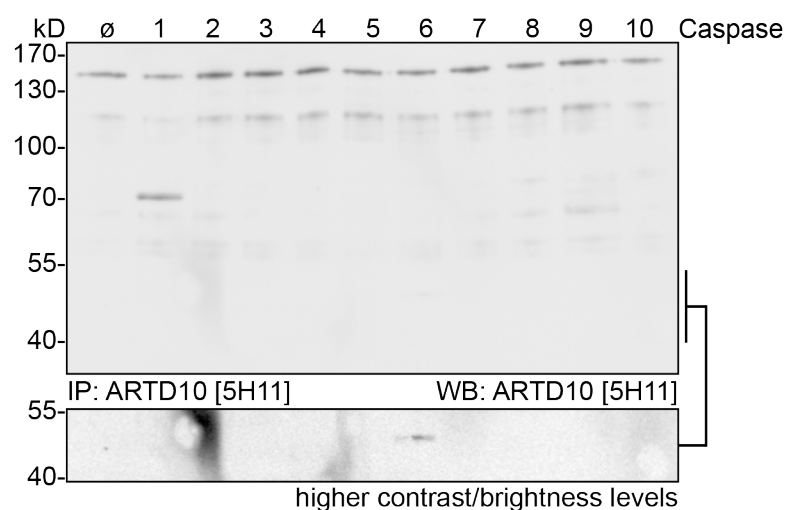


Figure 26. *In vitro* caspase assay with immunoprecipitated ARTD10 from THP-1.

THP-1 cells were used to immunoprecipitate endogenous ARTD10, which was subjected to a caspase assay with recombinant caspases. After separation in SDS-PAGE and western blotting, ARTD10 and its fragments were detected using the 5H11 antibody.

Regarding the efficiency of cleavage during these experiments one has to bear in mind that the purchased caspases are not very pure and concentration variations are very likely. In addition substrate priorities and assay conditions play a role in caspase activity. To at least ensure that the specific tubes contained the advertised caspases 4 of them were subjected to SDS-PAGE and western blotting and detected with specific antibodies. All antibodies recognize either the p20 or p10 subunit of the active caspase and all showed a signal with their respective target [Figure 27]. As there is no information by the supplying company on the constructs and eventual tags to purify the caspases further statements on the quality cannot be made.

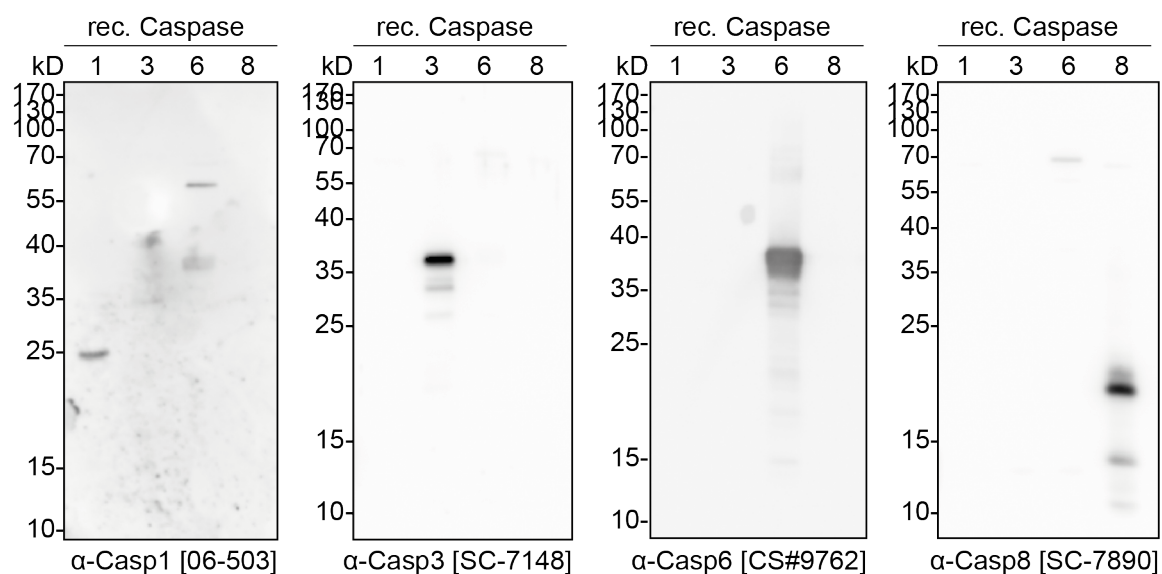


Figure 27. Immunoblot to control recombinant caspases.

Recombinant caspases 1, 3, 6 and 8 were run in SDS-PAGE and blotted before detection with specific antibodies. Location of epitopes: 06-503: p20-subunit; SC-7148: p20-subunit; CS#9762: p15-subunit; SC-7890: p18-subunit.

Although it needs further testing, especially in cells using knockouts or specific inhibitors of single caspases, caspase-6 seemed to be a promising candidate for the apoptotic processing of ARTD10. As there are concerns using inhibitors to discriminate between caspases due to low specificity, it is good that small molecule inhibitors are emerging which will be more suitable to the task (Chu et al., 2009; McStay et al., 2008). Caspase-6 was identified as ced-3 related protein MCH-2 and later classified as executioner caspase, which is responsible for the cleavage of nuclear lamins (Fernandes-Alnemri et al., 1995; Orth et al., 1996). Similar to caspase-3 and -7 during activation the short pro-domain as well as the linker domain

are separated through cleavage at three different sites from the p20 and p10 subunits, which form the active caspase. In contrast to the other effector caspases caspase-6 is also able to auto-activate, a unique ability, the function of which is still unclear (Klaiman et al., 2009; Wang et al., 2010). Apart from lamins more than 60 proteins have been reported over time to be target of caspase-6 (Graham et al., 2011). Among those are structural proteins like alpha-tubulin, NuMa or lamin A, signaling proteins, transcription factors like NF- κ B (p65) as well as the bona-fide executioner targets like ARTD1 (Hirata et al., 1998; Orth et al., 1996). The cleavage results in the typical apoptotic phenotype like breakdown of the cytoskeleton and nuclear matrix, shutdown of DNA repair and inhibition of anti-apoptotic signaling (Levkau et al., 1999). Interestingly caspase-6 also processes proteins of the autophagy machinery like ATG3 and ATG6 as well as p62, the autophagic adapter protein, which was recently shown to co-localize with ARTD10 in dynamic bodies (Kleine et al., 2012; Norman et al., 2010). Given a possible implication of ARTD10 in the autophagy process, its cleavage together with other key players in the autophagic process by the same caspase seems probable. The same is true for ARTD10 and the NF- κ B pathway where a link is also provided by p62 as discussed earlier [see 5.1.3].

The knowledge on caspase-6 has extended over the last decade, especially its implication in neuronal development and associated neurodegenerative diseases. During development of the nervous system inappropriate axons and redundant neurons are eliminated (Buss et al., 2006; Luo and O'Leary, 2005). Whereas caspase-3 is mainly responsible for disassembly of the neuronal body, caspase-6 was shown to be the mediator of axon degeneration, a process that shows hallmarks of apoptosis like membrane blebbing and fragmentation (Graham et al., 2011; Nikolaev et al., 2009). This essential role in neurons also ties caspase-6 to neurodegeneration in Alzheimer's, Huntington's and Parkinson's syndrome (Graham et al., 2011). Relevant proteins in those diseases like htt and TAU are caspase-6 substrates and high expression and activation of the protease can be seen in affected tissues (de Calignon et al., 2010; Graham et al., 2010; Graham et al., 2011). Low amounts of ARTD10 mRNA were detected in the brain in a tissues screen using northern blotting (Yu et al., 2005). But especially this could render such tissues susceptible to elevated ARTD10 levels, as HeLa cells and the HFT cells used

throughout our experiments also showed no detectable endogenous protein in a western blot. These small amounts of ARTD10 are nonetheless essential for the cells, as knockdown of ARTD10 also reduces colony formation (Feijs, 2009). Processing of ARTD10 by caspase-6 in neuronal tissues could hint towards the importance of ARTD10 homeostasis in healthy cells and link ARTD10 to processes not necessarily involved in apoptosis.

5.2.3 Definition of the caspase-6 cleavage site

Experiments using *in vitro* caspase assays and antibodies recognizing different epitopes of ARTD10 located the *in vivo* caspase cleavage site to a position around amino acid 420 [5.2.2]. As caspases prefer an aspartate at position P1 [see 4.2.2.1] the sequence of ARTD10 was examined for potential restriction sites. Only a single aspartate at position 406 is present in ARTD10-(263-464). Hydrolysis at D₄₀₆ would be consistent with the observed size of the fragments in apoptotic cells and the products both seen with full length and the GST-tagged part of ARTD10 [Figure 25]. Although caspases are reported to also cleave after glutamates, the majority prefers an aspartate at position P1 (Krippner-Heidenreich et al., 2001; Stennicke et al., 2000). The confirmation of the site D₄₀₆ was approached by site directed mutagenesis of this residue to a glycine, which is known to abolish caspase-mediated processing (Bischof et al., 2001). HeLa cells were transiently transfected with HA-ARTD10 and HA-ARTD10-D406G and subsequently apoptosis was induced with UV irradiation or staurosporine. Z-VAD-fmk was used to demonstrate the caspase dependence. The cells were lysed and analyzed by SDS-PAGE and western blotting using a tubulin antibody as loading control and an ARTD1 antibody to indicate the induction of the caspase cascade [Figure 28]. As expected staurosporine [middle panel] as well as UV treatment [right panel] resulted in the appearance of the N-terminal ARTD10 fragment in cells containing HA-ARTD10, which was abolished when caspases were inhibited by Z-VAD-fmk. Processing of ARTD1 was not inhibited to the same extent, but a clear reduction was visible. In the case of the mutated ARTD10 no cleavage band could be observed with either of the apoptotic stimuli, leading to the conclusion that amino acid D₄₀₆ is indeed the *in vivo* target site of caspases.

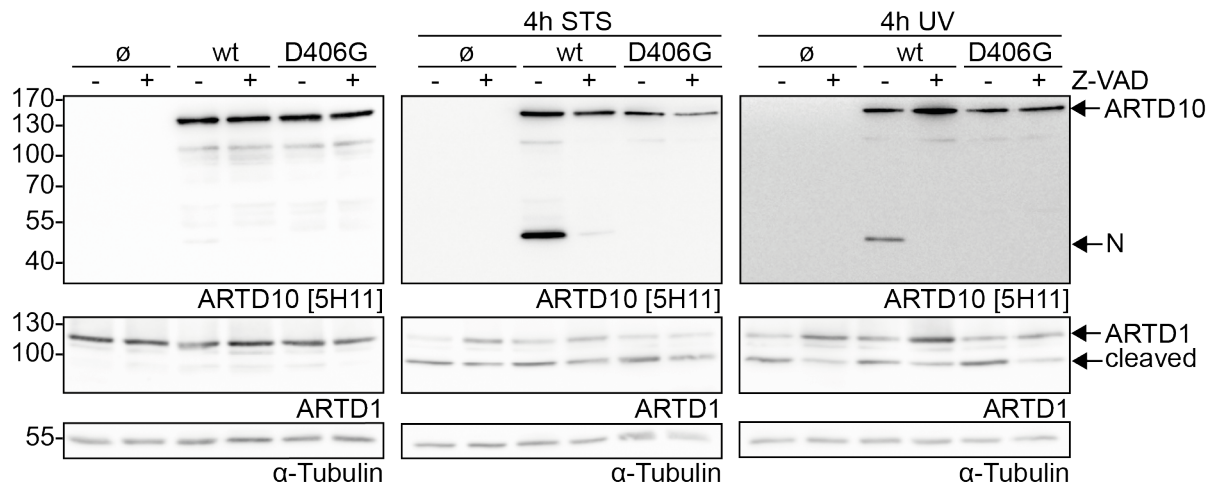


Figure 28. *In vivo* test of suspected caspase restriction site at D₄₀₆.

HeLa cells expressing HA-ARTD10 or HA-ARTD10-D406G or control cells were treated with either staurosporine (1 μ M) or UV (20 mJ/cm² at 254 nm) to induce apoptosis or left untreated. In addition cells were incubated or not with Z-VAD. ARTD10 expression was analyzed with the 5H11 monoclonal antibody. Apoptosis induction was monitored using an ARTD1 antibody and α -tubulin was detected as loading control.

Experiments in 5.2.2 showed that the caspases cleaving ARTD10 were somehow connected to the source of the protein. TAP-tagged exogenous protein was targeted by caspases 1, 6, 7 and 8, whereas immunoprecipitated ARTD10 was only cleaved by caspase-1 and -6. In addition the second fragment seen for caspase-1 in Figure 25A also did not appear. To clarify the type of involved caspase the new mutant D406G was now tested in an *in vitro* caspase assay with immunoprecipitated HA-tagged ARTD10. As TAP-tagged ARTD10 was produced in HEK293 cells those were additionally used to express the protein and see if the sensitivity to specific caspases was dependent on the cell line. The wild-type protein as well as the D406G mutant were immunoprecipitated with an HA-tag antibody (3F10) and subsequently used in caspase assays with caspases 1, 6, 7 and 8. The protein and fragments thereof were detected by western blot analysis using the N-terminal antibody 5H11. The observations confirmed those seen with immunoprecipitated endogenous ARTD10 in Figure 26. Regardless whether the proteins were obtained from HeLa or HEK293 cells, only caspase-6 caused the 50 kD fragment seen *in vivo*, whereas caspase-1 showed furthermore the band at 70 kD [Figure 29, left panels]. No processing of ARTD10 could be observed with either caspase-7 or -8. The use of the ARTD10-D406G mutant abolished the cleavage by caspase-6 whereas the fragment produced by caspase-1 was still present [Figure 29, right panels]. Signals seen with caspase-7 and -8 and ARTD10 immunoprecipitated from HeLa cells were probably background, as they do not appear in any of the other blots [Figure 29, upper right panel]. Taken

together one can conclude that *in vitro* caspase-6 is the main responsible caspase for cleavage at position D₄₀₆, the site also targeted in exogenous ARTD10 upon induction of apoptosis. Caspase-1 however processed ARTD10 at a different site *in vitro*, an activity that has yet to be shown in cells.

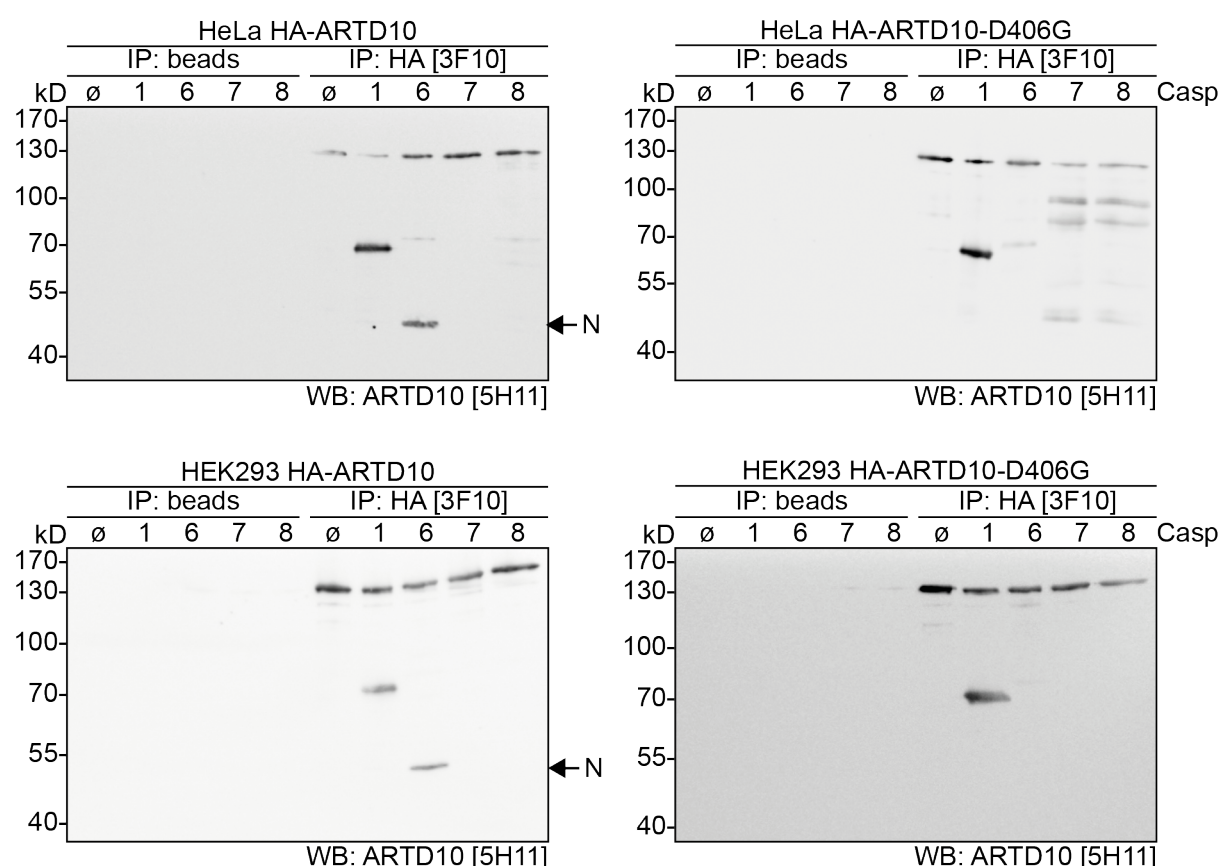


Figure 29. *In vitro* caspase assay with ARTD10 and ARTD10-D406G from HEK293 and HeLa.

HA-ARTD10 and HA-ARTD10-D406G were immunoprecipitated from lysates of transiently transfected HEK293 and HeLa cells. The immunoprecipitated proteins were subjected to an *in vitro* caspase assay with the indicated caspases and subsequently analyzed by western blotting using the N-terminal 5H11 antibody. The N-terminal fragment produced by caspase-6 is indicated.

The full cleavage site from P4 to P2' is 'I A M D₄₀₆ / S P' for the caspase-6 site. As stated before the serine following the aspartate could be a point of regulation regarding recognition and cleavage. Several targets of caspases like BID, Max, or PTEN are phosphorylated within their cleavage site, influencing their processing (Desagher et al., 2001; Krippner-Heidenreich et al., 2001; Torres et al., 2003). The protein kinase CK2 is responsible for those phosphorylations and Duncan et al. took this as opportunity to summarize the implications of the overlap of kinase consensus sites with known caspase cleavage sites (Duncan et al., 2010). This kind of cleavage control could also be the case for ARTD10. The serine/proline combination is

common in motifs of kinases and among those are for example ERK2 and CDK1/2 (Duncan et al., 2010; Schweigreiter et al., 2007). The latter was also reported to phosphorylate ARTD10 at T₁₀₁, a modification that was connected to altered localization in the same study (Chou et al., 2006). Modification of serine 407 in ARTD10 and an inhibition of cleavage would add another level of regulation to ARTD10. Phosphorylation by a MAP kinase or a CDK would link ARTD10 cleavage control to the cells environment and the cell cycle. A substrate screen for ARTD10 revealed that many of its targets are kinases, which adds the possibility for mutual regulation (Feijs et al. submitted). This could be similar to the interplay between kinases, phosphatases and caspases, where gain or loss of function through cleavage and phosphorylation controls the balance between life and death of the cell (Kurokawa and Kornbluth, 2009).

5.2.4 Definition of the caspase-1 restriction site

Compared to the N-terminal fragment produced by caspase-6 the cut executed by caspase-1 had to be around 20 kD (~180 amino acids) more C-terminal [Figure 25A and Figure 29, left panels]. To further verify the location, five overlapping GST-tagged parts of ARTD10 were expressed in *E. coli* and used in an *in vitro* caspase assay similar to Figure 25B, where fragment 2 was used. Only part 3 encompassing amino acids 408-649 was cleaved by caspase-1 into an approximately 6-12 kD shorter protein. With an average molecular weight of 110 Dalton per amino acid this would suggest that the cleavage site is located somewhere between amino acids 540 and 595. Consistently GST-fragment 4 encompassing amino acids 600 to 868 was not cleaved.

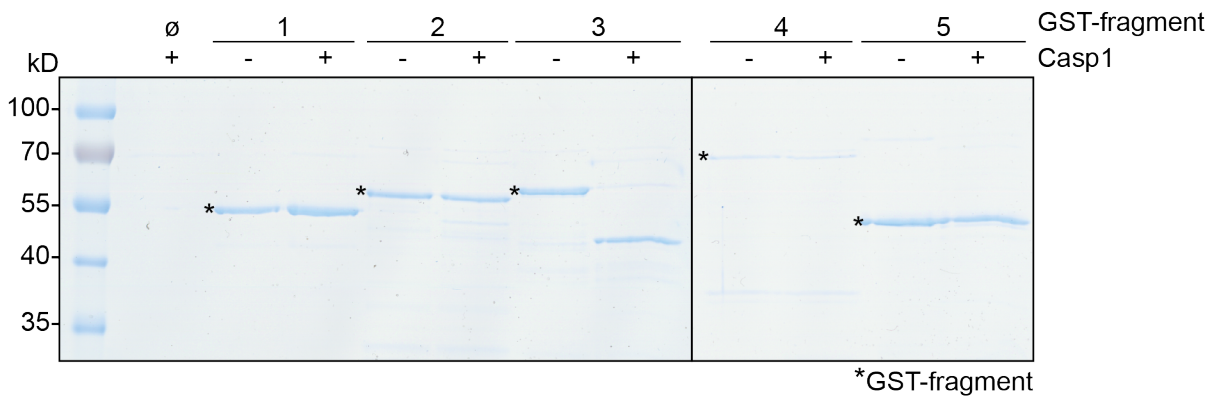


Figure 30. *In vitro* caspase assay with caspase-1 and purified ARTD10 GST-fragments. 5 different overlapping GST-fragments, about 250 amino acids in size, covering ARTD10 were used in a caspase assay with and without recombinant caspase-1. The assay was stopped using sample buffer, the samples separated in SDS-PAGE and the proteins subsequently stained with coomassie brilliant blue.

Taking into account the studies conducted by Shen et al. the surroundings of the 5 aspartates within the region of 540 to 595 were analyzed (Shen et al., 2010). Using probabilities for amino acids from positions P10 to P10', which were calculated using caspase-1 substrates, scores were made for the possible site in ARTD10. The two sites with the highest scores, amino acids 555 and 581, were mutated to glycine.

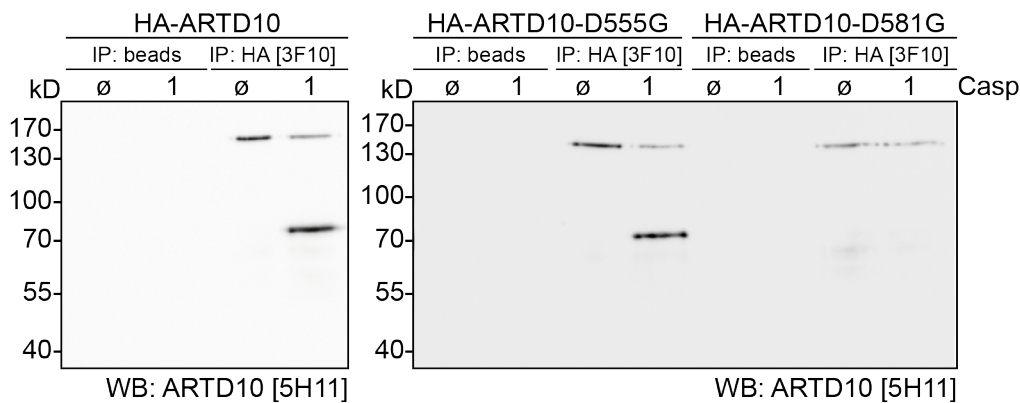


Figure 31. *In vitro* caspase assay with different restriction site mutants for the caspase-1 site. HA-ARTD10 and mutants thereof were immunoprecipitated from transiently transfected HeLa cells. The samples were used in a caspase assay with caspase-1 and ARTD10 was detected in an immunoblot using the N-terminal 5H11 antibody.

Similar to Figure 29 wild-type ARTD10 and the two new mutants were tested in an *in vitro* caspase assay. As the bigger caspase-1 fragment was visible in all protein

sources used so far, only HeLa cells were transfected with the constructs. Western blot analysis revealed that the ARTD-D555G was still targeted by caspase-1 whereas the mutation of D₅₈₁ abolished the caspase-mediated cleavage, confirming it as the cleavage site [Figure 31].

Caspase-1, together with caspases 4 and 5, belongs to the group of inflammatory caspases that mediate the processing and release of pro-inflammatory cytokines like IL-1 β and IL-18 in response to a variety of stimuli [see also 4.3]. Although the exact mechanism is not known the caspase-1-mediated cleavage is commonly thought to represent an unconventional way of secretion (Keller et al., 2008). The data in this chapter showed ARTD10 as caspase-1 target *in vitro* and the associated cleavage site was mapped to 'W T P D₅₈₁ / S T'. Follow-up experiments with overexpressed ARTD10 in HeLa cells as well as endogenous protein in THP-1 cells were not successful, i.e. did not show the observed fragmentation of ARTD10. In those systems the expression of inflammasome components was stimulated with LPS, monitored by IL-1 β production. The activation of the inflammasome with described secondary stimuli like nigericin and ATP as well as a subsequent release of pro-inflammatory cytokines however could not be shown (Bauernfeind et al., 2011a). Therefore preemptive conclusions, that ARTD10 is not cleaved by caspase-1 *in vivo* should not be made and further experiments are in need. Like the caspase-6 cleavage the processing by caspase-1 separates the RRM and glycine-rich region from the NES, UIMs and catalytic domain with the difference that the nuclear targeting sequence represented by amino acids 435-528 localizes to the N-terminal fragment (Kleine et al., 2012). This should have a crucial impact on the localization of the fragments and subsequently could change the biological function of ARTD10. A similar fluorescently labeled fragment from amino acids 552-1025 described in Kleine et al. shows a strictly cytoplasmic localization even when Leptomycin B is applied, a treatment which results in nuclear accumulation of the wild-type protein through inhibition of NES mediated export. The fragment from amino acids 1-581 on the other hand should now locate to the nucleus due to the NLS, regardless of the Leptomycin B status. Similar to the fragment 435-555 visualized in immunofluorescence microscopy during the same study it could also distribute throughout the cell depending on the strength of the NLS (Kleine et al., 2012). A

changed cellular function of the single fragments compared to the full-length protein linked to their different localization would represent an interesting gain of function mechanism.

Another possibility taking into account the involvement of the inflammasome in unconventional protein secretion would be the externalization of parts of ARTD10. Especially the C-terminal fragment containing the catalytic domain would fit into a model where ARTD10 upon an inflammatory stimulus is cleaved, secreted and subsequently modifies targets outside the cell. Of note is that the ARTD10 substrate screen revealed several secreted proteins. Among those was for example PDGF-B, which could be verified in experiments with recombinant protein (Feijs et al submitted). ADP-ribosylation of soluble factors or cell-surface receptors outside of cells is well described and mediated by the so-called ecto-mARTs (Zolkiewska, 2005). The secretion of ARTD10 or parts of it with maintained catalytic activity would provide an explanation for where ARTD10 and extracellular proteins could interact. In contrast to these models a loss of function as was discussed for the caspase-6 cleavage site could also be true for inflammation-linked cleavage of ARTD10. Taking into account its inhibitory effect on the pro-inflammatory NF- κ B pathway, cleavage and inactivation of ARTD10 as part of an inflammation activation loop would be a mechanism worth considering (Verheugd et al. submitted). In analogy to the discussion regarding the connection of NF- κ B, ARTD10 induced cell death and p62 (5.1.3) it is of note that the latter protein is also involved in the regulation of the inflammasome (Shi et al., 2012). Upon aggregation polyubiquitination of the inflammasome complex recruits p62 and subsequently autophagy is triggered, which is thought to regulate inflammasome activity. As stated before colocalization of ARTD10 bodies with p62 bodies was shown and could provide the foundation of a model wherein p62 links ARTD10 to sites of active caspase-1 (Kleine et al., 2012).

5.3 Cleavage of ARTD10 and cell viability

ARTD10 induced apoptosis in HeLa cells and at the same time was targeted by caspases during the process. To address whether the cleavage of ARTD10 diminished its pro-apoptotic properties additional stable HFT cells lines were established. The D406G mutant was used as non-cleavable ARTD10, as well as the

resulting fragments encompassing amino acids 1-406 and 407-1025. The cleavage at D₄₀₆ resulted in the loss of the potential RNA recognition motif in the far N-terminal region [see Figure 3]. A fourth construct (Δ RRM) lacking this N-terminal part from amino acid 1-256 was generated to see whether the absence of this domain influenced the apoptotic effect.

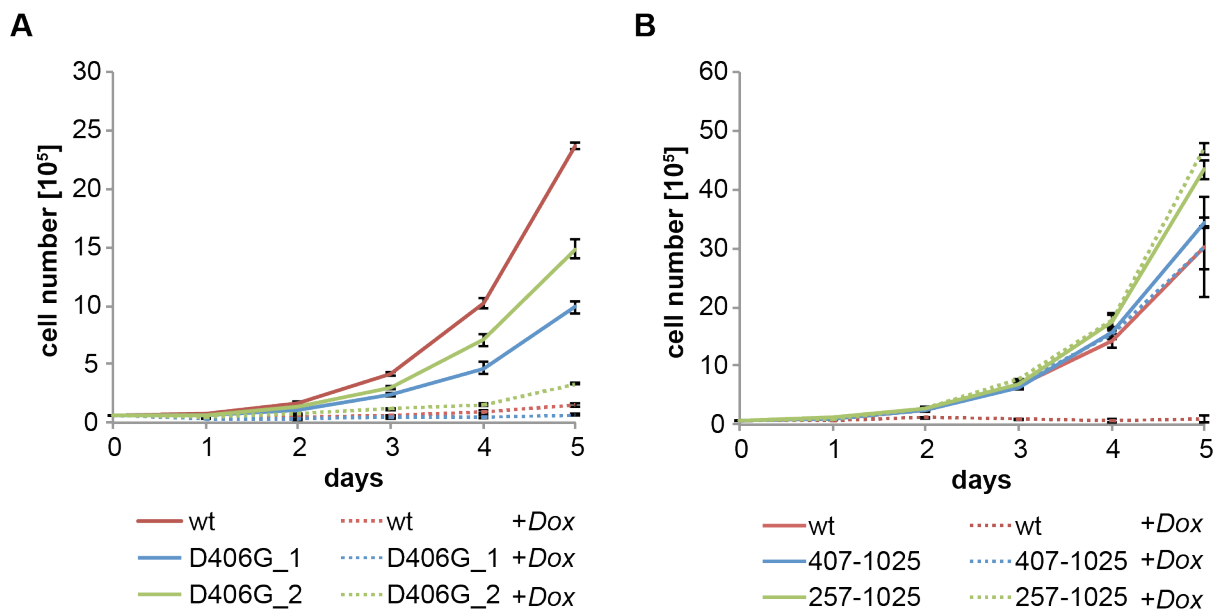


Figure 32. Growth curves of stable cell lines expressing different ARTD10 constructs.

(A) HeLa cells expressing either ARTD10 or ARTD10-D406G were grown with or without doxycycline [200 ng/ml] over 5 days and counted each day. Two different clones of the mutant cell line were used. All experiments were done in triplicates.

(B) HeLa cells expressing either ARTD10 or ARTD10 lacking the RRM and/or the glycine-rich region were grown with or without doxycycline [200 ng/ml] over 5 days and counted each day. All experiments were done in triplicates.

Proliferation assays conducted with the new HFT cells revealed that the non-cleavable mutant of ARTD10 inhibits proliferation [Figure 32A]. Similar to experiments done before the two clones used showed a slightly different growth rate. Addition of doxycycline resulted in the loss of cell proliferation approximately at the same rate as the cells expressing the wild-type ARTD10. In contrast the two fragments either lacking the RRM and glycine-rich region or the RRM alone did not show any inhibitory effect [Figure 32B]. The cells expressing the N-terminal fragment 1-406 were not used in this experiment, as the growth inhibitory effect was dependent on catalytic activity.

To rule out the possibility of different expression levels influencing this effect all constructs were expressed over 24 hours and detected by western blotting [Figure

33A/B]. All full-length constructs were detected with the polyclonal E09 antibody and show an equal expression level [Figure 33A]. The fragment protein levels were compared to the wild-type protein using the C-terminal antibody 9E12 as the epitope for the E09 antibody is lost [Figure 33B]. The visible ARTD10 reflected the sizes of the constructs and showed, when standardized to the tubulin control blot, an equal expression.

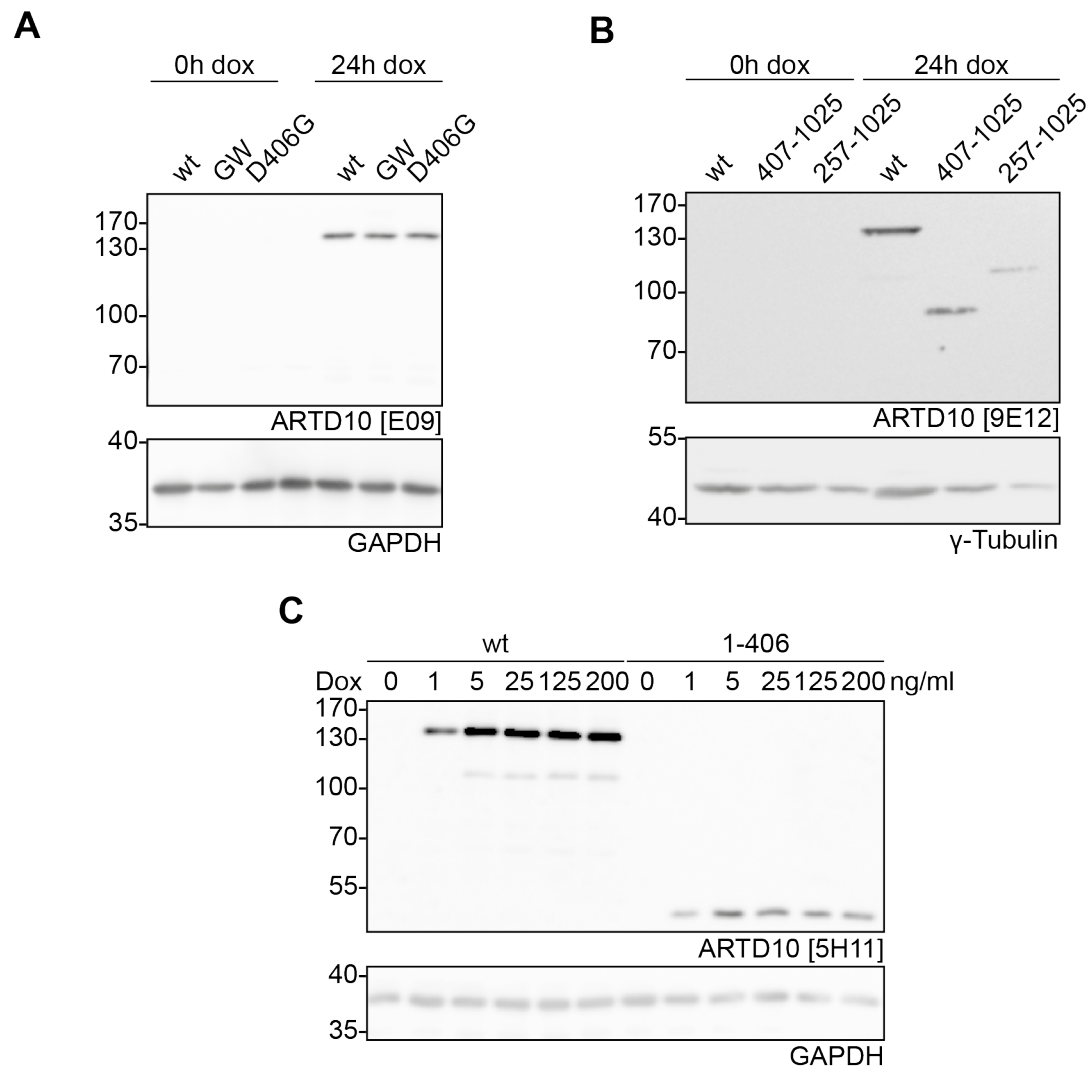


Figure 33. Expression comparison of different ARTD10 constructs.

(A) The expression of ARTD10, ARTD10-G888W, ARTD10-D406G was analyzed in lysates of uninduced and induced stably transfected HeLa cells. The full-length proteins were analyzed using the polyclonal antibody E09. GAPDH detection was used as loading control.

(B) Same as in (A) with C-terminal fragments ARTD10-(407-1025) and ARTD10-(257-1025) and detection by the C-terminal 9E12 antibody and γ-Tubulin was used as loading control.

(C) Expression comparison of wt3 and HFT cells expressing ARTD10-(1-406). Expression was induced for 24 h using different amounts of doxycycline. Proteins were detected using the monoclonal 5H11 antibody. GAPDH detection was used as loading control.

The HFT-ARTD10-(1-406) cells were additionally tested using different concentrations of doxycycline and subsequently compared to the expression of full-length ARTD10 in wt3 cells [Figure 33C].

The reduced growth rate is as mentioned in chapters 5.1.2 as well as 5.1.3 not sufficient to make further conclusions regarding the reason for the diminished growth. Therefore the cells were used in FACS experiments where simultaneously dead cells were stained by propidium iodide and apoptosis could be measured and quantified by cell cycle analysis, i.e. measurement of the sub-G1 cells. All HFT cells containing the different constructs were induced for ARTD10 expression over 24 or 48 hours. All cells including non-adherent cells were collected and simultaneously stained with PI (50 µg/ml) and Vybrant DyeCycle Violet in standard culture medium for 30 minutes at a cell density of 10^6 cells/ml. The cells were subjected to FACS analysis and the percentage of PI positive cells was quantified [Figure 34B, upper panel]. Similar to the results obtained from the growth curve experiments above ARTD10 and ARTD10-D406G showed an increase of cells with lost cell membrane integrity up to around 40%. This toxic effect was neither induced by the catalytically inactive mutant, which was also assessed before [see 5.1.3], nor by any other used construct. The rate of apoptotic cells analyzed by quantification of the sub-G1 peak was comparable to the cell death rates and again only observed using the wild-type and D406G mutant which was in line with the growth curves [Figure 33B, lower panel].

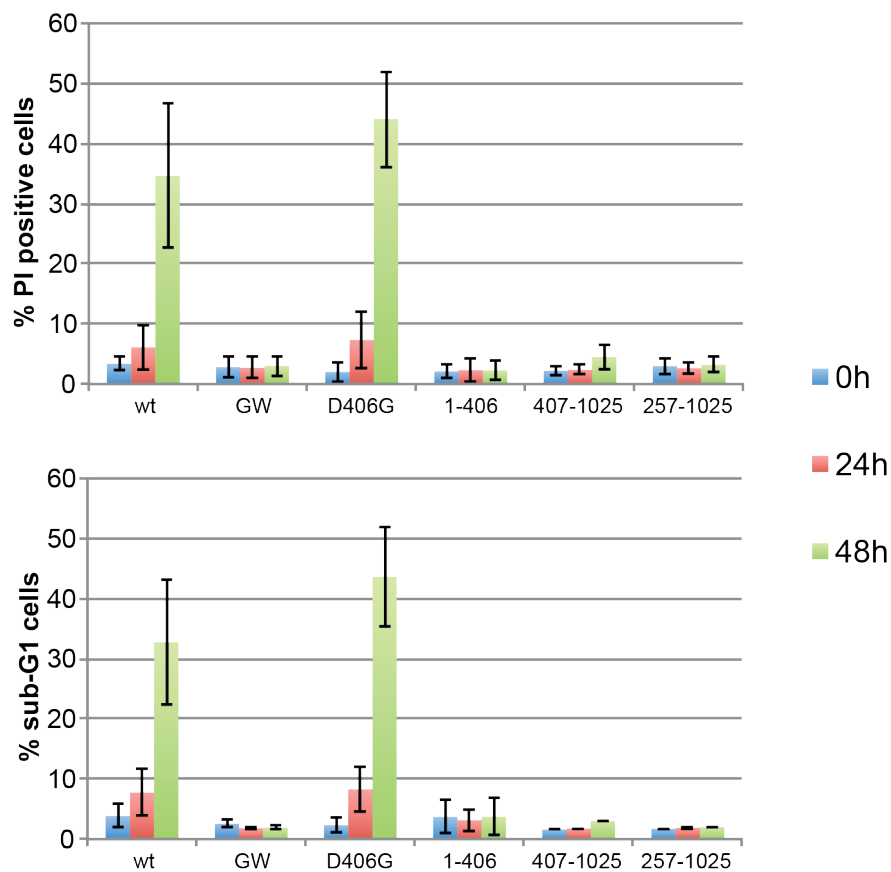


Figure 34. N-terminal truncation of ARTD10 abolishes apoptosis induction.

Stable cells lines containing different ARTD10 transgenes were induced for the indicated times with doxycycline. Subsequently the cells were analyzed by FACS. Dead cells were stained with propidium iodide, gated and counted (Upper panel). The number of sub-G1 cells in was calculated in the cell cycle visualized by Vybrant Dycycle Violet stain (Lower panel).

A potential lack of cytotoxicity of the ARTD10 C-terminal fragments could be due to lost catalytic activity, which would as well abolish apoptosis. Evidence pointing towards an active protein comes from experiments using the GST-purified catalytic domain, a fragment ranging from amino acid 818-1025. This protein obtained from *E. coli* is catalytically active and was repeatedly used in ADP-ribosylation assays in our group. To ensure the functionality of the catalytic mechanism regarding the ARTD10 fragment 407-1025 GFP-tagged versions of ARTD10 wild-type, -G888W and -(407-1025) were expressed in U2OS cells to circumvent any toxic effects and immunoprecipitated using a GFP antibody. The obtained protein was used in an radioactive ADP-ribosylation assay with either active GST-ARTD10-(818-1025) as positive control or GST-ARTD10-(818-1025)-G888W as substrate. Not only was the C-terminal fragment active in this setup, but normalized to the protein amounts visible

in coomassie staining the catalytic activity seemed to be comparable to the one of the full length protein [Figure 35].

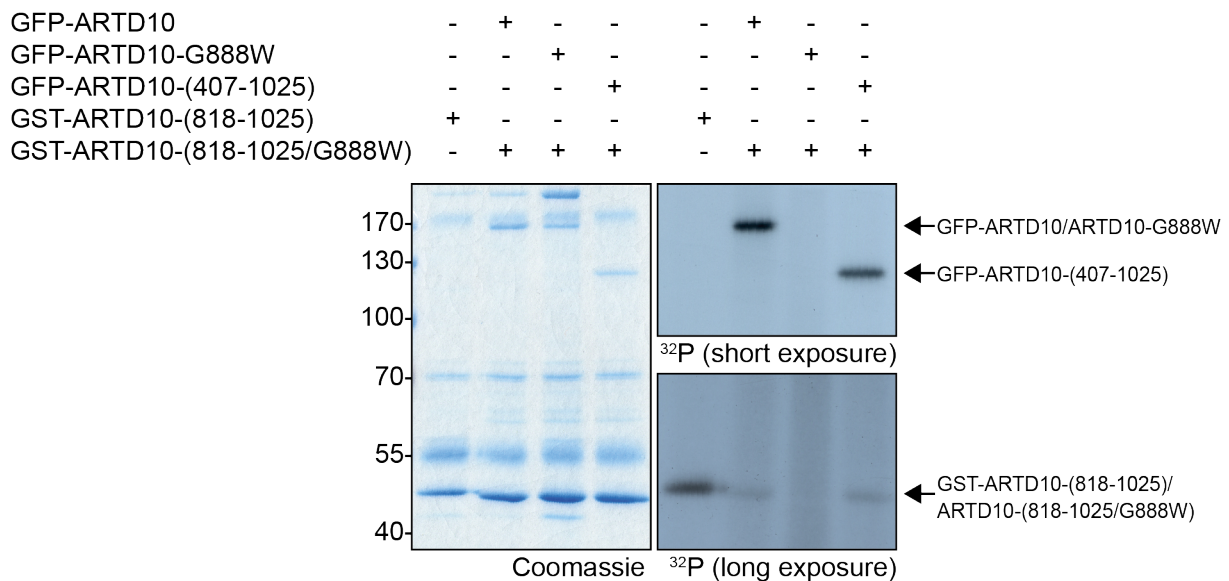


Figure 35. Activity comparison of ARTD10 and its caspase-6 fragment ARTD10-(407-1025).

U2OS cells were transfected with vectors expressing GFP-ARTD10, -G888W, -(407-1025) or the respective control vector. After 24 hours the cells were lysed with TAP-lysis buffer and ARTD10 was immunoprecipitated using a GFP antibody and IgG sepharose beads. Following washing steps the beads were subjected to a PARP assay containing either GST-ARTD10-(818-1025) in the case of the vector control or catalytically inactive GST-ARTD10-(818-1025)-G888W in the case of the GFP-ARTD10 proteins. The proteins were separated using SDS-PAGE. The gel was subsequently dried and incubated with medical X-ray films for different time periods.

Given the maintained catalytic activity of the caspase-cleaved fragment, the question arises why these N-terminally truncated mutants of ARTD10 are incapable of inducing apoptosis. During the cleavage the RRM as well as the glycine-rich region of ARTD10 are separated from the rest of the protein [Figure 3], indicating their possible functional relevance. RRMs belong to a group of RNA binding domains that are found in proteins involved in divers aspects of RNA metabolism, ranging from splicing and editing to export, translational regulation and degradation (Finn et al., 2006; Maris et al., 2005). They mainly interact with RNA, hence their name, but certain RRMs were also reported to bind to DNA or proteins (Clery et al., 2008). A combination with glycine-rich regions, like in ARTD10, is also reported for many other proteins in eukaryotes and this additional domain either assists in binding or confers binding itself (Cartegni et al., 1996; Dreyfuss et al., 1993; Kim et al., 2007; Mangeon et al., 2010). Some of these proteins including members of the hnRNP family are targets of caspases (Luthi and Martin, 2007; Van Damme et al., 2005). This is part of

a broad response in apoptotic cells to halt many house keeping processes in order to allow efficient apoptosis (Taylor et al., 2008). The processing of ARTD10 during apoptosis could be associated with an analogue mechanism, wherein the RRM and/or the glycine-rich region provide a vital function to the protein, which is abolished after cleavage. Activity changes upon binding of an interaction partner, be it RNA, DNA or protein, could be such a function, but initial experiments with sheared salmon sperm DNA, plasmid DNA or total cellular RNA did not alter activity dependent on the RRM (Kleine et al., 2008). Sequence specific binding or protein-protein interaction however cannot be excluded by these experiments and the search for binding molecules would be an opportunity to get further insides into the molecular function of ARTD10.

Considering the information about RRM containing proteins the N-terminal part of ARTD10 could also confer targeting and substrate recognition purposes. Interesting in this regard is the diminished development of the characteristic ARTD10 foci using ARTD10-(257-1025) or -(552-1025), a fact which led to the assumption that the RRM is important for localization (Schuchlautz, 2008). However colocalization of the full length ARTD10 foci with common RNA containing bodies like P-bodies or stress granules could not be shown (Kleine et al., 2012). Nonetheless the involvement of ARTD10 in an RRM directed process seems likely and the extensive shuttling between nucleus und cytoplasm could place ARTD10 in a model wherein it regulates the export or import of RNA (Kleine et al., 2012). At last the deregulation of an essential housekeeping function through overexpression of ARTD10 could also explain the onset of apoptosis, an assumption which is strengthened by the fact that also the knockdown of ARTD10 interferes with cell proliferation (Feijs, 2009).

6 Conclusions

ARTD10 was reported to inhibit proliferation in HeLa cells upon overexpression (Yu et al., 2005). Expanding on these earlier findings using stable inducible HeLa cell lines this work showed that the prior observed effect is due to the induction of apoptosis. The mono-ADP-ribosylation as catalytic activity of ARTD10 has proven to be essential as the catalytic inactive mutant ARTD10-G888W does not drive these cells into programmed death. Modifications of the protein, e.g. lysine depletion or destruction of UIM, NES or NLS, abolish the apoptotic phenotype as well, hinting at the importance of the overall structural integrity of ARTD10. Although it is possible that a protein's function is dependent on all of its domains, conclusions on the underlying mechanisms are complicated.

The main question in this regard comes back to whether ARTD10 itself is involved in apoptosis regulation or whether the cell death is just the effect of ARTD10's overexpression, i.e. the disturbance of a basic vital cellular pathway? Taking into account the late onset of cell death after 24 hours and the relatively high numbers of cells surviving ARTD10 overexpression, a direct pro-apoptotic function of ARTD10 seems unlikely. The little information on physiological functions of ARTD10 however allows the discussion of several indirect links to apoptosis. Inhibition of NEMO ubiquitination and p65 translocation could be responsible for the shutdown of an essential residual NF- κ B activity in those tumor cells (Verheugd et al. submitted). p62, a poly-ubiquitin adapter protein functioning in different pathways including pro-survival signaling through NF- κ B, colocalizes with ARTD10 bodies and links ARTD10's function to NF- κ B regulation (Duran et al., 2008; Kleine et al., 2012). The mentioned bodies are also known to decrease in numbers when the RRM is deleted in ARTD10. Although known RNA containing dot structures in the cytoplasm were ruled out, the involvement of ARTD10 in RNA processing is a valid option and the disturbance of this basic cellular process could explain apoptosis (Kleine et al., 2012). In addition ARTD10 modifies several mitosis-regulating kinases, whose functional inhibition is known to induce apoptosis or error prone mitosis, the latter of which would fit to the 24 hours cell death delay in the HeLa model system.

These models will have to be investigated in future studies to pinpoint ARTD10's exact function in cellular pathways and induction of apoptosis.

During the work with apoptosis we noted that ARTD10 was cleaved at 'I A M D₄₀₆ S P' into two fragments. Analogous to the processing of ARTD1 this was mediated by caspases, the main effectors during apoptosis. Both fragments were rather stable and appeared in a time window in response to apoptotic signals that was similar to ARTD1 cleavage. The N-terminal part contained the RRM as well as the glycine-rich region, separating a possible interaction with RNA or other macromolecules from the catalytic domain. Surprisingly, although the catalytic activity was maintained, the overexpression of the C-terminal part of ARTD10 did not lead to the induction of apoptosis. With this knowledge a model wherein ARTD10 is directly involved in the apoptotic process becomes even more unlikely, as the inactivation of a pro-apoptotic protein during apoptosis is hard to explain. The separation of the RRM however could very well influence a possible targeting or regulation of ARTD10 and subsequently its ability to modulate an important cellular pathway.

Using *in vitro* caspase assays we could demonstrate that predominantly caspase-6 is responsible for cleavage at D₄₀₆. This caspase, apart from its functions as executioner during apoptosis, is also implicated in neuronal development, i.e. axonal breakdown and neurodegenerative diseases. Targeting of ARTD10 outside the normal apoptotic process is an interesting possibility and would clear the way for studies analyzing ARTD10's role in the neuronal system.

Using recombinant caspases we observed an additional cleavage of ARTD10 by caspase-1, the best characterized member of the inflammatory caspases. The target site was located 175 amino acids further C-terminal in the protein to 'W T P D₅₈₁ / S T', placing the NLS (435-528) in the N-terminal fragment. This small difference should have an impact on its localization, abrogate shuttling of the C-terminal part, and subsequently influence their functions. As yet the *in vivo* processing by caspase-1 could not be shown, but a role of ARTD10 in inflammation, linking perhaps NF- κ B signaling and the inflammasome, is an interesting path to follow in future studies. In addition the unconventional protein secretion mediated by caspase-1 cleavage is commonly known (Keller et al., 2008). Releasing parts of ARTD10 containing the catalytic domain from the cell would facilitate explanations on how ARTD10 meets its substrates that are secreted.

Findings in our group revealed that ARTD10 is heavily modified by acetylation, ubiquitination and phosphorylation, the latter of which could play a role in regulating

caspase-mediated cleavage through modification of the serines in P1' or the threonine in P2'. The questions whether these sites are actually targeted in cells and which kinases and pathways potentially act, will have to be addressed in future studies.

In conclusion the HeLa system used throughout this study helped us to make a step forward in understanding the physiological role of ARTD10 by showing that ARTD10 induction leads to apoptosis and that ARTD10 is cleaved itself during this process. These results provide new starting points for further interesting studies connecting ARTD10 to apoptosis, RNA metabolism or inflammation. Additionally, this cell system will be highly useful in order to solve upcoming questions.

7 Experimental procedures

Materials and Methods are described according to standard protocols used in the Institute of Biochemistry and Molecular Biology, RWTH Aachen University, and modified regarding individual differences in experimental procedures.

7.1 Oligonucleotides

	Sequence (5'→3')
Mutagenesis of D406G in ARTD10	
PARP10_D406G	GTGGAAATTGCCATGGGCTCACCAGAGCAAGAG
PARP10_D406G_antisense	CTCTTGCTCTGGTGAGCCCATGGCAATTTCCAC
Mutagenesis of D581G in ARTD10	
D581G	CCTGTGGACCCCAGGCAGTACAGGTGGTG
D581G_antisense	CACCACCTGTACTGCCTGGGGTCCACAGG
Amplification of attB-PARP10	
attB1-PARP-10	GGGGACAAGTTTGTACAAAAAAGCAGGCTCCATGGTTGCAATG GCGGAGG
attB2-PARP-10	GGGGACCACTTTGTACAAGAAAGCTGGGTCTTAAGTGTCTGGG GAGCGGC
Amplification of attB-PARP10_1-406	
attB1-PARP-10	GGGGACAAGTTTGTACAAAAAAGCAGGCTCCATGGTTGCAATG GCGGAGG
attB2_ARTD10_1-406	GGGGACCACTTTGTACAAGAAAGCTGGGTCTTAGTCCATGGCA ATTCCACCAG
Amplification of attB-PARP10_407-1025	
attB1-PARP10_407-1025	GGGGACAAGTTTGTACAAAAAAGCAGGCTCCTCACCAGAGCAA GAGGGGCTG
attB2-PARP-10	GGGGACCACTTTGTACAAGAAAGCTGGGTCTTAAGTGTCTGGG GAGCGGC
Amplification of attB-PARP10_407-1025+M	
attB1-ARTD10_407+M	GGGGACAAGTTTGTACAAAAAAGCAGGCTCCATGTCACCAGAG CAAGAGGGGCTGGTGGGTCC
attB2-PARP-10	GGGGACCACTTTGTACAAGAAAGCTGGGTCTTAAGTGTCTGGG GAGCGGC

7.2 Plasmids

Vector	Reference
GW-pEGFP	Gateway compatible expression vector established by insertion of the Gateway cassette B into peGFP-C1 (Clontech)
pBabePuro	(Morgenstern and Land, 1990)
pEQ176P2	Derivate of pEQ176 (Schleiss et al., 1991) lacking a greater part of β -galactosidase (J. Lüscher-Firzlaff)

pOG44	Mammalian expression vector encoding the Flp recombinase (Invitrogen)
pcDNA5/FRT/TO	Mammalian expression vector used for integration of a target gene into the FRT site of Flp-In™ cells (Invitrogen)
pDonR/Zeo	Standard donor vector in the Gateway® cloning system (Invitrogen)
pcs2+p27	Vector driving the expression of p27 under the control of a CMV promoter (J. Vervoorts).
pEVRF0-HA	(Matthias et al., 1989)
GW-pcDNA5/FRT/TO	Gateway® compatible pcDNA5/FRT/TO with the Gateway® cassette A cloned into blunted HindIII site. (A. Forst)
pEVRF0-HA-ARTD10	(Yu et al., 2005)
pEVRF0-HA-ARTD10-G888W	(Yu et al., 2005)
pEVRF0-HA-ARTD10-ΔNES	(Schuchlautz, 2008)
pEVRF0-HA-ARTD10-ΔUIM	(Milke, 2007)
pEVRF0-HA-ARTD10-Δ219-502	Expression vector for ARTD10 lacking the amino acids 219-502
pEVRF0-HA-ARTD10-ΔK	(Chauvistré, 2008)
pEVRF0-HA-ARTD10-D406G	Constructed using site directed mutagenesis
pEVRF0-HA-ARTD10-D581G	Constructed using site directed mutagenesis
pcDNA5/FRT/TO-ARTD10	Constructed from pcDNA5/FRT/TO and the respective pEVRF0-HA-ARTD10 plasmid using standard cloning techniques.
pcDNA5/FRT/TO-ARTD10-G888W	
pcDNA5/FRT/TO-ARTD10-ΔNES	
pcDNA5/FRT/TO-ARTD10-ΔUIM	
pcDNA5/FRT/TO-ARTD10-Δ219-502	
pcDNA5/FRT/TO-ARTD10-ΔK	
pcDNA5/FRT/TO-ARTD10-D406G	
pcDNA5/FRT/TO-ARTD10-D581G	
pDonR/Zeo-ARTD10	(Montzka, 2006)
pDonR/Zeo-ARTD10-G888W	(Montzka, 2006)
pDonR/Zeo-ARTD10-D406G	Constructed by Gateway cloning (Primers see 7.1)
pDonR/Zeo-ARTD10-1-406	Constructed by Gateway cloning (Primers see 7.1)
pDonR/Zeo-ARTD10-407-1025	Constructed by Gateway cloning (Primers see 7.1)
pDonR/Zeo-ARTD10-407-1025+M	Constructed by Gateway cloning (Primers see 7.1)
GW-peGFP-ARTD10	Constructed by Gateway® cloning using GW-pEGFP and the respective pDonR/Zeo-ARTD10 construct.
GW-peGFP-ARTD10-G888W	
GW-peGFP-ARTD10-D406G	
GW-peGFP-ARTD10-1-406	
GW-peGFP-ARTD10-407-1025	
GW-pGEX-PARP10-1	Prokaryotic expression vector encoding GST-tagged fragments of ARTD10 (Montzka, 2006)
GW-pGEX-PARP10 (206-459)	
GW-pGEX-PARP10 (408-649)	
GW-pGEX-PARP10 (600-868)	
GW-pGEX-PARP10 (818-1025)	

7.3 Antibodies

Antigen	Antibody	Species	Type	Provided by	Order number	Reference
Actin	C4	mouse	monoclonal	MP Biomedicals	69100	
ARTD10	891-6	rabbit	polyclonal			(Yu et al., 2005)
ARTD10	5h11	rat	monoclonal	E. Kremmer		
ARTD10	E09	rabbit	polyclonal	Eurogentec		
ARTD10	3H5	rat	monoclonal	E. Kremmer		
Flag	M2	mouse	monoclonal	Sigma	F-3165	
GAPDH	4G5	mouse	monoclonal	AbD Serotec	MCA4740	
GFP	9F9.F9	mouse	monoclonal	Rockland	600-301-215	
HA-tag	3F10	rat	monoclonal	Roche	1 867 423	
PARP1		rabbit	polyclonal	Roche	11835238001	
α -Tub	B-5-1-2	mouse	monoclonal	Sigma	T-5168	
γ -Tub	GTU88	mouse	monoclonal	Sigma	T-6557	
Casp-1		rabbit	polyclonal	Millipore	06-503	
Casp-3	H-277	rabbit	polyclonal	Santa Cruz	SC-7148	
Casp-6		rabbit	polyclonal	Cell Signaling	CS#9762	
Casp-8	H-134	rabbit	polyclonal	Santa Cruz	SC-7890	

Secondary antibodies used for immunodetection were HRP labeled goat- α -mouse (115-035-146), goat- α -rabbit (111-035-144) and goat- α -rat (112-035-008) antibodies purchased from Jackson Immunoresearch. A rat-IgG2a specific secondary antibody labeled with HRP was a kind gift of E. Kremmer.

For immunofluorescence analysis goat- α -rat-Alexa-488 (Invitrogen) secondary antibody was used.

7.4 Work with nucleic acids

7.4.1 DNA preparation and extraction

Zymo Research

Zyppy™ Plasmid Miniprep Kit

Macherey-Nagel

Zymoclean™ Gel DNA Recovery Kit

Invitrogen

NucleoBond® Xtra Maxi / Maxi Plus

PureLink™ Quick Plasmid Miniprep Kit

All kits were used according to the manufacturer's manual. Samples, which were subjected to sequencing, were eluted with ddH₂O to exclude any negative effects of EDTA in the elution buffer. DNA concentrations were measured using a NanoDrop™ 1000 Spectrophotometer (PeqLab).

7.4.2 RNA preparation, cDNA synthesis and RT-PCR

Qiagen	QIAshredder RNeasy Mini Kit RNase-Free DNase Set
Diagenode	QuantiTect Reverse Transcription Kit 2x Universal Mastermix

RNA purification was performed using Qiagen QIAshredder columns and the RNeasy Mini Kit following the manufacturer's protocol with the optional on-column DNase digestion. cDNA synthesis was carried out using 1 µg RNA. RT-PCR was run on a Corbett Life Science Rotor-Gene 6000 in a 10 µl reaction volume containing 1 µM of each primer and 2 µl of 1:100 diluted cDNA.

7.4.3 Molecular cloning

Restriction enzymes from either NEB or Fermentas were used according to the manufacturer's protocol in a total volume of 10 µl. Ligations were performed using T4 DNA ligase (Fermentas) for 1 hour at room temperature. In the case of blunt end ligation, vector backbones were treated first with FastAP™ Thermosensitive Alkaline Phosphatase (Fermentas) and PEG2000 was added to the reaction mixture (1:10).

7.4.4 Agarose gel electrophoresis

TBE:	89 mM Tris-Base 89 mM boric acid 2 mM EDTA
------	--

Agarose Low EEO (Applichem)
O'GeneRuler™ 1 kb Plus DNA Ladder, ready-to-use, 75-20,000 bp (Fermentas)

Depending on the separating capacity needed, different agarose concentrations ranging from 0.8 to 2 % were used. If not indicated otherwise O'GeneRuler™ 1 kb Plus DNA Ladder was used as DNA marker.

7.4.5 Gateway cloning

Gateway cloning was performed using pDONR™/Zeo following the manufacturer's protocol. Due to the high performance all reactions were done with half the recommended volumes.

Invitrogen
 Gateway® BP Clonase® enzyme mix
 Gateway® LR Clonase® enzyme mix
 pDONR™/Zeo

AttB products were generated using the Finnzymes Phusion Polymerase, the respective attB1/attB2 primers [7.1] and a vector containing the target gene in a PCR with standard conditions.

7.4.6 Site-directed mutagenesis

Primers for mutagenesis were designed using the QuikChange Primer Design program (Agilent Technologies). PCR was performed using Finnzymes Phusion polymerase with standard conditions. Following the amplification the methylated DNA was digested with DpnI and *E. coli* DH5α were transformed.

7.5 Work with prokaryotic cells

7.5.1 Bacteria strains

<i>E. coli</i> BI21 (DE3)pLysS (Stratagene)	B F ⁻ <i>dcm ompT hsdS</i> (r _B ⁻ m _B ⁻) gal λ(DE3) [pLysS Cam ^r]
<i>E. coli</i> DH5α (Invitrogen)	F ⁻ Φ80 <i>lacZ</i> ΔM15 Δ(<i>lacZYA-argF</i>) U169 <i>recA1 endA1 hsdR17</i> (rK ⁻ , mK ⁺) <i>phoA supE44 λ⁻ thi-1 gyrA96 relA1</i>
<i>E. coli</i> Rosetta-gami™ B(DE3)pLysS (Merck)	F ⁻ <i>ompT hsdSB</i> (rB ⁻ mB ⁻) <i>gal dcm lacY1 ahpC</i> (DE3) <i>gor522::Tn10 trxB</i> pLysSRARE (Cam ^R , Kan ^R , Tet ^R)
<i>E. coli</i> XL10-Gold (Stratagene)	Tet ^r Δ(<i>mcrA</i>)183 Δ(<i>mcrCB-hsdSMR-mrr</i>)173 <i>endA1 supE44 thi-1 recA1 gyrA96 relA1 lac Hte</i> [F' <i>proAB lac^rZΔM15 Tn10</i> (Tet ^r) Amy Cam ^r]

7.5.2 Standard materials

LB Medium:
 1 % (w/v) tryptone
 0.5 % (w/v) yeast extract
 1 % (w/v) NaCl
 pH7.0

Low Salt LB Medium:	1 % (w/v) tryptone 0.5 % (w/v) yeast extract 0.5 % (w/v) NaCl pH 7.5
Agar plates (Amp/Kan):	LB Medium 1.5 % (w/v) Bacto Agar (Applichem) 100 µg/ml ampicillin (Binotal) or 30 µg/ml kanamycin (Seromed)
Agar Plates (Zeo):	Low Salt LB Medium 1.5 % (w/v) Bacto Agar (Applichem) 50 µg/ml zeocin (Invivogen)

7.5.3 Transformation

100 µl chemically competent bacteria were thawed on ice and mixed with either 500 ng plasmid DNA or 20 µl of ligation mixture. After 30 minutes on ice, the bacteria were incubated for 45 seconds at 42°C, cooled on ice again for 2 minutes and afterwards directly plated on agar plates containing the appropriate antibiotic. The plates were then incubated over night at 37°C.

7.5.4 GST-purification

TNE Buffer:	20 mM Tris pH 8.0 150 mM NaCl 1 mM EDTA 5 mM DTT 1 mM Pefabloc SC (Roche) 14 µg /ml aprotinin
GST Wash Buffer:	100 mM Tris pH 8.0 120 mM NaCl
GST Elution Buffer:	100 mM Tris pH 8.0 120 mM NaCl 20 mM glutathione

Colonies from *E. coli* BL21 (DE3)pLysS or *E. coli* Rosetta-gami™ B(DE3)pLysS were picked and used for inoculation of a 50ml pre-culture containing a final glucose concentration of 0,4 % (w/v), which was grown over night at 37 °C. The next day a 300 ml main culture was inoculated with 25 ml pre-culture. The culture was incubated further until an OD₆₀₀ of 0,5-0,8 and 1 mM IPTG was added to induce protein expression over night.

The cells were harvested at 3500 xg at 4 °C, resuspended in 30 ml TNE-buffer and 100 µg/ml lysozyme was added, before chilling on ice for 30 minutes.

The cells were disrupted by sonication and cell debris was removed by centrifugation at 10,000 xg for 30 minutes. 500 µl Glutathione Sepharose 4B beads (Amersham Biosciences) were added to the supernatant and the mixture was rotated for 1 hour at 4 °C. Washing of the beads was performed with 1 ml ice cold PBS + 1 % (v/v) Triton X-100 and 1 ml GST wash buffer. The purified protein was eluted with three times 300 µl GST elution buffer and subsequently stored at -80 °C. Purity and concentration of the desired protein were checked by SDS-PAGE and coomassie staining with a BSA standard.

7.6 Work with eukaryotic cells (cell culture)

7.6.1 Eukaryotic cell lines

Cell line	ATCC	Reference
HEK293-C-TAP-ARTD10		(Kleine et al., 2008)
HEK293-C-TAP-ARTD10-G888W		(Kleine et al., 2008)
HeLa	CCL-2™	
HeLa Flp-In T-Rex		Steven Taylor, University of Manchester
THP-1	TIB-202™	
U2OS	HTB-96™	

Stable inducible cell lines using the Flp-In T-Rex system (Invitrogen) were selected using 5 µg/ml blasticidin and 200 µg/ml hygromycin. After initial selection monoclonal cells were established. Therefore cells were seeded at a very low density and grown until visible colonies emerged from single cells. The colonies transferred to new separate wells using cloning rings.

7.6.2 Standard materials

PBS: 140 mM NaCl
2.6 mM KCl
2 mM Na₂HPO₄
1.45 mM KH₂PO₄

1.2 ml cryotubes (Thermo scientific)
Blasticidin S (Invivogen)
DMEM (Gibco) with 4,5 g/l Glucose
Doxycycline (Sigma)
Etoposide (Calbiochem)
FCS (Gibco)
Hygromycin B (Invivogen)
10,000 µg/ml Penicillin / 10,000 U/ml Streptomycin (Gibco)
RPMI + Glutamax (Gibco)
Staurosporine (Biomol)
Tissue culture dishes (Sarstedt)
Tissue culture plates (Sarstedt)
Trypsin (Gibco)

7.6.3 Cell culture

All cell lines were cultured at 37 °C with 5 % CO₂. RPMI medium was used for THP-1 cells. DMEM-Glutamax I medium was used for all other cell lines. All media were supplemented with 10 % FCS and 1 % penicillin/streptomycin. 5 µg/ml blasticidin and 100 µg/ml hygromycin (200 µg/ml for initial selection) were added as selection markers to the medium of the stable cell lines. Transfections of plasmids were carried out using the calcium phosphate method. UV was applied on PBS washed cells using 20 mJ/cm² at 254 nm.

7.6.4 Cryoconservation

Cells were grown on 10 cm dishes to density of roughly 70 %. They were trypsinized, spun down (200 xg, 2 minutes) and subsequently resuspended in 1 ml FCS containing 10 % DMSO. The cells were slowly frozen in cryotubes to -80 °C using styrofoam boxes. After 3-4 days they were transferred to a -150 °C freezer for longterm storage.

Thawing of the cells was achieved by quickly raising the temperature to 37 °C in a waterbath and transfer to pre-warmed medium. To get rid of residual DMSO the medium was changed directly by centrifugation.

7.6.5 Calcium phosphate transfection

HEBS buffer:	138 mM NaCl 17 mM Hepes 5 mM KCl 0.71 mM Na ₂ HPO ₄ • 2 H ₂ O pH 6.95
--------------	--

HEPES buffer:	142 mM NaCl 10 mM HEPES 6.7 mM KCl pH 7.3
---------------	--

2.5 M CaCl₂

To introduce plasmid DNA into cells the calcium phosphate precipitation method was used routinely. Amounts of total DNA and buffers, as well as number of cells, depend on the area of the dishes used. Cells were seeded at an approximate density of $8\text{--}10 \times 10^4$ cells per cm². 0.25 µg/cm² total plasmid DNA were mixed with 11.875 µl/cm² HEBS buffer. 0.625 µl/cm² 2.5 M CaCl₂ was added afterwards and vortexed. The suspension was incubated between 20–40 minutes at room temperature before the dropwise application to the cells. The ratio between transfection mixture and medium should be at 1:10.

7.6.6 Colony formation assay

Stable HeLa cells expressing the different ARTD10 proteins were seeded at the indicated cell number and treatment was started with 1 µg/ml doxycycline. Medium was changed after 4 days. On day 11 the cells were washed and subsequently stained with 0.2 % methylene blue in methanol for 30 minutes. The staining solution was removed by washing with ddH₂O and afterwards dried and scanned for documentation.

In colony formations with transfected cells, HeLa cells were seeded in 6-well plates at a density of 80,000 cells per well. The following morning the cells were transfected with 2.5 µg total plasmid DNA, including 0.25 µg puromycin resistance vector (pBabePuro) using the calcium phosphate transfection. After 24 hours the cells were washed with HEPES buffer and subsequently selected with medium containing puromycin (2 µg/ml, Sigma) for another 24 hours. Medium was replaced during the following days as necessary. At a density on the control plate (puromycin resistance

vector only) of roughly 90 % the colonies were stained and digitized as described above. Density was quantified using the free software ImageJ (v1.46).

7.6.7 Cell proliferation assays

HeLa cells were seeded at a density of 3×10^4 cells/well for each counting day in triplicates. Protein expression was induced by addition of doxycycline (1 µg/ml). The cell count on the respective plates was determined each day after trypsinization using the CASY® Technology Cell Counter with 3 measurements per sample.

For analysis of the cell cycle the respective clones were seeded in 6 cm dishes at a density of 1×10^4 cells/dish. Expression of the proteins was induced by doxycycline (0.2 µg/ml) for 0-72 hours. The cells were trypsinized from the plates and harvested by centrifugation (200 xg, 2 minutes) including the cells from the supernatant. They were stained with Vybrant Dycycle Violet (1 µl/ 10^6 cells in 1 ml DMEM) (Invitrogen) and propidium iodide (PI) (50 µg/ml) for 30 minutes in the dark and subsequently measured using a FACSCanto II. Analysis and quantification of the PI positive cells and the subG1-peak was done using FlowJo (v8.8.7).

Early apoptotic cells were detected using an annexin V binding assay. The cells were seeded in 6 cm dishes at a density of 8×10^4 cells/dish, incubated for 24 hours and then stimulated with 1 µg/ml doxycycline for 3 days. Control cells were treated with 20 µM etoposide. At the indicated time points the cells were treated using the FITC Annexin V Apoptosis Detection Kit I (BD Pharmingen) and measured by FACS. Annexin V / PI negative cells were quantified using FlowJo (v8.8.7).

7.7 Work with proteins

7.7.1 Cell lysis and immunoprecipitations

RIPA:	10 mM Tris-HCl, pH 7.4
	150 mM NaCl
	1 % NP-40
	1 % DOC
	0.1 % SDS
	0.5 % Trasylol
	ProteoBlock™ Protease Inhibitor Cocktail (Fermentas)

Cells were routinely lysed in 12,5 µl/cm² RIPA buffer containing a protease inhibitor cocktail on ice. The cells were scraped from the plates and sonified for 15 minutes

using a BioRaptor (Diagenode) to destroy the genomic DNA and afterwards cleared by centrifugation at 16,100 xg.

Lysates used for immunoprecipitation of proteins were incubated with IgG sepharose (Amersham Biosciences) and a specific antibody at 4 °C for at least 16 hours. The beads were washed twice with RIPA and twice with high salt RIPA buffer (containing 500 mM NaCl), followed by a washing step with the assay specific buffer. To ensure the catalytic activity of ARTD10, the immunoprecipitations for PARP assays were done using TAP lysis buffer [7.7.5] instead of RIPA during all steps.

7.7.2 SDS-PAGE

4x Sample Buffer:	320 mM Tris, pH 6.8 40 % (v/v) glycerol 8 % (w/v) SDS 0.5 % (w/v) BPB 200 mM β -Mercaptoethanol
Running Buffer (Laemmli):	25 mM Tris base 250 mM glycine 0.1 % (w/v) SDS
Protein Ladder:	PageRuler Prestained Protein Ladder, 11-170 kDa (Fermentas)

Separation of proteins was done by SDS-PAGE (sodium dodecyl sulfate polyacrylamide gel electrophoresis) in Bio-Rad electrophoresis chambers. Samples were mixed with 4x sample buffer and boiled for 5 minutes at 98 °C before the application to the gel. Depending on the molecular size of the detected protein, separating gels from 10 to 15 % and a 5 % stacking gel were used.

7.7.3 Western Blot and Immunodetection

Semi-dry Transfer Buffer:	25 mM Tris base 192 mM glycine 20 % (v/v) methanol
PBS-T:	PBS 0.05 % (v/v) Tween-20
Blocking Buffer:	PBS-T 5 % (w/v) non-fat dried milk powder (Applichem)
Ponceau S ECL solutions (Pierce)	0,2 % (w/v) Ponceau S in 3 % (v/v) Trichloroacetic acid

To detect separated proteins by specific antibodies, they were transferred onto nitrocellulose membranes (Whatman) by semi-dry blotting. The SDS-PAG and membrane were lined on each site with three layers of thin whatman paper (Whatman), soaked with semi-dry transfer buffer and blotted for 75 minutes at 1.75 mA/cm².

Transferred proteins were transiently stained with Ponceau S to check the transfer efficiency. After blocking with blocking buffer for 30 minutes the blot was washed with PBS-T and agitated with the desired antibody at 4 °C over night. Antibody dilutions ranged from 1:200 to 1:5000 depending on the quality of the antibody. Following a second washing step, the appropriate HRP coupled secondary antibody was added in PBS-T at a dilution of 1:5000 and shaken for 60 minutes. Proteins were detected using Pico or Femto ECL solution (Pierce) and a LAS-3000 image reader (Fuji).

7.7.4 Coomassie staining

Staining Solution:	10 % (v/v) acetic acid 0.006 % (w/v) Coomassie brilliant blue G250
Destaining Solution:	10 % acetic acid

Visualization of purified proteins in SDS-PAGs was done by coomassie staining. The gels were incubated in staining solution for 1 hour, followed by incubation in destaining solution or ddH₂O until the protein bands were clearly visible. The gels were dried on whatman paper under vacuum to store them.

7.7.5 Tandem affinity purification

TAP Lysis Buffer:	50 mM Tris pH 7.5 150 mM NaCl 1 mM EDTA 10 % (v/v) glycerol 1 % (v/v) NP-40 1 mM DTT 100 µM sodium vanadate 14 µg/ml aprotinin 4 µM leupeptin 0.5 mM PMSF
-------------------	--

TEV Buffer:	50 mM Tris pH 7.5 150 mM NaCl 0.5 mM EDTA 1 mM DTT
Calmodulin Binding Buffer:	10 mM Tris pH 7.5 150 mM NaCl 0.2 % (v/v) NP-40 1 mM magnesium acetate 2 mM calcium chloride 1 mM imidazole 10 mM β -ME
Calmodulin Wash Buffer:	50 mM ammonium bicarbonate pH 8.0 75 mM NaCl 1 mM magnesium acetate 1 mM imidazole 2 mM calcium chloride
Calmodulin Elution Buffer :	50 mM ammonium bicarbonate pH8.0 25 mM EGTA
IgG affinity matrix:	IgG Sepharose 6 Fast Flow (Amersham Biosciences)
Calmodulin affinity matrix:	Calmodulin Sepharose 4B (Amersham Biosciences)

HEK293-C-TAP-PARP10 (wildtype and G888W mutant) cells were grown in spinner culture. They were induced for expression of the protein by addition of 1 μ g/ml doxycycline for 16 hours. The cells were harvested at 200 xg and 4 °C and washed with 20 ml ice-cold PBS. All following steps were carried out at 4 °C.

After resuspension in 15 ml lysis buffer per 500 ml suspension culture, lysis was carried out with slight agitation for 30 minutes. The resulting lysate was cleared by centrifugation (20.000 xg, 4 °C, 20 min) and the supernatant was incubated with 125 μ l equilibrated IgG Sepharose 6 FF per 15 ml lysate for 1 hour under rotation. The beads were spun down (200 xg, 2 min) and washed three times with TEV buffer before resuspension in 5 volumes of TEV buffer. Approximately 200-500 ng of His-tagged TEV protease (Invitrogen) per 10 μ l beads was added and cleavage was carried out for 2 hours under permanent agitation. The beads were again separated and the supernatant transferred to a new tube containing equilibrated Calmodulin Sepharose 4B (equal volume as for IgG sepharose). The remaining IgG sepharose was washed with 3 volumes calmodulin binding buffer, which was also added to the calmodulin sepharose after repeated separation.

With a CaCl_2 concentration of 5 mM the suspension was incubated for 90 minutes. The beads were again spun down and washed 3 times with calmodulin wash buffer, before the final elution in 2 volumes elution buffer. The resulting supernatant with the eluted protein was stored with a final MgCl_2 concentration of 25 mM at -80°C .

7.8 Enzymatic assays

7.8.1 ADP-ribosylation assay

2x Reaction Buffer: 100 mM Tris pH 8.0
 0.4 mM DTT
 8 mM MgCl_2

$[\text{}^{32}\text{P}]\text{-NAD}^+$ 370 MBq/ml (10 $\mu\text{Ci}/\mu\text{l}$) (Perkin Elmer)
 $\beta\text{-NAD}^+$ (Sigma)

The activity of ARTD10 was measured with incorporation of radioactive labeled NAD^+ . The immunoprecipitated proteins and substrates were incubated in 30 μl reaction volume at 30°C . The reaction was carried out in ADP-ribosylation assay buffer containing additionally 50 μM $\beta\text{-NAD}^+$ and 1 μCi $[\text{}^{32}\text{P}]\text{-NAD}^+$. After 30 minutes the reaction was stopped by the addition of 4x sample buffer and the samples were subjected to SDS-PAGE. After coomassie staining and drying of the gel, medical X-ray films (Fujifilm, 100NIF) were used to visualize modified proteins.

7.8.2 Caspase assay

2x caspase reaction buffer 100 mM Hepes
 100 mM NaCl
 0.2 % Chaps
 20 mM EDTA
 5 % Glycerol
 10 mM DTT
 pH 7.2

Caspases Set IV, human, recombinant (PromoKine)

0.1 unit recombinant human caspase was used in a 30 μl volume, containing the protein of interest and buffered with caspase reaction buffer. After incubation for 1-2 hours at 37°C the reaction was stopped by addition of 4x sample buffer and the fragments were analyzed by SDS-PAGE followed by western blotting and immunodetection or a coomassie staining.

7.9 Immunofluorescence

Fixing Solution:	3.7 % PFA in PBS
Permeabilizing Solution:	0.1 % Triton-X100 in PBS
Blocking Solution:	1 % BSA in Permeabilizing Solution
Antibody Solution:	0.2 % BSA in PBS

Hoechst 33258 [10 mg/ml] (Sigma)
Mowiol 4-88 (Calbiochem)
Glass coverslips
PBS

Cells were seeded on coverslips in a 12 well plate and induced for expression of ARTD10 for 4 hours. The slides were washed twice with PBS and the cells were fixed with fixing solution for 15-30 minutes. The PFA was removed by a washing step with permeabilizing solution and the coverslips were blocked with blocking solution for 30 minutes. The primary antibody was diluted 1:20 in antibody solution and applied to the coverslips before a 1 hour incubation at 37 °C. The cells were again washed three times with antibody solution before the appropriate fluophore coupled secondary antibody diluted 1:1000 was applied for 1 hour at 37 °C in the dark.

Subsequently the glass slides were washed with antibody solution, PCS and ddH₂O. To stain the nucleus Hoechst 33258 at a final concentration of 0.5 µg/ml was added for 5 minutes and removed with ddH₂O. Mowiol 4-88 was used to fix the coverslips on microscope slides and embed the cells. Images of the stained cells were taken using an epifluorescence microscopy on an Olympus IX50.

8 References

- Acehan, D., Jiang, X., Morgan, D.G., Heuser, J.E., Wang, X., and Akey, C.W. (2002). Three-dimensional structure of the apoptosome: implications for assembly, procaspase-9 binding, and activation. *Mol Cell* 9, 423-432.
- Agostini, L., Martinon, F., Burns, K., McDermott, M.F., Hawkins, P.N., and Tschopp, J. (2004). NALP3 forms an IL-1 β -processing inflammasome with increased activity in Muckle-Wells autoinflammatory disorder. *Immunity* 20, 319-325.
- Ahel, D., Horejsi, Z., Wiechens, N., Polo, S.E., Garcia-Wilson, E., Ahel, I., Flynn, H., Skehel, M., West, S.C., Jackson, S.P., *et al.* (2009). Poly(ADP-ribose)-dependent regulation of DNA repair by the chromatin remodeling enzyme ALC1. *Science* 325, 1240-1243.
- Ahel, I., Ahel, D., Matsusaka, T., Clark, A.J., Pines, J., Boulton, S.J., and West, S.C. (2008). Poly(ADP-ribose)-binding zinc finger motifs in DNA repair/checkpoint proteins. *Nature* 451, 81-85.
- Alkhatib, H.M., Chen, D.F., Cherney, B., Bhatia, K., Notario, V., Giri, C., Stein, G., Slattery, E., Roeder, R.G., and Smulson, M.E. (1987). Cloning and expression of cDNA for human poly(ADP-ribose) polymerase. *Proc Natl Acad Sci U S A* 84, 1224-1228.
- Alnemri, E.S., Livingston, D.J., Nicholson, D.W., Salvesen, G., Thornberry, N.A., Wong, W.W., and Yuan, J. (1996). Human ICE/CED-3 protease nomenclature. *Cell* 87, 171.
- Altmeyer, M., Barthel, M., Eberhard, M., Rehrauer, H., Hardt, W.D., and Hottiger, M.O. (2010). Absence of poly(ADP-ribose) polymerase 1 delays the onset of *Salmonella enterica* serovar Typhimurium-induced gut inflammation. *Infect Immun* 78, 3420-3431.
- Ame, J.C., Spenlehauer, C., and de Murcia, G. (2004). The PARP superfamily. *Bioessays* 26, 882-893.
- Amiri, K.I., Ha, H.C., Smulson, M.E., and Richmond, A. (2006). Differential regulation of CXC ligand 1 transcription in melanoma cell lines by poly(ADP-ribose) polymerase-1. *Oncogene* 25, 7714-7722.
- Andrabi, S.A., Dawson, T.M., and Dawson, V.L. (2008). Mitochondrial and nuclear cross talk in cell death: parthanatos. *Ann N Y Acad Sci* 1147, 233-241.
- Andrabi, S.A., Kang, H.C., Haince, J.F., Lee, Y.I., Zhang, J., Chi, Z., West, A.B., Koehler, R.C., Poirier, G.G., Dawson, T.M., *et al.* (2011). Iduna protects the brain from glutamate excitotoxicity and stroke by interfering with poly(ADP-ribose) polymer-induced cell death. *Nat Med* 17, 692-699.
- Aravind, L. (2001). The WWE domain: a common interaction module in protein ubiquitination and ADP ribosylation. *Trends Biochem Sci* 26, 273-275.
- Ba, X., Gupta, S., Davidson, M., and Garg, N.J. (2010). *Trypanosoma cruzi* induces the reactive oxygen species-PARP-1-RelA pathway for up-regulation of cytokine expression in cardiomyocytes. *J Biol Chem* 285, 11596-11606.
- Bauernfeind, F., Ablasser, A., Bartok, E., Kim, S., Schmid-Burgk, J., Cavar, T., and Hornung, V. (2011a). Inflammasomes: current understanding and open questions. *Cell Mol Life Sci* 68, 765-783.
- Bauernfeind, F., Bartok, E., Rieger, A., Franchi, L., Nunez, G., and Hornung, V. (2011b). Cutting edge: reactive oxygen species inhibitors block priming, but not activation, of the NLRP3 inflammasome. *J Immunol* 187, 613-617.
- Bauernfeind, F.G., Horvath, G., Stutz, A., Alnemri, E.S., MacDonald, K., Speert, D., Fernandes-Alnemri, T., Wu, J., Monks, B.G., Fitzgerald, K.A., *et al.* (2009). Cutting edge: NF- κ B activating

pattern recognition and cytokine receptors license NLRP3 inflammasome activation by regulating NLRP3 expression. *J Immunol* 183, 787-791.

Bell, C.E., and Eisenberg, D. (1996). Crystal structure of diphtheria toxin bound to nicotinamide adenine dinucleotide. *Biochemistry* 35, 1137-1149.

Bella, J., Hindle, K.L., McEwan, P.A., and Lovell, S.C. (2008). The leucine-rich repeat structure. *Cell Mol Life Sci* 65, 2307-2333.

Belmokhtar, C.A., Hillion, J., and Segal-Bendirdjian, E. (2001). Staurosporine induces apoptosis through both caspase-dependent and caspase-independent mechanisms. *Oncogene* 20, 3354-3362.

Benedict, C.A., Norris, P.S., and Ware, C.F. (2002). To kill or be killed: viral evasion of apoptosis. *Nat Immunol* 3, 1013-1018.

Bernardi, P., and Azzone, G.F. (1981). Cytochrome c as an electron shuttle between the outer and inner mitochondrial membranes. *J Biol Chem* 256, 7187-7192.

Bertrand, M.J., Milutinovic, S., Dickson, K.M., Ho, W.C., Boudreault, A., Durkin, J., Gillard, J.W., Jaquith, J.B., Morris, S.J., and Barker, P.A. (2008). cIAP1 and cIAP2 facilitate cancer cell survival by functioning as E3 ligases that promote RIP1 ubiquitination. *Mol Cell* 30, 689-700.

Bessman, M.J., Frick, D.N., and O'Handley, S.F. (1996). The MutT proteins or "Nudix" hydrolases, a family of versatile, widely distributed, "housecleaning" enzymes. *J Biol Chem* 271, 25059-25062.

Bischof, O., Galande, S., Farzaneh, F., Kohwi-Shigematsu, T., and Campisi, J. (2001). Selective cleavage of BLM, the bloom syndrome protein, during apoptotic cell death. *J Biol Chem* 276, 12068-12075.

Boucher, D., Blais, V., and Denault, J.B. (2012). Caspase-7 uses an exosite to promote poly(ADP ribose) polymerase 1 proteolysis. *Proc Natl Acad Sci U S A* 109, 5669-5674.

Brown, S., Heinisch, I., Ross, E., Shaw, K., Buckley, C.D., and Savill, J. (2002). Apoptosis disables CD31-mediated cell detachment from phagocytes promoting binding and engulfment. *Nature* 418, 200-203.

Bruey, J.M., Bruey-Sedano, N., Luciano, F., Zhai, D., Balpai, R., Xu, C., Kress, C.L., Bailly-Maitre, B., Li, X., Osterman, A., *et al.* (2007). Bcl-2 and Bcl-XL regulate proinflammatory caspase-1 activation by interaction with NALP1. *Cell* 129, 45-56.

Burd, C.G., and Dreyfuss, G. (1994). Conserved structures and diversity of functions of RNA-binding proteins. *Science* 265, 615-621.

Buss, R.R., Sun, W., and Oppenheim, R.W. (2006). Adaptive roles of programmed cell death during nervous system development. *Annu Rev Neurosci* 29, 1-35.

Cande, C., Cohen, I., Daugas, E., Ravagnan, L., Larochette, N., Zamzami, N., and Kroemer, G. (2002). Apoptosis-inducing factor (AIF): a novel caspase-independent death effector released from mitochondria. *Biochimie* 84, 215-222.

Cartegni, L., Maconi, M., Morandi, E., Cobianchi, F., Riva, S., and Biamonti, G. (1996). hnRNP A1 selectively interacts through its Gly-rich domain with different RNA-binding proteins. *J Mol Biol* 259, 337-348.

Castedo, M., Perfettini, J.L., Roumier, T., Andreau, K., Medema, R., and Kroemer, G. (2004). Cell death by mitotic catastrophe: a molecular definition. *Oncogene* 23, 2825-2837.

Chai, J., Du, C., Wu, J.W., Kyin, S., Wang, X., and Shi, Y. (2000). Structural and biochemical basis of apoptotic activation by Smac/DIABLO. *Nature* 406, 855-862.

- Chambon, P., Weill, J.D., and Mandel, P. (1963). Nicotinamide mononucleotide activation of new DNA-dependent polyadenylic acid synthesizing nuclear enzyme. *Biochem Biophys Res Commun* **11**, 39-43.
- Chauvistré, H. (2008). Regulation von Poly-ADP-Ribose-Polymerase 10 durch Ubiquitinierung (Diploma thesis, RWTH Aachen University).
- Cheng, E.H., Kirsch, D.G., Clem, R.J., Ravi, R., Kastan, M.B., Bedi, A., Ueno, K., and Hardwick, J.M. (1997). Conversion of Bcl-2 to a Bax-like death effector by caspases. *Science* **278**, 1966-1968.
- Cheng, E.H., Levine, B., Boise, L.H., Thompson, C.B., and Hardwick, J.M. (1996). Bax-independent inhibition of apoptosis by Bcl-XL. *Nature* **379**, 554-556.
- Cheng, E.H., Wei, M.C., Weiler, S., Flavell, R.A., Mak, T.W., Lindsten, T., and Korsmeyer, S.J. (2001). BCL-2, BCL-X(L) sequester BH3 domain-only molecules preventing BAX- and BAK-mediated mitochondrial apoptosis. *Mol Cell* **8**, 705-711.
- Chinnaiyan, A.M., O'Rourke, K., Tewari, M., and Dixit, V.M. (1995). FADD, a novel death domain-containing protein, interacts with the death domain of Fas and initiates apoptosis. *Cell* **81**, 505-512.
- Choi, Y.E., Butterworth, M., Malladi, S., Duckett, C.S., Cohen, G.M., and Bratton, S.B. (2009). The E3 ubiquitin ligase cIAP1 binds and ubiquitinates caspase-3 and -7 via unique mechanisms at distinct steps in their processing. *J Biol Chem* **284**, 12772-12782.
- Chou, H.Y., Chou, H.T., and Lee, S.C. (2006). CDK-dependent activation of poly(ADP-ribose) polymerase member 10 (PARP10). *J Biol Chem* **281**, 15201-15207.
- Chu, W., Rothfuss, J., Chu, Y., Zhou, D., and Mach, R.H. (2009). Synthesis and in vitro evaluation of sulfonamide isatin Michael acceptors as small molecule inhibitors of caspase-6. *J Med Chem* **52**, 2188-2191.
- Clarke, A.R., Purdie, C.A., Harrison, D.J., Morris, R.G., Bird, C.C., Hooper, M.L., and Wyllie, A.H. (1993). Thymocyte apoptosis induced by p53-dependent and independent pathways. *Nature* **362**, 849-852.
- Clarke, P., and Tyler, K.L. (2009). Apoptosis in animal models of virus-induced disease. *Nat Rev Microbiol* **7**, 144-155.
- Clery, A., Blatter, M., and Allain, F.H. (2008). RNA recognition motifs: boring? Not quite. *Curr Opin Struct Biol* **18**, 290-298.
- Cogswell, J.P., Brown, C.E., Bisi, J.E., and Neill, S.D. (2000). Dominant-negative polo-like kinase 1 induces mitotic catastrophe independent of cdc25C function. *Cell Growth Differ* **11**, 615-623.
- Cowling, V., and Downward, J. (2002). Caspase-6 is the direct activator of caspase-8 in the cytochrome c-induced apoptosis pathway: absolute requirement for removal of caspase-6 prodomain. *Cell Death Differ* **9**, 1046-1056.
- Crook, N.E., Clem, R.J., and Miller, L.K. (1993). An apoptosis-inhibiting baculovirus gene with a zinc finger-like motif. *J Virol* **67**, 2168-2174.
- D'Amours, D., Desnoyers, S., D'Silva, I., and Poirier, G.G. (1999). Poly(ADP-ribosyl)ation reactions in the regulation of nuclear functions. *Biochem J* **342** (Pt 2), 249-268.
- David, K.K., Andrabi, S.A., Dawson, T.M., and Dawson, V.L. (2009). Parthanatos, a messenger of death. *Front Biosci* **14**, 1116-1128.
- Davidovic, L., Vodenicharov, M., Affar, E.B., and Poirier, G.G. (2001). Importance of poly(ADP-ribose) glycohydrolase in the control of poly(ADP-ribose) metabolism. *Exp Cell Res* **268**, 7-13.

- de Calignon, A., Fox, L.M., Pitstick, R., Carlson, G.A., Bacskai, B.J., Spires-Jones, T.L., and Hyman, B.T. (2010). Caspase activation precedes and leads to tangles. *Nature* **464**, 1201-1204.
- Debatin, K.M., and Krammer, P.H. (2004). Death receptors in chemotherapy and cancer. *Oncogene* **23**, 2950-2966.
- Denecker, G., Ovaere, P., Vandenabeele, P., and Declercq, W. (2008). Caspase-14 reveals its secrets. *J Cell Biol* **180**, 451-458.
- Desagher, S., Osen-Sand, A., Montessuit, S., Magnenat, E., Vilbois, F., Hochmann, A., Journot, L., Antonsson, B., and Martinou, J.C. (2001). Phosphorylation of bid by casein kinases I and II regulates its cleavage by caspase 8. *Mol Cell* **8**, 601-611.
- Desagher, S., Osen-Sand, A., Nichols, A., Eskes, R., Montessuit, S., Lauper, S., Maundrell, K., Antonsson, B., and Martinou, J.C. (1999). Bid-induced conformational change of Bax is responsible for mitochondrial cytochrome c release during apoptosis. *J Cell Biol* **144**, 891-901.
- Deveraux, Q.L., and Reed, J.C. (1999). IAP family proteins--suppressors of apoptosis. *Genes Dev* **13**, 239-252.
- Dostert, C., Petrilli, V., Van Bruggen, R., Steele, C., Mossman, B.T., and Tschopp, J. (2008). Innate immune activation through Nalp3 inflammasome sensing of asbestos and silica. *Science* **320**, 674-677.
- Dreyfuss, G., Matunis, M.J., Pinol-Roma, S., and Burd, C.G. (1993). hnRNP proteins and the biogenesis of mRNA. *Annu Rev Biochem* **62**, 289-321.
- Du, C., Fang, M., Li, Y., Li, L., and Wang, X. (2000). Smac, a mitochondrial protein that promotes cytochrome c-dependent caspase activation by eliminating IAP inhibition. *Cell* **102**, 33-42.
- Duncan, J.A., Bergstralh, D.T., Wang, Y., Willingham, S.B., Ye, Z., Zimmermann, A.G., and Ting, J.P. (2007). Cryopyrin/NALP3 binds ATP/dATP, is an ATPase, and requires ATP binding to mediate inflammatory signaling. *Proc Natl Acad Sci U S A* **104**, 8041-8046.
- Duncan, J.S., Turowec, J.P., Duncan, K.E., Vilks, G., Wu, C., Luscher, B., Li, S.S., Gloor, G.B., and Litchfield, D.W. (2011). A peptide-based target screen implicates the protein kinase CK2 in the global regulation of caspase signaling. *Sci Signal* **4**, ra30.
- Duncan, J.S., Turowec, J.P., Vilks, G., Li, S.S., Gloor, G.B., and Litchfield, D.W. (2010). Regulation of cell proliferation and survival: convergence of protein kinases and caspases. *Biochim Biophys Acta* **1804**, 505-510.
- Duran, A., Linares, J.F., Galvez, A.S., Wikenheiser, K., Flores, J.M., Diaz-Meco, M.T., and Moscat, J. (2008). The signaling adaptor p62 is an important NF-kappaB mediator in tumorigenesis. *Cancer Cell* **13**, 343-354.
- Eckelman, B.P., and Salvesen, G.S. (2006). The human anti-apoptotic proteins cIAP1 and cIAP2 bind but do not inhibit caspases. *J Biol Chem* **281**, 3254-3260.
- Eckelman, B.P., Salvesen, G.S., and Scott, F.L. (2006). Human inhibitor of apoptosis proteins: why XIAP is the black sheep of the family. *EMBO Rep* **7**, 988-994.
- Eisenbarth, S.C., Colegio, O.R., O'Connor, W., Sutterwala, F.S., and Flavell, R.A. (2008). Crucial role for the Nalp3 inflammasome in the immunostimulatory properties of aluminium adjuvants. *Nature* **453**, 1122-1126.
- Elmore, S. (2007). Apoptosis: a review of programmed cell death. *Toxicol Pathol* **35**, 495-516.
- Elward, K., Griffiths, M., Mizuno, M., Harris, C.L., Neal, J.W., Morgan, B.P., and Gasque, P. (2005). CD46 plays a key role in tailoring innate immune recognition of apoptotic and necrotic cells. *J Biol Chem* **280**, 36342-36354.

- Eskes, R., Desagher, S., Antonsson, B., and Martinou, J.C. (2000). Bid induces the oligomerization and insertion of Bax into the outer mitochondrial membrane. *Mol Cell Biol* 20, 929-935.
- Fairbrother, W.J., Gordon, N.C., Humke, E.W., O'Rourke, K.M., Starovasnik, M.A., Yin, J.P., and Dixit, V.M. (2001). The PYRIN domain: a member of the death domain-fold superfamily. *Protein Sci* 10, 1911-1918.
- Fan, T.J., Han, L.H., Cong, R.S., and Liang, J. (2005). Caspase family proteases and apoptosis. *Acta Biochim Biophys Sin (Shanghai)* 37, 719-727.
- Faustin, B., Lartigue, L., Bruey, J.M., Luciano, F., Sergienko, E., Bailly-Maitre, B., Volkmann, N., Hanein, D., Rouiller, I., and Reed, J.C. (2007). Reconstituted NALP1 inflammasome reveals two-step mechanism of caspase-1 activation. *Mol Cell* 25, 713-724.
- Feijs, K.L. (2009). PARP10 - Insights into its mono-ADP-ribosylation, nuclear import & influence on cell proliferation (Master thesis, RWTH Aachen).
- Fernandes-Alnemri, T., Litwack, G., and Alnemri, E.S. (1995). Mch2, a new member of the apoptotic Ced-3/Ice cysteine protease gene family. *Cancer Res* 55, 2737-2742.
- Fernandes-Alnemri, T., Yu, J.W., Datta, P., Wu, J., and Alnemri, E.S. (2009). AIM2 activates the inflammasome and cell death in response to cytoplasmic DNA. *Nature* 458, 509-513.
- Ferrari, D., Pizzirani, C., Adinolfi, E., Lemoli, R.M., Curti, A., Idzko, M., Panther, E., and Di Virgilio, F. (2006). The P2X7 receptor: a key player in IL-1 processing and release. *J Immunol* 176, 3877-3883.
- Ferraro-Peyret, C., Quemeneur, L., Flacher, M., Revillard, J.P., and Genestier, L. (2002). Caspase-independent phosphatidylserine exposure during apoptosis of primary T lymphocytes. *J Immunol* 169, 4805-4810.
- Finn, R.D., Mistry, J., Schuster-Bockler, B., Griffiths-Jones, S., Hollich, V., Lassmann, T., Moxon, S., Marshall, M., Khanna, A., Durbin, R., *et al.* (2006). Pfam: clans, web tools and services. *Nucleic Acids Res* 34, D247-251.
- Fornerod, M., Ohno, M., Yoshida, M., and Mattaj, I.W. (1997). CRM1 is an export receptor for leucine-rich nuclear export signals. *Cell* 90, 1051-1060.
- Franchi, L., Amer, A., Body-Malapel, M., Kanneganti, T.D., Ozoren, N., Jagirdar, R., Inohara, N., Vandenabeele, P., Bertin, J., Coyle, A., *et al.* (2006). Cytosolic flagellin requires Ipaf for activation of caspase-1 and interleukin 1beta in salmonella-infected macrophages. *Nat Immunol* 7, 576-582.
- Fuentes-Prior, P., and Salvesen, G.S. (2004). The protein structures that shape caspase activity, specificity, activation and inhibition. *Biochem J* 384, 201-232.
- Fulda, S., Meyer, E., Friesen, C., Susin, S.A., Kroemer, G., and Debatin, K.M. (2001). Cell type specific involvement of death receptor and mitochondrial pathways in drug-induced apoptosis. *Oncogene* 20, 1063-1075.
- Gagne, J.P., Isabelle, M., Lo, K.S., Bourassa, S., Hendzel, M.J., Dawson, V.L., Dawson, T.M., and Poirier, G.G. (2008). Proteome-wide identification of poly(ADP-ribose) binding proteins and poly(ADP-ribose)-associated protein complexes. *Nucleic Acids Res* 36, 6959-6976.
- Gaur, U., and Aggarwal, B.B. (2003). Regulation of proliferation, survival and apoptosis by members of the TNF superfamily. *Biochem Pharmacol* 66, 1403-1408.
- Gavathiotis, E., Suzuki, M., Davis, M.L., Pitter, K., Bird, G.H., Katz, S.G., Tu, H.C., Kim, H., Cheng, E.H., Tjandra, N., *et al.* (2008). BAX activation is initiated at a novel interaction site. *Nature* 455, 1076-1081.
- George, N.M., Evans, J.J., and Luo, X. (2007). A three-helix homo-oligomerization domain containing BH3 and BH1 is responsible for the apoptotic activity of Bax. *Genes Dev* 21, 1937-1948.

- Gibson, B.A., and Kraus, W.L. (2012). New insights into the molecular and cellular functions of poly(ADP-ribose) and PARPs. *Nat Rev Mol Cell Biol* 13, 411-424.
- Gill, D.M., Pappenheimer, A.M., Jr., Brown, R., and Kurnick, J.T. (1969). Studies on the mode of action of diphtheria toxin. VII. Toxin-stimulated hydrolysis of nicotinamide adenine dinucleotide in mammalian cell extracts. *J Exp Med* 129, 1-21.
- Glowacki, G., Braren, R., Firner, K., Nissen, M., Kuhl, M., Reche, P., Bazan, F., Cetkovic-Cvrlje, M., Leiter, E., Haag, F., *et al.* (2002). The family of toxin-related ecto-ADP-ribosyltransferases in humans and the mouse. *Protein Sci* 11, 1657-1670.
- Graham, R.K., Deng, Y., Carroll, J., Vaid, K., Cowan, C., Pouladi, M.A., Metzler, M., Bissada, N., Wang, L., Faull, R.L., *et al.* (2010). Cleavage at the 586 amino acid caspase-6 site in mutant huntingtin influences caspase-6 activation in vivo. *J Neurosci* 30, 15019-15029.
- Graham, R.K., Ehrnhoefer, D.E., and Hayden, M.R. (2011). Caspase-6 and neurodegeneration. *Trends Neurosci* 34, 646-656.
- Halle, A., Hornung, V., Petzold, G.C., Stewart, C.R., Monks, B.G., Reinheckel, T., Fitzgerald, K.A., Latz, E., Moore, K.J., and Golenbock, D.T. (2008). The NALP3 inflammasome is involved in the innate immune response to amyloid-beta. *Nat Immunol* 9, 857-865.
- Hassa, P.O., and Hottiger, M.O. (2002). The functional role of poly(ADP-ribose)polymerase 1 as novel coactivator of NF-kappaB in inflammatory disorders. *Cell Mol Life Sci* 59, 1534-1553.
- Hengartner, M.O., and Horvitz, H.R. (1994). *C. elegans* cell survival gene *ced-9* encodes a functional homolog of the mammalian proto-oncogene *bcl-2*. *Cell* 76, 665-676.
- Hinds, M.G., Norton, R.S., Vaux, D.L., and Day, C.L. (1999). Solution structure of a baculoviral inhibitor of apoptosis (IAP) repeat. *Nat Struct Biol* 6, 648-651.
- Hirata, H., Takahashi, A., Kobayashi, S., Yonehara, S., Sawai, H., Okazaki, T., Yamamoto, K., and Sasada, M. (1998). Caspases are activated in a branched protease cascade and control distinct downstream processes in Fas-induced apoptosis. *J Exp Med* 187, 587-600.
- Honjo, T., Nishizuka, Y., and Hayaishi, O. (1968). Diphtheria toxin-dependent adenosine diphosphate ribosylation of aminoacyl transferase II and inhibition of protein synthesis. *J Biol Chem* 243, 3553-3555.
- Hornung, V., Ablasser, A., Charrel-Dennis, M., Bauernfeind, F., Horvath, G., Caffrey, D.R., Latz, E., and Fitzgerald, K.A. (2009). AIM2 recognizes cytosolic dsDNA and forms a caspase-1-activating inflammasome with ASC. *Nature* 458, 514-518.
- Hornung, V., Bauernfeind, F., Halle, A., Samstad, E.O., Kono, H., Rock, K.L., Fitzgerald, K.A., and Latz, E. (2008). Silica crystals and aluminum salts activate the NALP3 inflammasome through phagosomal destabilization. *Nat Immunol* 9, 847-856.
- Horvath, G.L., Schrum, J.E., De Nardo, C.M., and Latz, E. (2011). Intracellular sensing of microbes and danger signals by the inflammasomes. *Immunol Rev* 243, 119-135.
- Hottiger, M.O., Hassa, P.O., Luscher, B., Schuler, H., and Koch-Nolte, F. (2010). Toward a unified nomenclature for mammalian ADP-ribosyltransferases. *Trends Biochem Sci* 35, 208-219.
- Hsu, H., Xiong, J., and Goeddel, D.V. (1995). The TNF receptor 1-associated protein TRADD signals cell death and NF-kappa B activation. *Cell* 81, 495-504.
- Hsu, L.C., Ali, S.R., McGillivray, S., Tseng, P.H., Mariathasan, S., Humke, E.W., Eckmann, L., Powell, J.J., Nizet, V., Dixit, V.M., *et al.* (2008). A NOD2-NALP1 complex mediates caspase-1-dependent IL-1beta secretion in response to *Bacillus anthracis* infection and muramyl dipeptide. *Proc Natl Acad Sci U S A* 105, 7803-7808.

- Hu, S., and Yang, X. (2003). Cellular inhibitor of apoptosis 1 and 2 are ubiquitin ligases for the apoptosis inducer Smac/DIABLO. *J Biol Chem* 278, 10055-10060.
- Huigsloot, M., Tijdens, I.B., Mulder, G.J., and van de Water, B. (2001). Differential regulation of phosphatidylserine externalization and DNA fragmentation by caspases in anticancer drug-induced apoptosis of rat mammary adenocarcinoma MTLn3 cells. *Biochem Pharmacol* 62, 1087-1097.
- Ikejima, M., Noguchi, S., Yamashita, R., Ogura, T., Sugimura, T., Gill, D.M., and Miwa, M. (1990). The zinc fingers of human poly(ADP-ribose) polymerase are differentially required for the recognition of DNA breaks and nicks and the consequent enzyme activation. Other structures recognize intact DNA. *J Biol Chem* 265, 21907-21913.
- Janicke, R.U., Ng, P., Sprengart, M.L., and Porter, A.G. (1998). Caspase-3 is required for alpha-fodrin cleavage but dispensable for cleavage of other death substrates in apoptosis. *J Biol Chem* 273, 15540-15545.
- Jin, Z., Li, Y., Pitti, R., Lawrence, D., Pham, V.C., Lill, J.R., and Ashkenazi, A. (2009). Cullin3-based polyubiquitination and p62-dependent aggregation of caspase-8 mediate extrinsic apoptosis signaling. *Cell* 137, 721-735.
- Johansen, T., and Lamark, T. (2011). Selective autophagy mediated by autophagic adapter proteins. *Autophagy* 7, 279-296.
- Johnson, C.E., and Kornbluth, S. (2008). Caspase cleavage is not for everyone. *Cell* 134, 720-721.
- Kalisch, T., Ame, J.C., Dantzer, F., and Schreiber, V. (2012). New readers and interpretations of poly(ADP-ribosyl)ation. *Trends Biochem Sci*.
- Kang, H.C., Lee, Y.I., Shin, J.H., Andrabi, S.A., Chi, Z., Gagne, J.P., Lee, Y., Ko, H.S., Lee, B.D., Poirier, G.G., *et al.* (2011). Iduna is a poly(ADP-ribose) (PAR)-dependent E3 ubiquitin ligase that regulates DNA damage. *Proc Natl Acad Sci U S A* 108, 14103-14108.
- Kanneganti, T.D., Lamkanfi, M., Kim, Y.G., Chen, G., Park, J.H., Franchi, L., Vandenabeele, P., and Nunez, G. (2007). Pannexin-1-mediated recognition of bacterial molecules activates the cryopyrin inflammasome independent of Toll-like receptor signaling. *Immunity* 26, 433-443.
- Kanneganti, T.D., Ozoren, N., Body-Malapel, M., Amer, A., Park, J.H., Franchi, L., Whitfield, J., Barchet, W., Colonna, M., Vandenabeele, P., *et al.* (2006). Bacterial RNA and small antiviral compounds activate caspase-1 through cryopyrin/Nalp3. *Nature* 440, 233-236.
- Karpnich, N.O., Tafani, M., Rothman, R.J., Russo, M.A., and Farber, J.L. (2002). The course of etoposide-induced apoptosis from damage to DNA and p53 activation to mitochondrial release of cytochrome c. *J Biol Chem* 277, 16547-16552.
- Karras, G.I., Kustatscher, G., Buhecha, H.R., Allen, M.D., Pugieux, C., Sait, F., Bycroft, M., and Ladurner, A.G. (2005). The macro domain is an ADP-ribose binding module. *Embo J* 24, 1911-1920.
- Kashima, L., Idogawa, M., Mita, H., Shitashige, M., Yamada, T., Ogi, K., Suzuki, H., Toyota, M., Ariga, H., Sasaki, Y., *et al.* (2012). CHFR protein regulates mitotic checkpoint by targeting PARP-1 protein for ubiquitination and degradation. *J Biol Chem* 287, 12975-12984.
- Keller, M., Ruegg, A., Werner, S., and Beer, H.D. (2008). Active caspase-1 is a regulator of unconventional protein secretion. *Cell* 132, 818-831.
- Kerr, J.F., Wyllie, A.H., and Currie, A.R. (1972). Apoptosis: a basic biological phenomenon with wide-ranging implications in tissue kinetics. *Br J Cancer* 26, 239-257.
- Kiehlbauch, C.C., Aboul-Ela, N., Jacobson, E.L., Ringer, D.P., and Jacobson, M.K. (1993). High resolution fractionation and characterization of ADP-ribose polymers. *Anal Biochem* 208, 26-34.

- Kim, J.S., Park, S.J., Kwak, K.J., Kim, Y.O., Kim, J.Y., Song, J., Jang, B., Jung, C.H., and Kang, H. (2007). Cold shock domain proteins and glycine-rich RNA-binding proteins from *Arabidopsis thaliana* can promote the cold adaptation process in *Escherichia coli*. *Nucleic Acids Res* 35, 506-516.
- Kim, M.Y., Zhang, T., and Kraus, W.L. (2005). Poly(ADP-ribosyl)ation by PARP-1: 'PAR-laying' NAD⁺ into a nuclear signal. *Genes Dev* 19, 1951-1967.
- Kirkin, V., McEwan, D.G., Novak, I., and Dikic, I. (2009). A role for ubiquitin in selective autophagy. *Mol Cell* 34, 259-269.
- Klaiman, G., Champagne, N., and LeBlanc, A.C. (2009). Self-activation of Caspase-6 in vitro and in vivo: Caspase-6 activation does not induce cell death in HEK293T cells. *Biochim Biophys Acta* 1793, 592-601.
- Kleine, H., Herrmann, A., Lamark, T., Forst, A.H., Verheugd, P., Luscher-Firzlaff, J., Lippok, B., Feijs, K.L., Herzog, N., Kremmer, E., *et al.* (2012). Dynamic subcellular localization of the mono-ADP-ribosyltransferase ARTD10 and interaction with the ubiquitin receptor p62. *Cell Commun Signal* 10, 28.
- Kleine, H., Poreba, E., Lesniewicz, K., Hassa, P.O., Hottiger, M.O., Litchfield, D.W., Shilton, B.H., and Luscher, B. (2008). Substrate-assisted catalysis by PARP10 limits its activity to mono-ADP-ribosylation. *Mol Cell* 32, 57-69.
- Koh, D.W., Lawler, A.M., Poitras, M.F., Sasaki, M., Wattler, S., Nehls, M.C., Stoger, T., Poirier, G.G., Dawson, V.L., and Dawson, T.M. (2004). Failure to degrade poly(ADP-ribose) causes increased sensitivity to cytotoxicity and early embryonic lethality. *Proc Natl Acad Sci U S A* 101, 17699-17704.
- Kraus, W.L. (2008). Transcriptional control by PARP-1: chromatin modulation, enhancer-binding, coregulation, and insulation. *Curr Opin Cell Biol* 20, 294-302.
- Krippner-Heidenreich, A., Talanian, R.V., Sekul, R., Kraft, R., Thole, H., Ottleben, H., and Luscher, B. (2001). Targeting of the transcription factor Max during apoptosis: phosphorylation-regulated cleavage by caspase-5 at an unusual glutamic acid residue in position P1. *Biochem J* 358, 705-715.
- Kroemer, G., Galluzzi, L., and Brenner, C. (2007). Mitochondrial membrane permeabilization in cell death. *Physiol Rev* 87, 99-163.
- Kroemer, G., Galluzzi, L., Vandenabeele, P., Abrams, J., Alnemri, E.S., Baehrecke, E.H., Blagosklonny, M.V., El-Deiry, W.S., Golstein, P., Green, D.R., *et al.* (2009). Classification of cell death: recommendations of the Nomenclature Committee on Cell Death 2009. *Cell Death Differ* 16, 3-11.
- Kroemer, G., and Martin, S.J. (2005). Caspase-independent cell death. *Nat Med* 11, 725-730.
- Krueger, A., Baumann, S., Krammer, P.H., and Kirchhoff, S. (2001). FLICE-inhibitory proteins: regulators of death receptor-mediated apoptosis. *Mol Cell Biol* 21, 8247-8254.
- Kurokawa, M., and Kornbluth, S. (2009). Caspases and kinases in a death grip. *Cell* 138, 838-854.
- Kurosaki, T., Ushiro, H., Mitsuuchi, Y., Suzuki, S., Matsuda, M., Matsuda, Y., Katunuma, N., Kangawa, K., Matsuo, H., Hirose, T., *et al.* (1987). Primary structure of human poly(ADP-ribose) synthetase as deduced from cDNA sequence. *J Biol Chem* 262, 15990-15997.
- Kuwana, T., Mackey, M.R., Perkins, G., Ellisman, M.H., Latterich, M., Schneider, R., Green, D.R., and Newmeyer, D.D. (2002). Bid, Bax, and lipids cooperate to form supramolecular openings in the outer mitochondrial membrane. *Cell* 111, 331-342.
- Langelier, M.F., Planck, J.L., Roy, S., and Pascal, J.M. (2012). Structural basis for DNA damage-dependent poly(ADP-ribosyl)ation by human PARP-1. *Science* 336, 728-732.
- Langelier, M.F., Servent, K.M., Rogers, E.E., and Pascal, J.M. (2008). A third zinc-binding domain of human poly(ADP-ribose) polymerase-1 coordinates DNA-dependent enzyme activation. *J Biol Chem* 283, 4105-4114.

- Lazebnik, Y.A., Kaufmann, S.H., Desnoyers, S., Poirier, G.G., and Earnshaw, W.C. (1994). Cleavage of poly(ADP-ribose) polymerase by a proteinase with properties like ICE. *Nature* **371**, 346-347.
- Lesniewicz, K., Luscher-Firzlaff, J., Poreba, E., Fuchs, P., Walsemann, G., Wiche, G., and Luscher, B. (2005). Overlap of the gene encoding the novel poly(ADP-ribose) polymerase Parp10 with the plectin 1 gene and common use of exon sequences. *Genomics* **86**, 38-46.
- Levkau, B., Scatena, M., Giachelli, C.M., Ross, R., and Raines, E.W. (1999). Apoptosis overrides survival signals through a caspase-mediated dominant-negative NF-kappa B loop. *Nat Cell Biol* **1**, 227-233.
- Li, G.Y., McCulloch, R.D., Fenton, A.L., Cheung, M., Meng, L., Ikura, M., and Koch, C.A. (2010). Structure and identification of ADP-ribose recognition motifs of APLF and role in the DNA damage response. *Proc Natl Acad Sci U S A* **107**, 9129-9134.
- Li, L.Y., Luo, X., and Wang, X. (2001). Endonuclease G is an apoptotic DNase when released from mitochondria. *Nature* **412**, 95-99.
- Li, X., Yang, Y., and Ashwell, J.D. (2002). TNF-RII and c-IAP1 mediate ubiquitination and degradation of TRAF2. *Nature* **416**, 345-347.
- Liaudet, L., Pacher, P., Mabley, J.G., Virag, L., Soriano, F.G., Hasko, G., and Szabo, C. (2002). Activation of poly(ADP-Ribose) polymerase-1 is a central mechanism of lipopolysaccharide-induced acute lung inflammation. *Am J Respir Crit Care Med* **165**, 372-377.
- Lindsten, T., Ross, A.J., King, A., Zong, W.X., Rathmell, J.C., Shiels, H.A., Ulrich, E., Waymire, K.G., Mahar, P., Frauwirth, K., *et al.* (2000). The combined functions of proapoptotic Bcl-2 family members bak and bax are essential for normal development of multiple tissues. *Mol Cell* **6**, 1389-1399.
- Liu, X., Zou, H., Slaughter, C., and Wang, X. (1997). DFF, a heterodimeric protein that functions downstream of caspase-3 to trigger DNA fragmentation during apoptosis. *Cell* **89**, 175-184.
- Liu, X., Zou, H., Widlak, P., Garrard, W., and Wang, X. (1999). Activation of the apoptotic endonuclease DFF40 (caspase-activated DNase or nuclease). Oligomerization and direct interaction with histone H1. *J Biol Chem* **274**, 13836-13840.
- Loffler, H., Lukas, J., Bartek, J., and Kramer, A. (2006). Structure meets function--centrosomes, genome maintenance and the DNA damage response. *Exp Cell Res* **312**, 2633-2640.
- Lomonosova, E., and Chinnadurai, G. (2008). BH3-only proteins in apoptosis and beyond: an overview. *Oncogene* **27 Suppl 1**, S2-19.
- Long, J.S., and Ryan, K.M. (2012). New frontiers in promoting tumour cell death: targeting apoptosis, necroptosis and autophagy. *Oncogene*.
- Lonskaya, I., Potaman, V.N., Shlyakhtenko, L.S., Oussatcheva, E.A., Lyubchenko, Y.L., and Soldatenkov, V.A. (2005). Regulation of poly(ADP-ribose) polymerase-1 by DNA structure-specific binding. *J Biol Chem* **280**, 17076-17083.
- Lopez, J., John, S.W., Tenev, T., Rautureau, G.J., Hinds, M.G., Francalanci, F., Wilson, R., Broemer, M., Santoro, M.M., Day, C.L., *et al.* (2011). CARD-mediated autoinhibition of cIAP1's E3 ligase activity suppresses cell proliferation and migration. *Mol Cell* **42**, 569-583.
- Lowe, S.W., and Lin, A.W. (2000). Apoptosis in cancer. *Carcinogenesis* **21**, 485-495.
- Lowe, S.W., Schmitt, E.M., Smith, S.W., Osborne, B.A., and Jacks, T. (1993). p53 is required for radiation-induced apoptosis in mouse thymocytes. *Nature* **362**, 847-849.
- Luo, L., and O'Leary, D.D. (2005). Axon retraction and degeneration in development and disease. *Annu Rev Neurosci* **28**, 127-156.

- Luo, X., and Kraus, W.L. (2012). On PAR with PARP: cellular stress signaling through poly(ADP-ribose) and PARP-1. *Genes Dev* 26, 417-432.
- Luthi, A.U., and Martin, S.J. (2007). The CASBAH: a searchable database of caspase substrates. *Cell Death Differ* 14, 641-650.
- Ma, H.T., and Poon, R.Y. (2011). How protein kinases co-ordinate mitosis in animal cells. *Biochem J* 435, 17-31.
- Malireddi, R.K., Ippagunta, S., Lamkanfi, M., and Kanneganti, T.D. (2010). Cutting edge: proteolytic inactivation of poly(ADP-ribose) polymerase 1 by the Nlrp3 and Nlr4 inflammasomes. *J Immunol* 185, 3127-3130.
- Mangeon, A., Junqueira, R.M., and Sachetto-Martins, G. (2010). Functional diversity of the plant glycine-rich proteins superfamily. *Plant Signal Behav* 5, 99-104.
- Manji, G.A., Wang, L., Geddes, B.J., Brown, M., Merriam, S., Al-Garawi, A., Mak, S., Lora, J.M., Briskin, M., Jurman, M., *et al.* (2002). PYPAF1, a PYRIN-containing Apaf1-like protein that assembles with ASC and regulates activation of NF-kappa B. *J Biol Chem* 277, 11570-11575.
- Mariathasan, S., Newton, K., Monack, D.M., Vucic, D., French, D.M., Lee, W.P., Roose-Girma, M., Erickson, S., and Dixit, V.M. (2004). Differential activation of the inflammasome by caspase-1 adaptors ASC and Ipaf. *Nature* 430, 213-218.
- Maris, C., Dominguez, C., and Allain, F.H. (2005). The RNA recognition motif, a plastic RNA-binding platform to regulate post-transcriptional gene expression. *Febs J* 272, 2118-2131.
- Marsischky, G.T., Wilson, B.A., and Collier, R.J. (1995). Role of glutamic acid 988 of human poly-ADP-ribose polymerase in polymer formation. Evidence for active site similarities to the ADP-ribosylating toxins. *J Biol Chem* 270, 3247-3254.
- Martin, S.J., and Green, D.R. (1995). Protease activation during apoptosis: death by a thousand cuts? *Cell* 82, 349-352.
- Martinon, F., Agostini, L., Meylan, E., and Tschopp, J. (2004). Identification of bacterial muramyl dipeptide as activator of the NALP3/cryopyrin inflammasome. *Curr Biol* 14, 1929-1934.
- Martinon, F., Burns, K., and Tschopp, J. (2002). The inflammasome: a molecular platform triggering activation of inflammatory caspases and processing of proIL-beta. *Mol Cell* 10, 417-426.
- Martinon, F., Petrilli, V., Mayor, A., Tardivel, A., and Tschopp, J. (2006). Gout-associated uric acid crystals activate the NALP3 inflammasome. *Nature* 440, 237-241.
- Martinou, J.C., and Green, D.R. (2001). Breaking the mitochondrial barrier. *Nat Rev Mol Cell Biol* 2, 63-67.
- Martinou, J.C., and Youle, R.J. (2011). Mitochondria in apoptosis: Bcl-2 family members and mitochondrial dynamics. *Dev Cell* 21, 92-101.
- Mashima, T., Naito, M., and Tsuruo, T. (1999). Caspase-mediated cleavage of cytoskeletal actin plays a positive role in the process of morphological apoptosis. *Oncogene* 18, 2423-2430.
- Masson, M., Niedergang, C., Schreiber, V., Muller, S., Menissier-de Murcia, J., and de Murcia, G. (1998). XRCC1 is specifically associated with poly(ADP-ribose) polymerase and negatively regulates its activity following DNA damage. *Mol Cell Biol* 18, 3563-3571.
- Masumoto, J., Taniguchi, S., Ayukawa, K., Sarvotham, H., Kishino, T., Niiikawa, N., Hidaka, E., Katsuyama, T., Higuchi, T., and Sagara, J. (1999). ASC, a novel 22-kDa protein, aggregates during apoptosis of human promyelocytic leukemia HL-60 cells. *J Biol Chem* 274, 33835-33838.

- Matsuzawa, A., Tseng, P.H., Vallabhapurapu, S., Luo, J.L., Zhang, W., Wang, H., Vignali, D.A., Gallagher, E., and Karin, M. (2008). Essential cytoplasmic translocation of a cytokine receptor-assembled signaling complex. *Science* 321, 663-668.
- Matthias, P., Muller, M.M., Schreiber, E., Rusconi, S., and Schaffner, W. (1989). Eukaryotic expression vectors for the analysis of mutant proteins. *Nucleic Acids Res* 17, 6418.
- Mayo, M.W., Wang, C.Y., Cogswell, P.C., Rogers-Graham, K.S., Lowe, S.W., Der, C.J., and Baldwin, A.S., Jr. (1997). Requirement of NF-kappaB activation to suppress p53-independent apoptosis induced by oncogenic Ras. *Science* 278, 1812-1815.
- McConnell, B.B., and Vertino, P.M. (2000). Activation of a caspase-9-mediated apoptotic pathway by subcellular redistribution of the novel caspase recruitment domain protein TMS1. *Cancer Res* 60, 6243-6247.
- McLennan, A.G. (2006). The Nudix hydrolase superfamily. *Cell Mol Life Sci* 63, 123-143.
- McStay, G.P., Salvesen, G.S., and Green, D.R. (2008). Overlapping cleavage motif selectivity of caspases: implications for analysis of apoptotic pathways. *Cell Death Differ* 15, 322-331.
- Menissier de Murcia, J., Ricoul, M., Tartier, L., Niedergang, C., Huber, A., Dantzer, F., Schreiber, V., Ame, J.C., Dierich, A., LeMeur, M., *et al.* (2003). Functional interaction between PARP-1 and PARP-2 in chromosome stability and embryonic development in mouse. *Embo J* 22, 2255-2263.
- Miao, E.A., Alpuche-Aranda, C.M., Dors, M., Clark, A.E., Bader, M.W., Miller, S.I., and Aderem, A. (2006). Cytoplasmic flagellin activates caspase-1 and secretion of interleukin 1beta via Ipaf. *Nat Immunol* 7, 569-575.
- Miao, E.A., Mao, D.P., Yudkovsky, N., Bonneau, R., Lorang, C.G., Warren, S.E., Leaf, I.A., and Aderem, A. (2010). Innate immune detection of the type III secretion apparatus through the NLRC4 inflammasome. *Proc Natl Acad Sci U S A* 107, 3076-3080.
- Micheau, O., and Tschopp, J. (2003). Induction of TNF receptor I-mediated apoptosis via two sequential signaling complexes. *Cell* 114, 181-190.
- Milke, L. (2007). Biochemische und funktionelle Analyse der Ubiquitinierung und des Kerntransports von PARP10 (Diploma thesis, RWTH Aachen University).
- Miwa, M., Tanaka, M., Matsushima, T., and Sugimura, T. (1974). Purification and properties of glycohydrolase from calf thymus splitting ribose-ribose linkages of poly(adenosine diphosphate ribose). *J Biol Chem* 249, 3475-3482.
- Montzka, K. (2006). Nucleo-cytoplasmatischer Transport von PARP10 (Diploma thesis, RWTH Aachen University).
- Morgenstern, J.P., and Land, H. (1990). Advanced mammalian gene transfer: high titre retroviral vectors with multiple drug selection markers and a complementary helper-free packaging cell line. *Nucleic Acids Res* 18, 3587-3596.
- Moscat, J., and Diaz-Meco, M.T. (2009). p62 at the crossroads of autophagy, apoptosis, and cancer. *Cell* 137, 1001-1004.
- Moss, J., Stanley, S.J., Nightingale, M.S., Murtagh, J.J., Jr., Monaco, L., Mishima, K., Chen, H.C., Williamson, K.C., and Tsai, S.C. (1992). Molecular and immunological characterization of ADP-ribosylarginine hydrolases. *J Biol Chem* 267, 10481-10488.
- Muchmore, S.W., Sattler, M., Liang, H., Meadows, R.P., Harlan, J.E., Yoon, H.S., Nettesheim, D., Chang, B.S., Thompson, C.B., Wong, S.L., *et al.* (1996). X-ray and NMR structure of human Bcl-xL, an inhibitor of programmed cell death. *Nature* 381, 335-341.

- Mundt, K.E., Golsteyn, R.M., Lane, H.A., and Nigg, E.A. (1997). On the regulation and function of human polo-like kinase 1 (PLK1): effects of overexpression on cell cycle progression. *Biochem Biophys Res Commun* 239, 377-385.
- Muppidi, J.R., Tschopp, J., and Siegel, R.M. (2004). Life and death decisions: secondary complexes and lipid rafts in TNF receptor family signal transduction. *Immunity* 21, 461-465.
- Muruve, D.A., Petrilli, V., Zaiss, A.K., White, L.R., Clark, S.A., Ross, P.J., Parks, R.J., and Tschopp, J. (2008). The inflammasome recognizes cytosolic microbial and host DNA and triggers an innate immune response. *Nature* 452, 103-107.
- Nakano, K., and Vousden, K.H. (2001). PUMA, a novel proapoptotic gene, is induced by p53. *Mol Cell* 7, 683-694.
- Nechushtan, A., Smith, C.L., Hsu, Y.T., and Youle, R.J. (1999). Conformation of the Bax C-terminus regulates subcellular location and cell death. *Embo J* 18, 2330-2341.
- Niere, M., Mashimo, M., Agledal, L., Dolle, C., Kasamatsu, A., Kato, J., Moss, J., and Ziegler, M. (2012). ADP-ribosylhydrolase 3 (ARH3), not poly(ADP-ribose) glycohydrolase (PARG) isoforms, is responsible for degradation of mitochondrial matrix-associated poly(ADP-ribose). *J Biol Chem* 287, 16088-16102.
- Nikolaev, A., McLaughlin, T., O'Leary, D.D., and Tessier-Lavigne, M. (2009). APP binds DR6 to trigger axon pruning and neuron death via distinct caspases. *Nature* 457, 981-989.
- Norman, J.M., Cohen, G.M., and Bampton, E.T. (2010). The in vitro cleavage of the hAtg proteins by cell death proteases. *Autophagy* 6, 1042-1056.
- O'Regan, L., and Fry, A.M. (2009). The Nek6 and Nek7 protein kinases are required for robust mitotic spindle formation and cytokinesis. *Mol Cell Biol* 29, 3975-3990.
- Oda, E., Ohki, R., Murasawa, H., Nemoto, J., Shibue, T., Yamashita, T., Tokino, T., Taniguchi, T., and Tanaka, N. (2000). Noxa, a BH3-only member of the Bcl-2 family and candidate mediator of p53-induced apoptosis. *Science* 288, 1053-1058.
- Oka, S., Kato, J., and Moss, J. (2006). Identification and characterization of a mammalian 39-kDa poly(ADP-ribose) glycohydrolase. *J Biol Chem* 281, 705-713.
- Okazaki, I.J., Kim, H.J., and Moss, J. (1996). Cloning and characterization of a novel membrane-associated lymphocyte NAD:arginine ADP-ribosyltransferase. *J Biol Chem* 271, 22052-22057.
- Orrenius, S., Nicotera, P., and Zhivotovsky, B. (2011). Cell death mechanisms and their implications in toxicology. *Toxicol Sci* 119, 3-19.
- Orth, K., Chinnaiyan, A.M., Garg, M., Froelich, C.J., and Dixit, V.M. (1996). The CED-3/ICE-like protease Mch2 is activated during apoptosis and cleaves the death substrate lamin A. *J Biol Chem* 271, 16443-16446.
- Otera, H., Ohsakaya, S., Nagaura, Z., Ishihara, N., and Mihara, K. (2005). Export of mitochondrial AIF in response to proapoptotic stimuli depends on processing at the intermembrane space. *Embo J* 24, 1375-1386.
- Otto, H., Reche, P.A., Bazan, F., Dittmar, K., Haag, F., and Koch-Nolte, F. (2005). In silico characterization of the family of PARP-like poly(ADP-ribosyl)transferases (pARTs). *BMC Genomics* 6, 139.
- Oumouna, M., Datta, R., Oumouna-Benachour, K., Suzuki, Y., Hans, C., Matthews, K., Fallon, K., and Boulares, H. (2006). Poly(ADP-ribose) polymerase-1 inhibition prevents eosinophil recruitment by modulating Th2 cytokines in a murine model of allergic airway inflammation: a potential specific effect on IL-5. *J Immunol* 177, 6489-6496.

- Patterson, S.D., Spahr, C.S., Daugas, E., Susin, S.A., Irinopoulou, T., Koehler, C., and Kroemer, G. (2000). Mass spectrometric identification of proteins released from mitochondria undergoing permeability transition. *Cell Death Differ* 7, 137-144.
- Pehrson, J.R., and Fried, V.A. (1992). MacroH2A, a core histone containing a large nonhistone region. *Science* 257, 1398-1400.
- Pelegri, P., and Surprenant, A. (2006). Pannexin-1 mediates large pore formation and interleukin-1 β release by the ATP-gated P2X7 receptor. *Embo J* 25, 5071-5082.
- Pereira, W.O., and Amarante-Mendes, G.P. (2011). Apoptosis: a programme of cell death or cell disposal? *Scand J Immunol* 73, 401-407.
- Petrilli, V., Papin, S., Dostert, C., Mayor, A., Martinon, F., and Tschopp, J. (2007). Activation of the NALP3 inflammasome is triggered by low intracellular potassium concentration. *Cell Death Differ* 14, 1583-1589.
- Pleschke, J.M., Kleczkowska, H.E., Strohm, M., and Althaus, F.R. (2000). Poly(ADP-ribose) binds to specific domains in DNA damage checkpoint proteins. *J Biol Chem* 275, 40974-40980.
- Poirier, G.G., de Murcia, G., Jongstra-Bilen, J., Niedergang, C., and Mandel, P. (1982). Poly(ADP-ribosylation) of polynucleosomes causes relaxation of chromatin structure. *Proc Natl Acad Sci U S A* 79, 3423-3427.
- Poyet, J.L., Srinivasula, S.M., Tnani, M., Razmara, M., Fernandes-Alnemri, T., and Alnemri, E.S. (2001). Identification of Ipaf, a human caspase-1-activating protein related to Apaf-1. *J Biol Chem* 276, 28309-28313.
- Puthalakath, H., O'Reilly, L.A., Gunn, P., Lee, L., Kelly, P.N., Huntington, N.D., Hughes, P.D., Michalak, E.M., McKimm-Breschkin, J., Motoyama, N., *et al.* (2007). ER stress triggers apoptosis by activating BH3-only protein Bim. *Cell* 129, 1337-1349.
- Rayet, B., and Gelinas, C. (1999). Aberrant rel/nfkb genes and activity in human cancer. *Oncogene* 18, 6938-6947.
- Reed, J.C. (2006). Proapoptotic multidomain Bcl-2/Bax-family proteins: mechanisms, physiological roles, and therapeutic opportunities. *Cell Death Differ* 13, 1378-1386.
- Reed, J.C., Doctor, K.S., and Godzik, A. (2004). The domains of apoptosis: a genomics perspective. *Sci STKE* 2004, re9.
- Reeder, R.H., Ueda, K., Honjo, T., Nishizuka, Y., and Hayaishi, O. (1967). Studies on the polymer of adenosine diphosphate ribose. II. Characterization of the polymer. *J Biol Chem* 242, 3172-3179.
- Ren, T., Zamboni, D.S., Roy, C.R., Dietrich, W.F., and Vance, R.E. (2006). Flagellin-deficient Legionella mutants evade caspase-1- and Naip5-mediated macrophage immunity. *PLoS Pathog* 2, e18.
- Riedl, S.J., and Shi, Y. (2004). Molecular mechanisms of caspase regulation during apoptosis. *Nat Rev Mol Cell Biol* 5, 897-907.
- Roberts, T.L., Idris, A., Dunn, J.A., Kelly, G.M., Burnton, C.M., Hodgson, S., Hardy, L.L., Garceau, V., Sweet, M.J., Ross, I.L., *et al.* (2009). HIN-200 proteins regulate caspase activation in response to foreign cytoplasmic DNA. *Science* 323, 1057-1060.
- Rolli, V., O'Farrell, M., Menissier-de Murcia, J., and de Murcia, G. (1997). Random mutagenesis of the poly(ADP-ribose) polymerase catalytic domain reveals amino acids involved in polymer branching. *Biochemistry* 36, 12147-12154.
- Ruffolo, S.C., and Shore, G.C. (2003). BCL-2 selectively interacts with the BID-induced open conformer of BAK, inhibiting BAK auto-oligomerization. *J Biol Chem* 278, 25039-25045.

- Saelens, X., Festjens, N., Vande Walle, L., van Gurp, M., van Loo, G., and Vandenabeele, P. (2004). Toxic proteins released from mitochondria in cell death. *Oncogene* 23, 2861-2874.
- Sakahira, H., Enari, M., and Nagata, S. (1998). Cleavage of CAD inhibitor in CAD activation and DNA degradation during apoptosis. *Nature* 391, 96-99.
- Salvesen, G.S., and Dixit, V.M. (1999). Caspase activation: the induced-proximity model. *Proc Natl Acad Sci U S A* 96, 10964-10967.
- Santiago, C., Ballesteros, A., Martinez-Munoz, L., Mellado, M., Kaplan, G.G., Freeman, G.J., and Casasnovas, J.M. (2007). Structures of T cell immunoglobulin mucin protein 4 show a metal-ion-dependent ligand binding site where phosphatidylserine binds. *Immunity* 27, 941-951.
- Sanz, L., Diaz-Meco, M.T., Nakano, H., and Moscat, J. (2000). The atypical PKC-interacting protein p62 channels NF-kappaB activation by the IL-1-TRAF6 pathway. *Embo J* 19, 1576-1586.
- Sanz, L., Sanchez, P., Lallena, M.J., Diaz-Meco, M.T., and Moscat, J. (1999). The interaction of p62 with RIP links the atypical PKCs to NF-kappaB activation. *Embo J* 18, 3044-3053.
- Scaffidi, C., Fulda, S., Srinivasan, A., Friesen, C., Li, F., Tomaselli, K.J., Debatin, K.M., Krammer, P.H., and Peter, M.E. (1998). Two CD95 (APO-1/Fas) signaling pathways. *Embo J* 17, 1675-1687.
- Schechter, I., and Berger, A. (1967). On the size of the active site in proteases. I. Papain. *Biochem Biophys Res Commun* 27, 157-162.
- Schleiss, M.R., Degnin, C.R., and Geballe, A.P. (1991). Translational control of human cytomegalovirus gp48 expression. *J Virol* 65, 6782-6789.
- Schreiber, V., Ame, J.C., Dolle, P., Schultz, I., Rinaldi, B., Fraulob, V., Menissier-de Murcia, J., and de Murcia, G. (2002). Poly(ADP-ribose) polymerase-2 (PARP-2) is required for efficient base excision DNA repair in association with PARP-1 and XRCC1. *J Biol Chem* 277, 23028-23036.
- Schuchlantz, H. (2008). Mechanistic insights into the PARP10-mediated ADP-ribosylation reaction and analysis of PARP10's subcellular localization (Phd thesis, RWTH Aachen University).
- Schweigreiter, R., Stasyk, T., Contarini, I., Frauscher, S., Oertle, T., Klimaschewski, L., Huber, L.A., and Bandtlow, C.E. (2007). Phosphorylation-regulated cleavage of the reticulon protein Nogo-B by caspase-7 at a noncanonical recognition site. *Proteomics* 7, 4457-4467.
- Shen, J., Yin, Y., Mai, J., Xiong, X., Pansuria, M., Liu, J., Maley, E., Saqib, N.U., Wang, H., and Yang, X.F. (2010). Caspase-1 recognizes extended cleavage sites in its natural substrates. *Atherosclerosis* 210, 422-429.
- Shi, C.S., Shenderov, K., Huang, N.N., Kabat, J., Abu-Asab, M., Fitzgerald, K.A., Sher, A., and Kehrl, J.H. (2012). Activation of autophagy by inflammatory signals limits IL-1beta production by targeting ubiquitinated inflammasomes for destruction. *Nat Immunol* 13, 255-263.
- Shi, Y. (2002). A conserved tetrapeptide motif: potentiating apoptosis through IAP-binding. *Cell Death Differ* 9, 93-95.
- Shi, Y. (2004a). Caspase activation, inhibition, and reactivation: a mechanistic view. *Protein Sci* 13, 1979-1987.
- Shi, Y. (2004b). Caspase activation: revisiting the induced proximity model. *Cell* 117, 855-858.
- Shieh, W.M., Ame, J.C., Wilson, M.V., Wang, Z.Q., Koh, D.W., Jacobson, M.K., and Jacobson, E.L. (1998). Poly(ADP-ribose) polymerase null mouse cells synthesize ADP-ribose polymers. *J Biol Chem* 273, 30069-30072.
- Shirley, S., and Micheau, O. (2010). Targeting c-FLIP in cancer. *Cancer Lett.*

- Srinivasula, S.M., and Ashwell, J.D. (2008). IAPs: what's in a name? *Mol Cell* 30, 123-135.
- Srinivasula, S.M., Hegde, R., Saleh, A., Datta, P., Shiozaki, E., Chai, J., Lee, R.A., Robbins, P.D., Fernandes-Alnemri, T., Shi, Y., *et al.* (2001). A conserved XIAP-interaction motif in caspase-9 and Smac/DIABLO regulates caspase activity and apoptosis. *Nature* 410, 112-116.
- Srinivasula, S.M., Poyet, J.L., Razmara, M., Datta, P., Zhang, Z., and Alnemri, E.S. (2002). The PYRIN-CARD protein ASC is an activating adaptor for caspase-1. *J Biol Chem* 277, 21119-21122.
- Stennicke, H.R., Renatus, M., Meldal, M., and Salvesen, G.S. (2000). Internally quenched fluorescent peptide substrates disclose the subsite preferences of human caspases 1, 3, 6, 7 and 8. *Biochem J* 350 Pt 2, 563-568.
- Strasser, A. (2005). The role of BH3-only proteins in the immune system. *Nat Rev Immunol* 5, 189-200.
- Sun, J., Maresso, A.W., Kim, J.J., and Barbieri, J.T. (2004). How bacterial ADP-ribosylating toxins recognize substrates. *Nat Struct Mol Biol* 11, 868-876.
- Susin, S.A., Lorenzo, H.K., Zamzami, N., Marzo, I., Snow, B.E., Brothers, G.M., Mangion, J., Jacotot, E., Costantini, P., Loeffler, M., *et al.* (1999). Molecular characterization of mitochondrial apoptosis-inducing factor. *Nature* 397, 441-446.
- Suzuki, M., Youle, R.J., and Tjandra, N. (2000). Structure of Bax: coregulation of dimer formation and intracellular localization. *Cell* 103, 645-654.
- Suzuki, Y., Nakabayashi, Y., and Takahashi, R. (2001). Ubiquitin-protein ligase activity of X-linked inhibitor of apoptosis protein promotes proteasomal degradation of caspase-3 and enhances its anti-apoptotic effect in Fas-induced cell death. *Proc Natl Acad Sci U S A* 98, 8662-8667.
- Takada, T., Iida, K., and Moss, J. (1993). Cloning and site-directed mutagenesis of human ADP-ribosylarginine hydrolase. *J Biol Chem* 268, 17837-17843.
- Takahashi, A., Musy, P.Y., Martins, L.M., Poirier, G.G., Moyer, R.W., and Earnshaw, W.C. (1996). CrmA/SPI-2 inhibition of an endogenous ICE-related protease responsible for lamin A cleavage and apoptotic nuclear fragmentation. *J Biol Chem* 271, 32487-32490.
- Talanian, R.V., Quinlan, C., Trautz, S., Hackett, M.C., Mankovich, J.A., Banach, D., Ghayur, T., Brady, K.D., and Wong, W.W. (1997). Substrate specificities of caspase family proteases. *J Biol Chem* 272, 9677-9682.
- Taylor, R.C., Cullen, S.P., and Martin, S.J. (2008). Apoptosis: controlled demolition at the cellular level. *Nat Rev Mol Cell Biol* 9, 231-241.
- Telford, W.G., King, L.E., and Fraker, P.J. (1991). Evaluation of glucocorticoid-induced DNA fragmentation in mouse thymocytes by flow cytometry. *Cell Prolif* 24, 447-459.
- Telford, W.G., King, L.E., and Fraker, P.J. (1992). Comparative evaluation of several DNA binding dyes in the detection of apoptosis-associated chromatin degradation by flow cytometry. *Cytometry* 13, 137-143.
- Tewari, M., Quan, L.T., O'Rourke, K., Desnoyers, S., Zeng, Z., Beidler, D.R., Poirier, G.G., Salvesen, G.S., and Dixit, V.M. (1995). Yama/CPP32 beta, a mammalian homolog of CED-3, is a CrmA-inhibitable protease that cleaves the death substrate poly(ADP-ribose) polymerase. *Cell* 81, 801-809.
- Thiemermann, C., Bowes, J., Myint, F.P., and Vane, J.R. (1997). Inhibition of the activity of poly(ADP-ribose) synthetase reduces ischemia-reperfusion injury in the heart and skeletal muscle. *Proc Natl Acad Sci U S A* 94, 679-683.
- Thornberry, N.A., Bull, H.G., Calaycay, J.R., Chapman, K.T., Howard, A.D., Kostura, M.J., Miller, D.K., Molineaux, S.M., Weidner, J.R., Aunins, J., *et al.* (1992). A novel heterodimeric cysteine protease is required for interleukin-1 beta processing in monocytes. *Nature* 356, 768-774.

- Thornberry, N.A., Rano, T.A., Peterson, E.P., Rasper, D.M., Timkey, T., Garcia-Calvo, M., Houtzager, V.M., Nordstrom, P.A., Roy, S., Vaillancourt, J.P., *et al.* (1997). A combinatorial approach defines specificities of members of the caspase family and granzyme B. Functional relationships established for key mediators of apoptosis. *J Biol Chem* 272, 17907-17911.
- Timinszky, G., Till, S., Hassa, P.O., Hothorn, M., Kustatscher, G., Nijmeijer, B., Colombelli, J., Altmeyer, M., Stelzer, E.H., Scheffzek, K., *et al.* (2009). A macrodomain-containing histone rearranges chromatin upon sensing PARP1 activation. *Nat Struct Mol Biol* 16, 923-929.
- Timmer, J.C., and Salvesen, G.S. (2007). Caspase substrates. *Cell Death Differ* 14, 66-72.
- Ting, J.P., Lovering, R.C., Alnemri, E.S., Bertin, J., Boss, J.M., Davis, B.K., Flavell, R.A., Girardin, S.E., Godzik, A., Harton, J.A., *et al.* (2008a). The NLR gene family: a standard nomenclature. *Immunity* 28, 285-287.
- Ting, J.P., Willingham, S.B., and Bergstralh, D.T. (2008b). NLRs at the intersection of cell death and immunity. *Nat Rev Immunol* 8, 372-379.
- Torres, J., Rodriguez, J., Myers, M.P., Valiente, M., Graves, J.D., Tonks, N.K., and Pulido, R. (2003). Phosphorylation-regulated cleavage of the tumor suppressor PTEN by caspase-3: implications for the control of protein stability and PTEN-protein interactions. *J Biol Chem* 278, 30652-30660.
- Tsuchiya, S., Yamabe, M., Yamaguchi, Y., Kobayashi, Y., Konno, T., and Tada, K. (1980). Establishment and characterization of a human acute monocytic leukemia cell line (THP-1). *Int J Cancer* 26, 171-176.
- Vakifahmetoglu, H., Olsson, M., and Zhivotovsky, B. (2008). Death through a tragedy: mitotic catastrophe. *Cell Death Differ* 15, 1153-1162.
- Van Damme, P., Martens, L., Van Damme, J., Hugelier, K., Staes, A., Vandekerckhove, J., and Gevaert, K. (2005). Caspase-specific and nonspecific in vivo protein processing during Fas-induced apoptosis. *Nat Methods* 2, 771-777.
- Varfolomeev, E., Goncharov, T., Fedorova, A.V., Dynek, J.N., Zobel, K., Deshayes, K., Fairbrother, W.J., and Vucic, D. (2008). c-IAP1 and c-IAP2 are critical mediators of tumor necrosis factor alpha (TNFalpha)-induced NF-kappaB activation. *J Biol Chem* 283, 24295-24299.
- Vaux, D.L. (2011). Apoptogenic factors released from mitochondria. *Biochim Biophys Acta* 1813, 546-550.
- Vaux, D.L., Weissman, I.L., and Kim, S.K. (1992). Prevention of programmed cell death in *Caenorhabditis elegans* by human bcl-2. *Science* 258, 1955-1957.
- Verhagen, A.M., Ekert, P.G., Pakusch, M., Silke, J., Connolly, L.M., Reid, G.E., Moritz, R.L., Simpson, R.J., and Vaux, D.L. (2000). Identification of DIABLO, a mammalian protein that promotes apoptosis by binding to and antagonizing IAP proteins. *Cell* 102, 43-53.
- Verhagen, A.M., Silke, J., Ekert, P.G., Pakusch, M., Kaufmann, H., Connolly, L.M., Day, C.L., Tikoo, A., Burke, R., Wrobel, C., *et al.* (2002). HtrA2 promotes cell death through its serine protease activity and its ability to antagonize inhibitor of apoptosis proteins. *J Biol Chem* 277, 445-454.
- Verhoven, B., Schlegel, R.A., and Williamson, P. (1995). Mechanisms of phosphatidylserine exposure, a phagocyte recognition signal, on apoptotic T lymphocytes. *J Exp Med* 182, 1597-1601.
- Vermes, I., Haanen, C., Steffens-Nakken, H., and Reutelingsperger, C. (1995). A novel assay for apoptosis. Flow cytometric detection of phosphatidylserine expression on early apoptotic cells using fluorescein labelled Annexin V. *J Immunol Methods* 184, 39-51.
- Vousden, K.H., and Lu, X. (2002). Live or let die: the cell's response to p53. *Nat Rev Cancer* 2, 594-604.

- Walensky, L.D., Pitter, K., Morash, J., Oh, K.J., Barbuto, S., Fisher, J., Smith, E., Verdine, G.L., and Korsmeyer, S.J. (2006). A stapled BID BH3 helix directly binds and activates BAX. *Mol Cell* 24, 199-210.
- Wang, H.G., Pathan, N., Ethell, I.M., Krajewski, S., Yamaguchi, Y., Shibasaki, F., McKeon, F., Bobo, T., Franke, T.F., and Reed, J.C. (1999). Ca²⁺-induced apoptosis through calcineurin dephosphorylation of BAD. *Science* 284, 339-343.
- Wang, X.J., Cao, Q., Liu, X., Wang, K.T., Mi, W., Zhang, Y., Li, L.F., LeBlanc, A.C., and Su, X.D. (2010). Crystal structures of human caspase 6 reveal a new mechanism for intramolecular cleavage self-activation. *EMBO Rep* 11, 841-847.
- Wang, Y., Kim, N.S., Haince, J.F., Kang, H.C., David, K.K., Andrabi, S.A., Poirier, G.G., Dawson, V.L., and Dawson, T.M. (2011). Poly(ADP-ribose) (PAR) binding to apoptosis-inducing factor is critical for PAR polymerase-1-dependent cell death (parthanatos). *Sci Signal* 4, ra20.
- Wang, Z., Michaud, G.A., Cheng, Z., Zhang, Y., Hinds, T.R., Fan, E., Cong, F., and Xu, W. (2012). Recognition of the iso-ADP-ribose moiety in poly(ADP-ribose) by WWE domains suggests a general mechanism for poly(ADP-ribosyl)ation-dependent ubiquitination. *Genes Dev* 26, 235-240.
- Wei, M.C., Zong, W.X., Cheng, E.H., Lindsten, T., Panoutsakopoulou, V., Ross, A.J., Roth, K.A., MacGregor, G.R., Thompson, C.B., and Korsmeyer, S.J. (2001). Proapoptotic BAX and BAK: a requisite gateway to mitochondrial dysfunction and death. *Science* 292, 727-730.
- Wilson, N.S., Dixit, V., and Ashkenazi, A. (2009). Death receptor signal transducers: nodes of coordination in immune signaling networks. *Nat Immunol* 10, 348-355.
- Wu, Y., Mehew, J.W., Heckman, C.A., Arcinas, M., and Boxer, L.M. (2001). Negative regulation of bcl-2 expression by p53 in hematopoietic cells. *Oncogene* 20, 240-251.
- Yin, M.J., Shao, L., Voehringer, D., Smeal, T., and Jallal, B. (2003). The serine/threonine kinase Nek6 is required for cell cycle progression through mitosis. *J Biol Chem* 278, 52454-52460.
- Yin, X.M., Oltvai, Z.N., and Korsmeyer, S.J. (1994). BH1 and BH2 domains of Bcl-2 are required for inhibition of apoptosis and heterodimerization with Bax. *Nature* 369, 321-323.
- Yu, M., Schreek, S., Cerni, C., Schamberger, C., Lesniewicz, K., Poreba, E., Vervoorts, J., Walsemann, G., Grotzinger, J., Kremmer, E., *et al.* (2005). PARP-10, a novel Myc-interacting protein with poly(ADP-ribose) polymerase activity, inhibits transformation. *Oncogene* 24, 1982-1993.
- Yu, S.W., Andrabi, S.A., Wang, H., Kim, N.S., Poirier, G.G., Dawson, T.M., and Dawson, V.L. (2006). Apoptosis-inducing factor mediates poly(ADP-ribose) (PAR) polymer-induced cell death. *Proc Natl Acad Sci U S A* 103, 18314-18319.
- Yu, S.W., Wang, H., Poitras, M.F., Coombs, C., Bowers, W.J., Federoff, H.J., Poirier, G.G., Dawson, T.M., and Dawson, V.L. (2002). Mediation of poly(ADP-ribose) polymerase-1-dependent cell death by apoptosis-inducing factor. *Science* 297, 259-263.
- Yuan, J., Shaham, S., Ledoux, S., Ellis, H.M., and Horvitz, H.R. (1993). The *C. elegans* cell death gene *ced-3* encodes a protein similar to mammalian interleukin-1 beta-converting enzyme. *Cell* 75, 641-652.
- Yuan, S., Yu, X., Topf, M., Ludtke, S.J., Wang, X., and Akey, C.W. (2010). Structure of an apoptosome-procaspase-9 CARD complex. *Structure* 18, 571-583.
- Zahradka, P., and Ebisuzaki, K. (1982). A shuttle mechanism for DNA-protein interactions. The regulation of poly(ADP-ribose) polymerase. *Eur J Biochem* 127, 579-585.
- Zamzami, N., Larochette, N., and Kroemer, G. (2005). Mitochondrial permeability transition in apoptosis and necrosis. *Cell Death Differ* 12 Suppl 2, 1478-1480.

- Zerfaoui, M., Errami, Y., Naura, A.S., Suzuki, Y., Kim, H., Ju, J., Liu, T., Hans, C.P., Kim, J.G., Abd Elmageed, Z.Y., *et al.* (2010). Poly(ADP-ribose) polymerase-1 is a determining factor in Crm1-mediated nuclear export and retention of p65 NF-kappa B upon TLR4 stimulation. *J Immunol* 185, 1894-1902.
- Zhang, S.Q., Kovalenko, A., Cantarella, G., and Wallach, D. (2000). Recruitment of the IKK signalosome to the p55 TNF receptor: RIP and A20 bind to NEMO (IKKgamma) upon receptor stimulation. *Immunity* 12, 301-311.
- Zhang, Y., Liu, S., Mickanin, C., Feng, Y., Charlat, O., Michaud, G.A., Schirle, M., Shi, X., Hild, M., Bauer, A., *et al.* (2011). RNF146 is a poly(ADP-ribose)-directed E3 ligase that regulates axin degradation and Wnt signalling. *Nat Cell Biol* 13, 623-629.
- Zhou, R., Yazdi, A.S., Menu, P., and Tschopp, J. (2011). A role for mitochondria in NLRP3 inflammasome activation. *Nature* 469, 221-225.
- Zhu, H., Fearnhead, H.O., and Cohen, G.M. (1995). An ICE-like protease is a common mediator of apoptosis induced by diverse stimuli in human monocytic THP.1 cells. *FEBS Lett* 374, 303-308.
- Zhu, P., Martinvalet, D., Chowdhury, D., Zhang, D., Schlesinger, A., and Lieberman, J. (2009). The cytotoxic T lymphocyte protease granzyme A cleaves and inactivates poly(adenosine 5'-diphosphate-ribose) polymerase-1. *Blood* 114, 1205-1216.
- Zolkiewska, A. (2005). Ecto-ADP-ribose transferases: cell-surface response to local tissue injury. *Physiology (Bethesda)* 20, 374-381.
- Zolkiewska, A., Nightingale, M.S., and Moss, J. (1992). Molecular characterization of NAD:arginine ADP-ribosyltransferase from rabbit skeletal muscle. *Proc Natl Acad Sci U S A* 89, 11352-11356.
- Zou, H., Li, Y., Liu, X., and Wang, X. (1999). An APAF-1.cytochrome c multimeric complex is a functional apoptosome that activates procaspase-9. *J Biol Chem* 274, 11549-11556.

9 Appendix

9.1.1 Abbreviations

Abbreviation	
ADP	adenosine diphosphate
ADPr	ADP-ribose
AIF	apoptosis inducing factor
ANT	adenine nucleotide translocase
APAF-1	apoptotic protease activating factor 1
ARH	ADP-ribosylhydrolase
ART	ADP-ribosyltransferase
ARTC	ADP-ribosyltransferase cholera toxin like
ARTD	ADP-ribosyltransferase diphtheria toxin like
ASC	apoptosis-associated speck-like protein containing a CARD
ATP	adenosine triphosphate
BAK	BCL-2 antagonist killer
BAX	BCL-2-associated protein X
BCRT	BRCA1 C-terminus
BER	base excision repair
BH	B-cell homology
BIR	baculoviral IAP repeat
CAD	caspase-activated DNase
CARD	caspase recruitment domain
CDK	cyclin dependent kinase
cFLIP	cellular FLICE-like inhibitory protein
CLR	C-type lectin receptors
CMV	cytomegalovirus
cyt c	cytochrome c
DAMP	damage-associated molecular pattern
DD	death domain
DED	death effector domain
DISC	death inducing signaling complex
DNA	desoxy-ribonucleic acid
dsDNA	double stranded DNA
E-rich	glutamate rich region
ER	endoplasmatic reticulum
FACS	fluorescence-activated cell sorting
G-rich	glycine rich region
GFP	green fluorescent protein
GST	glutathione S-transferase
HA	hemagglutinin
HFT	HeLa Flp-In T-Rex
HPLC	high-pressure liquid chromatography
IAP	inhibitor of apoptosis
IBM	IAP binding motif
ICAD	inhibitor of CAD
IF	immunofluorescence
IMS	intermembrane space
kb	kilo bases
kD	kilo Dalton
LMB	Leptomycin B
LRR	leucine rich repeat
LRR	leucine-rich repeat
LT	lethal toxin
mADPr	mono-ADPr
mART	mono-ADP-ribosyltransferase

MDP	muramyl dipeptide
MEF	murine embryo fibroblasts
MMP	mitochondrial membrane permeabilization
NAD	nicotinamide adenine dinucleotide
NBD	nucleotide binding domain
NES	nuclear export sequence
NF- κ B	nuclear factor κ -light chain enhancer of activated B cells
NLR	nucleotide-binding-and-oligomerization domain [Nod] and leucine-rich-repeat-containing receptors
NLS	nuclear localization sequence
NOD	nucleotide binding and oligomerization domain
PAMP	pathogen-associated molecular pattern
PAR	poly-ADP-ribose
PARG	poly-ADP-ribose glycohydrolase
PARP	poly-ADP-ribose polymerase
PARP	poly-ADP-ribose polymerase
PBM	PAR binding motif
PBZ	PAR binding zinc finger
PI	propidium iodide
PS	phosphatidyl serine
PTM	post translational modification
PYD	pyrin domain
REF	rat embryo fibroblast
RLR	RIG-I-like receptors
RNA	ribonucleic acid
ROS	reactive oxygen species
RRM	RNA recognition motif
SDS-PAGE	sodium dodecyl sulfate polyacrylamide gel electrophoresis
ssDNA	single stranded DNA
TAP	tandem affinity purification
TLR	toll-like receptor
TM	transmembrane
TNF	tumor necrosis factor
TNFR	tumor necrosis factor receptor
TpT	tRNA 2'phosphotransferase
tRNA	transfer ribonucleic acid
TUNEL	terminal deoxynucleotidyl transferase-mediated dUTP nick-end labeling
UIM	ubiquitin interacting motif
UV	ultraviolet
VDAC	voltage-dependent ion channel
ZF	zinc finger
$\Delta\Psi_m$	mitochondrial transmembrane permeabilization

9.2 Scientific contributions

9.2.1 Publications in scientific journals

Feijs KLH, Kleine H, Braczynski A, Forst AH, **Herzog N**, Verheugd P, Linzen U, Kremmer E, Lüscher B. Identification of ARTD10 substrates and regulation of GSK3 β by mono-ADP-ribosylation. *Journal of Biological Chemistry*, manuscript submitted

Herzog N, Hartkamp JDH, Verheugd P, Forst AH, Feijs KLH, Kremmer E, Kleine H, Lüscher B. Caspase-dependent cleavage of the mono-ADP-ribosyltransferase ARTD10 interferes with its pro-apoptotic function. *Molecular and Cellular Biology*, manuscript in revision

Verheugd P, Milke L, **Herzog N**, Feijs KLH, Forst AH, Kremmer E, Kleine H, Lüscher B. Regulation of NF- κ B signaling by the mono-ADP-ribosyltransferase ARTD10. *Nature Communications*, manuscript in revision

Forst AH, Karlberg T, **Herzog N**, Thorsell AG, Feijs KLH, Verheugd P, Kursula P, Nijmeijer B, Lippok B, Kleine H, Kremmer E, Ladurner A, Lüscher B, Schüler H. Recognition of mono-ADP-ribosylated ARTD10 substrates by ARTD8 macrodomains. *The EMBO journal*, manuscript submitted

Kleine H, Herrmann A, Lamark T, Forst AH, Verheugd P, Lüscher-Firzlaff J, Lippok B, Feijs KLH, **Herzog N**, Kremmer E, Johansen T, Müller-Newen G, Lüscher B. Dynamic subcellular localization of the mono-ADP-ribosyltransferase and interaction with the ubiquitin receptor p62. *Cell communication & signaling* (2012)

9.2.2 Presentations at scientific meetings

Herzog N, Feijs KHL, Forst AH, Verheugd P, Hartkamp JDH, Kleine H, Kremmer E, Lüscher B. Control of cell proliferation and induction of apoptosis by ARTD10 is dependent on its mono-ADP-ribosyltransferase activity. *Talk given at the 6th PARPregio Meeting, 6-7 September, Aachen, Germany (2012).*

Herzog N, Feijs KH, Verheugd P, Forst AH, Kleine H, Schuppert A, Lüscher B. Role of PARP10/ARTD10 in cell proliferation and apoptosis. *Poster presented at the 18th International Conference on ADP-ribose metabolism, 18-21 August, Zurich, Switzerland (2010).*

9.3 Curriculum Vitae

Persönliche Daten

Name:	Nicolas Herzog
Geburtsdatum/-ort:	30.11.1982 in Aachen
Anschrift:	Fischmarkt. 7, 52062 Aachen
Telefon:	0241/47589659
Email-Adresse:	nicolas.herzog@rwth-aachen.de

Schulische Ausbildung

2002	Erlangung der Allgemeinen Hochschulreife
1993-2002	Einhard Gymnasium in Aachen

Zivildienst

07/2002 – 04/2003	Zivildienst beim Deutschen Roten Kreuz Aachen
07/2002 – 10/2002	Ausbildung zum Rettungssanitäter

Hochschulausbildung

08/2009 – 10/2012	Promotionsstudium am Institut für Molekularbiologie und Biochemie, RWTH Aachen
03/2009	Abschluss des Studiums als Diplom-Biologe
05/2008 – 03/2009	Diplomarbeit am Fraunhofer Institut für Molekularbiologie und angewandte Ökologie mit dem Thema: <i>„Isolation muriner V-Gene und Herstellung funktionaler Antikörperfragmente“</i>
11/2006 – 01/2007	Zellbiologisch/Molekularbiologisches Forschungspraktikum am Institut für Botanik der RWTH Aachen
10/2003 – 03/2009	Studium der Biologie an der RWTH Aachen (Abschluss: 1,2) Hauptfach: Molekularbiologie & Zellbiologie Biol. Nebenfächer: Immunologie Biomaterialien Nicht-biol. Nebenfach: Proteinchemie

Sprachkenntnisse

Deutsch:	Muttersprache
Englisch:	fließend
Latein:	großes Latinum

9.4 Eidesstattliche Erklärung

Ich erkläre eidesstattlich, dass ich die vorliegende Dissertation selbständig verfasst und alle in Anspruch genommenen Hilfen in der Dissertation angegeben habe. Des Weiteren erkläre ich, dass die vorliegende Dissertation nicht bereits als Diplomarbeit oder vergleichbare Prüfungsarbeit verwendet worden ist.

30.10.2012

Nicolas Herzog

9.5 Acknowledgements

Erst einmal herzlichen Dank an Prof. Dr. Bernhard Lüscher für die Möglichkeit meine Promotion in einer so tollen Arbeitsgruppe an einem spannenden Thema anzufertigen. Danke auch für das stete Gegengewicht in Diskussionen und während Meetings, sei es Skepsis, Enthusiasmus oder Motivation.

Herrn Prof. Dr. Lothar Elling möchte ich für die bereitwillige Übernahme des Zweitgutachtens danken.

Dank gilt auch denen die an diesem Projekt mitgearbeitet haben, wie Patrice, Karla, Alex, Barbara, die beiden Jörgs, Juliane und Henning, welche durch Diskussionen, Ideen und Motivation dazu beigetragen haben Sackgassen zu umschiffen oder ihnen zu entrinnen. Vielen Dank auch an Elisabeth Kremmer für die Arbeit und Unterstützung bei unserer Suche nach guten Antikörpern und Steven Taylor für die HeLa Flp-In T-Rex Zellen ohne die diese Arbeit nicht möglich gewesen wäre.

Für die gute Arbeitsatmosphäre und viele schöne Stunden in Labor, Büro, Kaffeeküche und Mensa möchte ich mich bei allen bedanken mit denen ich diese verbracht habe. Danke vor allem an alle Insassen von Labor 3, welches trotz starker Konkurrenz, das mit Abstand coolste Labor war. Gleiches gilt für das Büro im 6. Stock. Ihr seid toll!

Auch außerhalb der Arbeit habe ich euch alle gerne gesehen und kann klar sagen, dass mir durchweg alle Spiele- und Filmabende, Ausflüge, Urlaube und Feiern viel Spaß gemacht haben und ich sie nicht so leicht vergessen werde.

Danke Annika für deine Unterstützung in allen Belangen.

Vielen Dank auch an meine Freunde und Familie die, trotz vieler offener Fragen aufgrund meiner Wortkargheit in Bezug auf meine Arbeit, immer wieder Interesse gezeigt haben und viel zu meiner Erholung beigetragen haben.